Shearing on the Great Glen Fault: Kinematic and Microstructural Evidence Preserved at Different Crustal Levels

Cassandra Becker

Thesis submitted to the faculty of the Virginia Polytechnic Institute and State University in partial fulfillment of the requirements for the degree of

Master of Science
In
Geosciences

Richard D. Law, Chair
Mark J. Caddick
James A. Spotila

May 8, 2023
Blacksburg, Virginia

Keywords: Dynamic Recrystallization, Kinematics, Shearing, Faulting, Scotland, Quartz

Shearing on the Great Glen Fault: Kinematic and Microstructural Evidence Preserved at Different Crustal Levels

Cassandra Becker

ABSTRACT

The NE-SW trending Great Glen Fault (GGF) is one of mainland Scotland's most significant crustal-scale faults, although our understanding of its early kinematics is in question. Previous studies generally agree that the GGF was initiated as a Silurian sinistral strike-slip fault displacing c. 425 Ma isotopically dated granitic plutons. Stewart et al. (2001) argued that dikes fed by these plutons were sinistrally sheared by the GGF while in the sub-magmatic state, suggesting continuous strike-slip motion on the GGF by 425 Ma. Strike-slip offset post-dating overlying Devonian sedimentary basins is likely only a few tens of kilometers, requiring substantial (100s of kms) Silurian-aged strike-slip movement on the GGF in most plate reconstruction models for the Caledonian mountain belt, now exposed in East Greenland, Scandinavia, and Scotland. In contrast, a recent study (Searle 2021) has argued that motion on the GGF may instead have initiated in the Upper Paleozoic and that off-set is therefore minimal, bringing current restoration models into question.

Several papers report widespread field and microstructural evidence from crystalline bedrock and overlying Devonian sedimentary rocks for brittle upper-crustal shearing on the GGF. However, evidence for high-temperature crystal plastic shearing at deeper crustal levels on the GGF, potentially of Silurian to Early Devonian age, is limited. During summer 2022, suites of oriented and plastically deformed metasedimentary rock samples were collected from the NW side (Moine/Lewisian gneisses and quartzites), center (Moine quartzites), and SE side (Dalradian quartzites) of the GGF. Additional samples included plutonic rocks from locations adjacent to the GGF and the associated Strathconnon fault that were believed to have been intruded during strike-slip motion, but after regional metamorphism and deformation in the surrounding Moine rocks. Microstructures and quartz c-axis fabrics from samples on the NW side and in the center of the GGF indicate a NW side up to the SW sense of displacement about NE to E plunging slip vectors, and these results are compatible with oblique sinistral motion on the GGF below the brittle-ductile transition zone during Silurian - Early Devonian times. However, radiometric dating is needed to prove the absolute timing of this shearing. In contrast, on the SE side of the GGF, NW side up or NW side down senses of shearing are indicated at different locations. Brittle fracturing is observed in all collected samples, overprinting the earlier high-temperature (300 - 650 °C) crystal fabrics and microstructures developed below the brittle-ductile transition zone. No convincing microstructural evidence for sub-magmatic shearing during pluton emplacement was found in the samples collected. However, the local presence of high-low temperature (c. 650 - 300 °C) solid-state deformation microstructures in both quartz and feldspar grains in these 430 - 425 Ma plutons suggests that the plutons were deforming internally in response to far-field stresses generated by shearing on the adjacent GGF and Strathconnon fault during cooling to background regional temperatures.

Shearing on the Great Glen Fault: Kinematic and Microstructural Evidence Preserved at Different Crustal Levels

Cassandra Becker

GENERAL AUDIENCE ABSTRACT

The Great Glen Fault (GGF) is one of mainland Scotland's most significant large-scale faults, although our understanding of its early motion is debated. Most geologists agree that the GGF began displacing existing rocks during the Silurian (c. 444 - 419 Ma), including igneous bodies, known as plutons, of approximately the same age (c. 425 Ma). Stewart et al. (2001) argued that during shearing, dikes fed by these plutons were deformed before cooling to background temperatures, which may suggest that the GGF was continuously undergoing lateral strike-slip motion by 425 Ma and that post-Silurian offset was likely only a few tens of kilometers. Most plate reconstruction models for the Caledonian mountain belt, now exposed in East Greenland, Scandinavia, and Scotland, assume that significant lateral motion and shearing occurred on the GGF during the Silurian. However, new research has suggested that the GGF was initiated several million years later, bringing current restoration models into question. Several published papers have reported widespread evidence for upper-crustal brittle shearing of crystalline bedrock and overlying Early Devonian (c. 420 - 359 Ma) sedimentary basins within the GGF. However, evidence for lower-crustal shearing during the same time frame, resulting in plastic deformation, is limited. To address this knowledge gap, I collected suites of oriented bedrock samples and 430 - 425 Ma plutonic rocks from locations adjacent to the GGF and associated Strathconnon Fault believed to have been intruded during strike-slip motion. Samples from the NW side and center of the GGF suggest oblique left-lateral motion within the fault zone, with the rocks on the NW side of the GGF moving upward relative to the SE side, compatible with current generally accepted models for the Silurian-Early Devonian age on the GGF; however, these results must be verified with radiometric dating to constrain the absolute timing of shearing. On the SE side of the GGF, vertical offset is variable at different locations. Brittle upper-crustal shearing is observed in all samples, which overprints early high-temperature (300 - 650 °C) deformation. Early lower-crustal shearing on the GGF is recorded by these deformation indicators and was followed by uplift and fracturing within the GGF of these initially lower-crust rocks. The local presence of solid-state deformation microstructures in the plutons suggest internal deformation due to shearing on the adjacent Great Glen and Strathconnon Faults during their cooling to regional background temperatures.

Dedication

I want to acknowledge my advisor, Dr. Rick Law, my committee members, Dr. Mark Caddick and Dr. Jim Spotila, and several others in the Department of Geosciences for their support during my time at Virginia Tech. I would also like to thank Dr. Ryan Thigpen from the University of Kentucky for allowing me to use unpublished maps for this thesis. Thank you to all my friends I made in Blacksburg for always being there for me and helping me when I needed it; I love you all dearly. I would specifically like to acknowledge, in no particular order, Kayla McCabe, Ella Davis, Jonny Prouty, Denise Burgett, David Bunin, Alaina Helm, Alix Ehlers, Carmen Atkins, Cece Wood, Ben Eppinger, Tarisa Ross, Amy Hagen, and Prescott Vayda. Also, I would like to thank my parents, Steve and Debbie Becker, and my sister, Dr. Dianna Souder, for their unconditional love and support during my time at Virginia Tech.

Contents

List of Figures

List of Tables

Chapter 1: Introduction to the Great Glen Fault

Background

The Great Glen Fault (GGF), also commonly referred to as the Great Glen Fault Zone (GGFZ), is one of Scotland's most significant crustal-scale faults (Figs. 1.1 & 1.2). The NE-trending fault zone is thought to have formed during the final stages of the Caledonian orogeny during Late Silurian to early Devonian times and has been periodically active through to the present day.

The GGF separates two terranes of the Caledonian orogen (Fig. 1.1) with markedly different geological histories (see review by Strachan et al. 2002). To the SE of the GGF, the Grampian Terrane (GT) is composed of late Neoproterozoic to Cambrian (~ 800 - 517 Ma) and possibly lowermost Ordovician (c. 470 Ma) metasedimentary rocks (the Dalradian). These rocks were pervasively metamorphosed and deformed during the Ordovician (Grampian) phase of Caledonian orogenesis. To the NW of the GGFZ, the Northern Highlands Terrain (NHT) is composed of Archean gneisses (the Lewisian Complex) and overlying early Neoproterozoic metasedimentary rocks (Moine Supergroup; ~ 1000 - 870 Ma). Lewisian and Moine rocks were pervasively deformed and metamorphosed during the Silurian (Scandian) phase of Caledonian orogenesis. Only limited evidence has been found for earlier phases of Neoproterozoic (Knoydartian) and Grampian age magmatism, deformation, and metamorphism within the NHT. It remains unclear if this lack of evidence for earlier stages of orogenesis is due to their only local development within the NHT or to pervasive overprinting during the Scandian. In contrast, within the Grampian Terrane, no convincing evidence has been found for Neoproterozoic or Scandian age deformation and metamorphism. Both the Grampian and Northern Highlands terranes are intruded by a swarm of late Silurian – early Devonian felsic plutons, often called the 'Newer Granites.'

The contrast in rock types and geologic histories across the Great Glen has historically been taken to indicate significant (tens to hundreds of kilometers) of strike-slip offset on the GGF. Within the Northern Highland and Grampian terranes (Fig. 1.1), there are several prominent NE trending sub-vertical faults referred to as the *'Great Glen set'* and most formed before the deposition of Devonian-age Old Red Sandstone (post-Caledonian sediments) (Mykura 1991; Watson 1984). The *Great Glen set* includes the Strathconnon fault within the NHT which will be referred to later in the thesis.

To the southwest, the GGF (e.g., Kennedy 1946; Holgate 1969; Smith & Watson 1983; Harris 1995) has been linked with the Loch Gruinart-Leannan Fault in Islay and Ireland (Alsop 1992; Pitcher et al. 1964) and potentially in pre-Atlantic opening reconstructions to strike-slip faults of similar age in Newfoundland (Wilson 1962). Additionally, the GGF has been linked to the Walls Boundary Fault, further north in Shetland (Flinn 1961, 1992; McGeary 1989; McBride 1994; Watts et al. 2007; Dewey et al. 2015). Offshore into the Moray Firth, the Great Glen Fault forms a significant near-vertical structure, which can be traced offshore to the NE (23 km) into Mesozoic metasedimentary rocks within the West Moray Firth Basin (Andrews et al. 1990; Bird et al. 1987; Underhill 1991; Underhill and

Brodie 1993; Thomson & Underhill 1993). Based on submarine topography Flinn (1961) proposed that the Great Glen Fault may link with the Walls Boundary Fault. Watts et al. (2007) have highlighted the similarities in the kinematic history of the two faults during the Paleozoic but have also pointed to their significantly different post-Triassic histories (see also Armitage et al. 2021; Searle 2021).

The previously mentioned offshore sub-vertical GGF has been studied using seismic reflection, which demonstrates that it can be traced to a depth of at least 40 km with lamprophyre dikes on both sides of the structure (Hall et al. 1984; McBride 1995). These late Caledonian dikes are mantle-derived, possessing varying isotopic signatures on opposing sides of the fault, suggesting some upper-mantle expression (Canning et al. 1996; 1998). Sinistral lateral displacements along the GGF have historically been recognized as the primary sense of motion, dominating during the Silurian and lowermost Devonian (Stewart et al. 1999). The Great Glen and the Walls Boundary fault systems have also experienced: sinistral displacement and extension during the later Devonian (Séranne, 1992; Dichiarente et al. 2016, 2020); late Carboniferous to Early Permian dextral displacements (Speight & Mitchell, 1979; Coward et al. 1989; Rogers et al. 1989; Kemp et al. 2019; Dichiarente et al. 2020); Permian-to-Mesozoic-aged transtension across the Moray Firth–Pentland Firth-Orkney region (Underhill, 1991; Underhill & Brodie, 1993; Dichiarente et al. 2016); and Paleocene-Eocene dextral oblique faulting during the opening of the Atlantic Ocean (Holgate, 1969; Watts et al., 2007; LeBreton et al. 2013).

Silurian-Devonian shearing on the Great Glen Fault

Main Caledonian sinistral displacements are constrained (c. 430 - 400 Ma) by structural relationships between dated igneous intrusions, post-orogenic sedimentary rocks, and fault zone structures (Stewart et al. 1999; but cf. Searle 2021, 2022; Dewey & Ryan 2022). A component of Silurian displacement is indicated by the 428 ± 2 Ma Clunes Tonalite that outcrops on the NW side of the fault (Fig. 1.3) and was emplaced and sinistrally sheared while still in a sub-magmatic state (Stewart et al. 2001). In contrast, Hutton (1988) has argued that the inner part of the Strontian granite dated at 418 ± 1 Ma (Patterson et al. 1993) was emplaced during dextral displacement on the Great Glen Fault. Early Devonian shearing is recorded in the Rosemarkie Inlier exposed on the Black Isle where Lewisian gneisses and Moine psammites intruded by 398– 400 ± 2 Ma leucogranite veins are all intensely deformed on the NW side of the fault zone with moderately-steeply NE plunging stretching lineations interpreted to be associated with transpression (Mendum and Noble 2010). Several indicators of shearing at mid-crustal levels are present, including deformation textures in leucogranites, syn-shearing mineral assemblages in the Moine pelites, as well as fold geometries and fabrics. The sheared basement rocks of the Rosemarkie Inlier are unconformably overlain by undeformed Old Red Sandstone conglomerates and sandstones of late Eifelian (c. 393 - 387 Ma) age (Marshall et al. 2007), indicating that the inlier has been exhumed from mid-crustal levels within no more than 6 million years (Mendum and Noble 2010).

The Great Glen Fault Zone in mainland Scotland is composed of a belt of cataclastic Moine and Dalradian rocks, measuring up to c. 3 km in width. Fault rocks typically include

(hydrated) cataclasites and phyllonites, although quartz mylonites and blastomylonites are occasionally present (Rathbone & Harris 1980; Stewart 1997; Stewart et al. 1997, 1999, 2000; Mendum & Noble 2010). Macro and micro kinematic indicators in the mylonitic core of the fault zone exposed at Torcastle near Fort William (Fig. 1.4) are consistently sinistrally displaced, with minor downthrow towards the southeast (Stewart et al. 1997, 1999, 2000; see also field guide by Stewart 2010) – although few details were given. Previous studies have reported microstructures in these fault-bounded mylonites to be consistent with deformation in the brittle-ductile transition zone with quartz plastic deformation and recrystallization reported to be by grain boundary migration - but accompanied by brittle deformation of feldspar – indicating shearing at crustal depths of 10-15 km (Stewart et al. 2000; Holdsworth et al. 2001). This mid-lower crustal deformation within the shear zone resulted in the growth of white mica and chlorite, compatible with greenschist facies metamorphism. Most of this shearing appears to have been completed while at mid-crustal levels, with no evidence for overprinting by later, upper-crustal brittle fracturing during uplift (Stewart 2010). Preserved mylonitic rocks in the center of the fault zone may indicate an exhumed positive flower structure, formed during sinistral transpression (Stewart et al. 1999).

Within the Great Glen fault zone, sedimentary rocks in the Old Red Sandstone basins are minimally deformed compared with the underlying metamorphic basement rocks (Stewart et al. 1999; Holdsworth et al. 2001; see also Mykura 1982; Stocker 1982). Late-stage deformation structures in both crystalline basement rocks and the overlying Old Red Sandstone times are strongly brittle, and fault products in individual fault zones are typically incohesive, containing poorly consolidated breccia and clay gouge (May et al. 1997; Stewart et al. 1999).

Magnitude of early displacement on the Great Glen Fault

Although the timing of sinistral motion on the Great Glen Fault is generally considered to be relatively well constrained (but cf. Searle 2021, 2022, Dewey & Ryan 2022), the magnitude of early fault displacement is in question due to the lack of unambiguous geologic markers pre-dating the Devonian that can be correlated across the fault. Kennedy (1946) proposed a sinistral movement of c. 104 km; this was based on various lines of evidence, including the notion that the Strontian and Foyers granites (Fig. 1.1) were once part of a single pluton that was separated into two pieces and displaced by the fault. However, although the two intrusive complexes are of similar age (Strontian 425 ± 3 Ma and 418 ± 1 Ma on outer and inner parts, Rogers & Dunning 1991, Paterson et al. 1993; Foyers 424 ± 4 Ma, Oliver et al. 2008; all zircon ages), differing internal structures (Marston 1971; Munro 1973), trace element content (Pankhurst 1979) and zircon distributions (Pidgeon & Aftalion 1978) suggest these complexes may never have been joint. Winchester (1973 proposed a sinistral offset of 160 km based on the apparent offset of regional metamorphic zones, within the Northern Highland and Grampian terranes on the NW and SE sides of the fault, respectively. Piasecki et al. (1981) argued for a similar displacement based on correlation of the youngest stratigraphic sequences (Glenfinnan and Loch Eil Groups) in the Moine Supergroup of the NHT with the oldest metasedimentary unit (Badenoch Group) recognized in the Grampian Terrane, a correlation supported by

more recent isotopic dating (see review by Krabbendam et al. 2021). Larger displacements are indicated by plate tectonics-based models for the Scandian phase of Caledonian orogenesis that place Baltica close to the NHT, suggesting that at least 500 km of sinistral displacement along the GGF is needed to place Moine of the NHT into its present position with respect to the Dalradian of the Grampian Terrane (Soper et al. 1992; Dewey & Strachan 2003; Dewey et al. 2015; Dalziel & Dewey 2018). Smith and Watson (1983) have argued that the main phase of movement on the Great Glen Fault was pre-Devonian or early Devonian with post-Devonian displacements of less than a few tens of kilometers based on the similarity of lithology and fauna in middle Old Red Sandstone strata on either side of the Great Glen fault (e.g., Donovan & Meyerhoff 1981; Parnell 1982; Mykura & Owens 1983; Rogers et al. 1989). These prevailing views of large-scale Silurian age displacement on the GGF have been challenged by Searle 2021, 2022 who has questioned both the field evidence for initiation of slip during the Silurian (at c. 430 Ma) and reconstruction models that call for large magnitudes of slip, suggesting instead that slip was probably initiated in Lower Devonian times and is of much smaller (although undefined) magnitude.

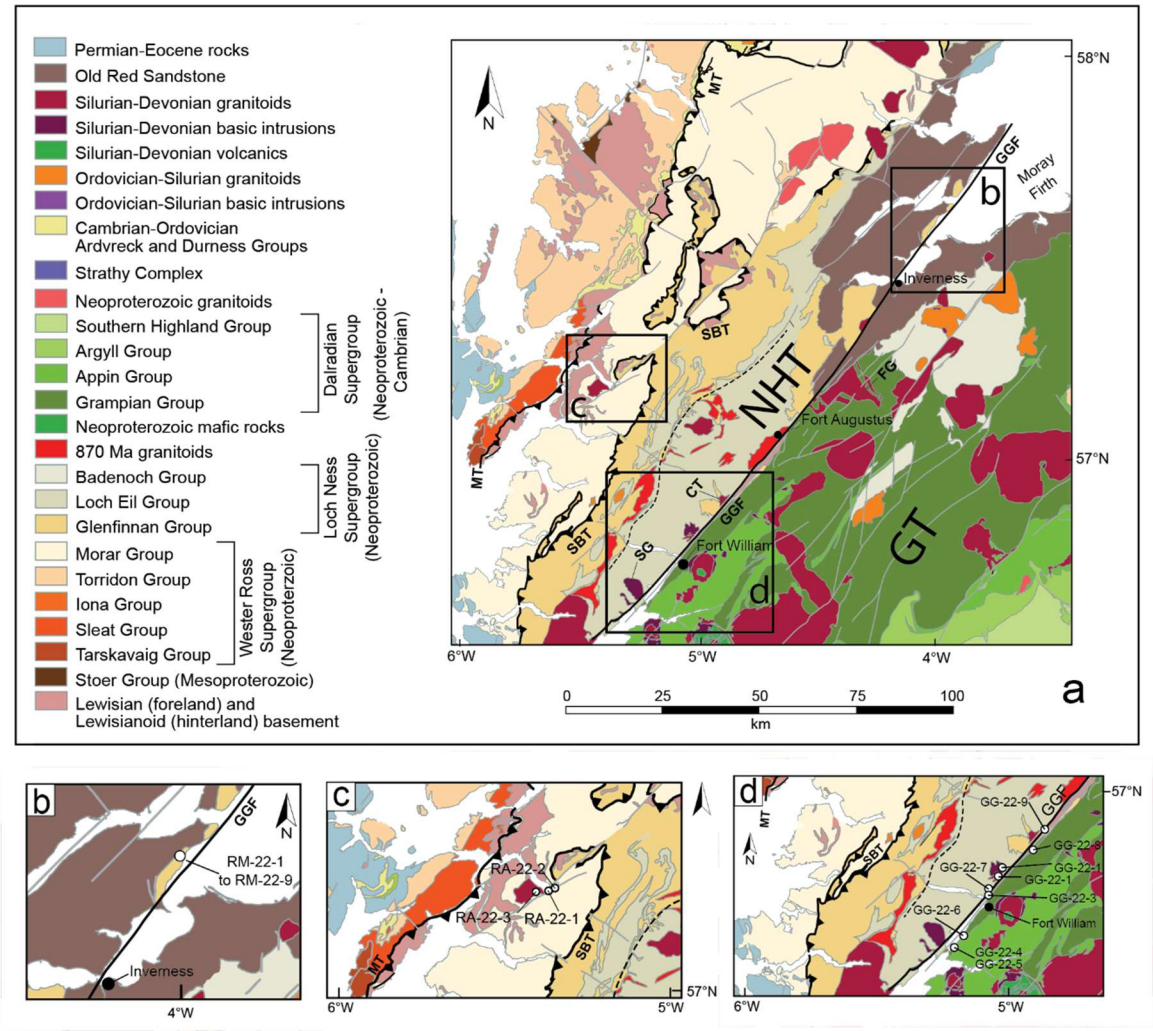

Figure 1.1. **(a)** Geologic map of the part of the Scottish Highlands, with groupings of sample locations indicated by black boxes; modified from Law et al. (in review; Figure 8.2). (*b*) Rosemarkie coastal section, (*c*) Ratagain pluton and Strathconnon Fault. (*d*) Great Glen locations centered on Fort William, Modified from Law et al. (in review; Figure 8.2). NHT = Northern Highlands Terrane, GT = Grampian Terrane, SG = Strontian Granite, CT = Clunes Tonalite, FG = Foyers Granite, GGF = Great Glen Fault, MT = Moine Thrust, SBT = Sgurr Beag Thrust.

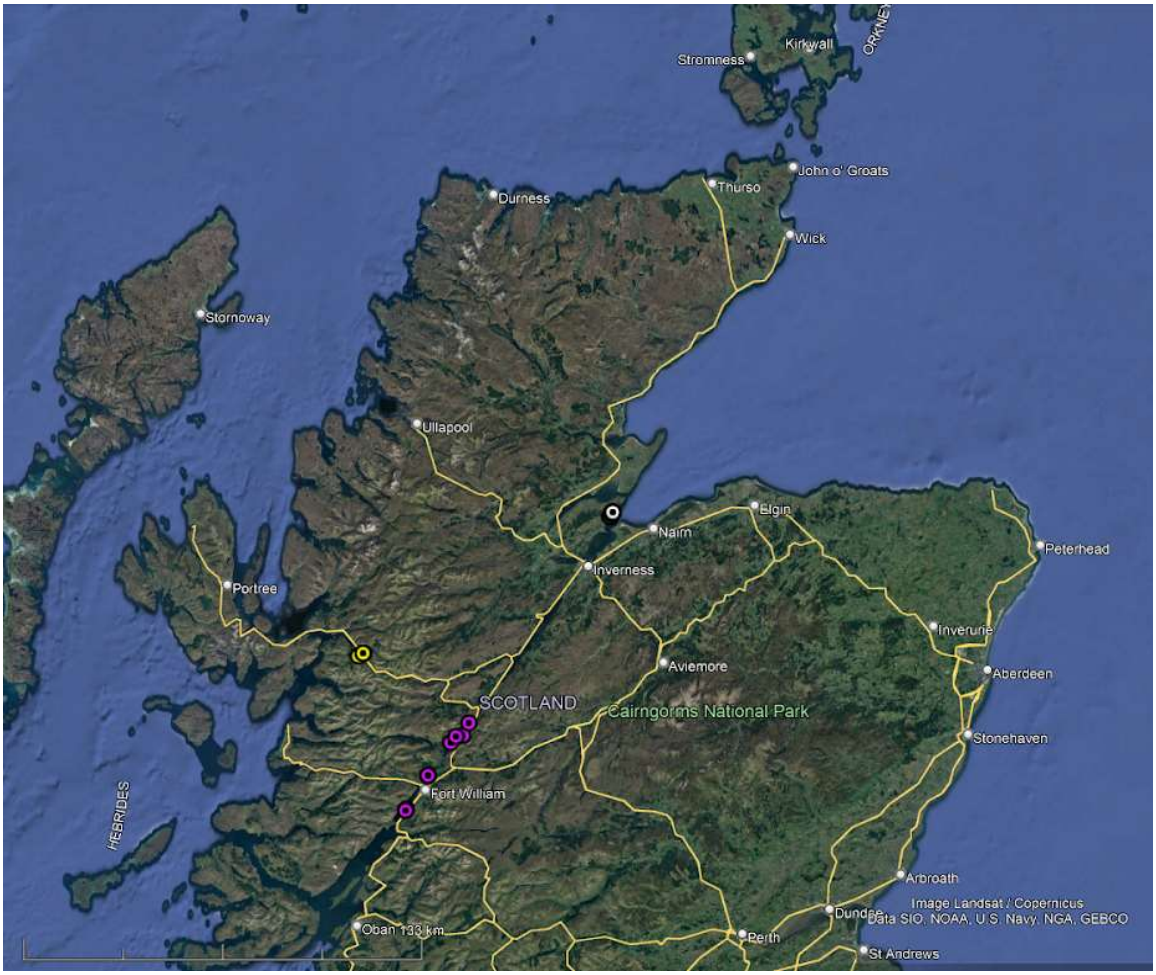

Figure 1.2. Sampling locations. Great Glen (GG) samples near Fort William are indicated by purple circles, a white circle indicates Rosemarkie (RM) coastal section samples, and Ratagain pluton (RA) samples are indicated by yellow circles. Screenshot from Google Earth.

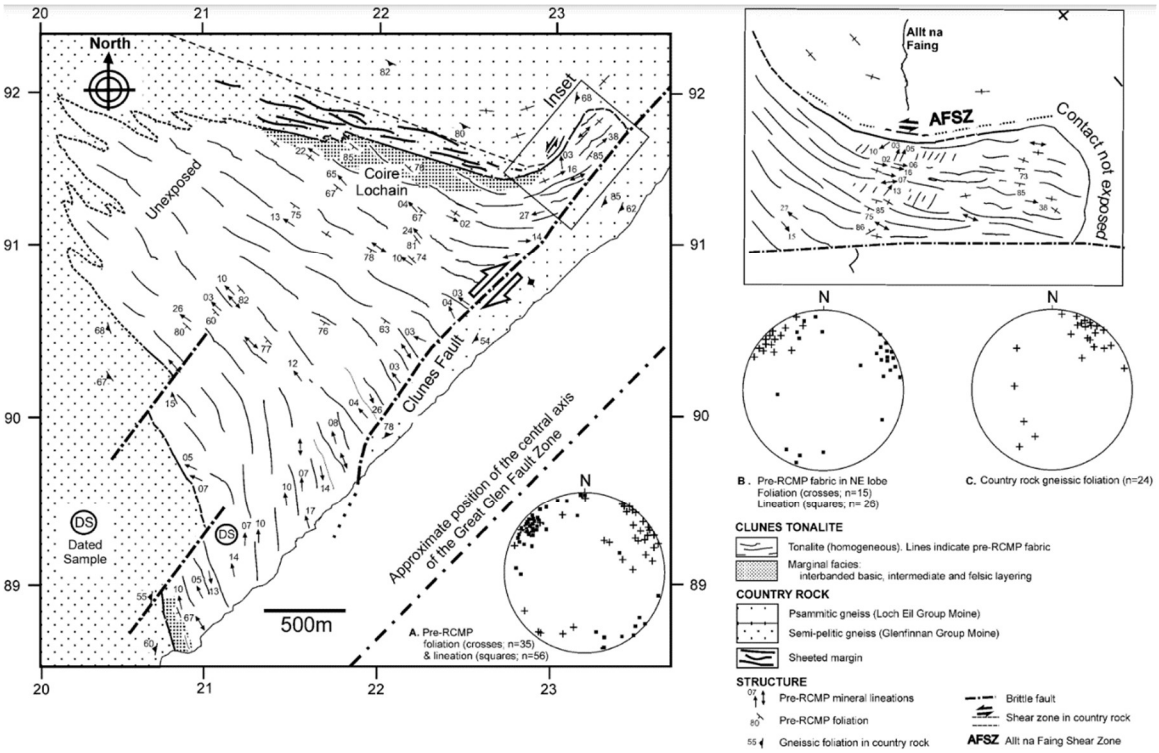

Figure 1.3. Structural map of the Clunes tonalite pluton adjacent to the Great Glen Fault Zone (GGFZ). Figure from Stewart et al. (2001). Figure 2; pg. 823. Fair Use determination attached.

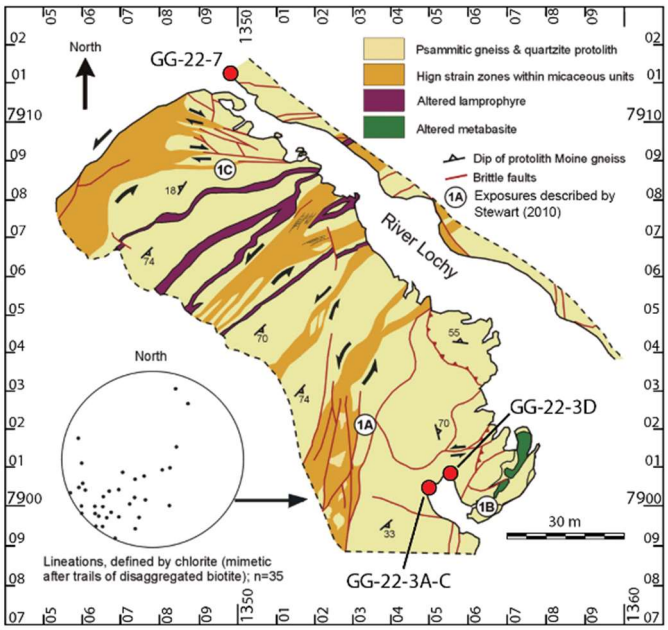

Figure 1.4. Geologic map of the Torcastle North exposures on both sides of River Lochy. Sample locations marked with red circles; UK grid coordinates indicated. Adapted from Stewart (2010). Figure 14.2; pg. 269. Used with permission from the Edinburgh Geological Society; email attached.

Chapter 2. Rosemarkie

Sampling area

The Rosemarkie sampling area is located on the Black Isle at approximately 12 - 20 km to the NNE of Inverness (Figs. 2.1 & 2.2). Crystalline bedrock in the sampling area is only accessible in an 8 km long NE-SW trending set of coastal exposures. Many of these exposures are located between high and low tidal water levels and are only accessible at close to low water times. These coastal exposures are shown on UK Ordnance Survey 1:50,000 scale (Sheets 21 & 27) and 1:25,000 scale (Sheet 432) topographic maps. The geology of the area is summarized on British Geological Survey 1:50,000 scale Sheets 94 and 84 and 84W (British Geological Survey 1958, 1973, 1997).

Geologic maps of the Rosemarkie Inlier have been published by Rathbone & Harris (1980), Highton (2009) and Mendum & Noble (2010). The structural evolution of the Rosemarkie Inlier has been reviewed by Highton (2009) and a field guide to exposures in the northern part of the Rosemarkie Inlier has been provided by Stewart (2010).

Tectonic setting

The Rosemarkie Inlier is one of two inliers of metasedimentary rocks exposed on the east coast of the Black Isle (Fig. 2.1). The Rosemarkie Inlier is the more southerly of these two inliers and is composed of Moine-like psammites and semi-pelites, together with amphibolites and hornblende-bearing gneisses in the northern part of the inlier that may be of Lewisianoid (Archean) affinity (Rathbone & Harris 1980; Highton 2009), although Fletcher et al. (1996) considered it more likely that all these rock types were of Moine affinity. The second inlier, exposed on either side of the Cromarty Firth and usually referred to as the Cromarty Inlier, is dominantly composed of semi-pelitic and psammitic metasedimentary rocks that have tentatively been attributed to the Glenfinnan Group of the Moine Supergroup (Rathbone & Harris 1980). These Inliers mark the most southeastern positioned exposures of Moine metasedimentary rocks in mainland Scotland. They are unconformably overlain on their NW side by the Mid-Devonian Kilmuir Conglomerate and Raddery Sandstone formations (Fletcher et al. 1996). Fossil pollen from this sequence indicates late Eifelian (c. 393 - 387 Ma) deposition of its basal beds (Marshall et al. 2007). Conglomerates, sandstones, and siltstones of interpreted Lower Devonian age are downfaulted against the southwestern margin of the Rosemarkie Inlier. Jurassic mudstones with ammonites are downfaulted against metasedimentary rocks at the northern margin of the inlier.

The Great Glen Fault is mapped as lying immediately offshore to the SE of the Rosemarkie and Cromarty inliers and coming onshore in the poorly exposed ground between Rosemarkie and Fortrose at the southern end of the Rosemarkie Inlier (Figs. 2.1 & 2.2). Offshore of the Rosemarkie Inlier the Great Glen Fault strikes 040° - 220°. Metasedimentary rocks in the southern part of the inlier and exposed between low and high-water marks are intensely fractured at the outcrop-to-hand-sample scale. These water-polished coastal exposures of intensely fractured metasedimentary rocks are the closest

exposures to the Great Glen Fault. In contrast, exposed metasedimentary rocks in the northern section of the inlier are much less intensely fractured, and grain shape fabrics (foliation and lineation) defined by plastically deformed mineral grains (quartz, feldspar, amphibole, mica) are well preserved. Fractures that are present in the northern part of the inlier are usually steeply dipping and oriented at a high angle to the NE-plunging grain shape lineation, and range in scale from individual transgranular fractures observed in thin section to cm to meter scale zones of brecciation and mineral growth between clasts (Fig. 2.3). Fluid flow within these fracture networks is indicated by carbonate veining, fluidized breccia dikes with carbonate matrices and by alkaline metasomatism (fenitization). Garson et al. (1984) have documented similar fracturing and mineralization processes in rocks from both sides of the Great Glen Fault and traced from the Rosemarkie Inlier southwestwards to the Foyers Granite. They suggested that all these fenitization zones that are concentrated along the Great Glen formed contemporaneously during the emplacement of at least one carbonatite structure deep within the Great Glen Fault Zone, likely during Early Devonian (c. 400 Ma) fault displacements. The pervasive fractures that cut the metasedimentary rocks of the Rosemarkie Inlier are not observed in the overlying Devonian sedimentary rocks, suggesting that pervasive fracturing and mineralization on the Great Glen Fault Zone had ceased by at least Middle Devonian times.

Geology of the northern part of the Rosemarkie Inlier

The metasedimentary rocks of the Rosemarkie Inlier are composed of amphibolite facies psammites with secondary semipelites and amphibole-rich mafic rocks, in addition to laminated gneisses of both felsic and mafic lithologies. All these units are cut by pink leucogranite veins and sheets (Fletcher et al. 1996, Mendum & Noble 2010, Rathbone & Harris 1980). The amphibole-rich bodies are concentrated in the northeast part of the inlier. Horne (1923, p. 58) originally suggested that these amphibole-rich bodies may be either a fault-bounded slice of Lewisian basement or a distinct group of Moine rocks exhumed by the GGF. Rathbone & Harris (1980) suggested that the stripped hornblende-rich mafic and felsic gneisses were of Lewisian(oid) affinity. There is no field evidence, however, for either an unconformity or discrete tectonic break between the Moine and these possible Lewisian rocks in the inlier, and Fletcher et al. (1998) regarded all these rock units as being of Moine affinity. It must be kept in mind, however, that all these rocks are highly strained (Rathbone & Harris 1980) and original contact relationships may now be obscured (Highton 2009).

Four phases of deformation within the Rosemarkie Inlier have been recognized (Rathbone & Harris 1980). The principal planar fabric observed in all outcrops is a composite S1/S2 grain shape foliation oriented parallel to compositional banding that presumably reflects original bedding in the metasedimentary rocks. This foliation strikes NE-SW sub-parallel to the off-shore trace of the Great Glen Fault and, at least in the northern part of the Inlier, dips steeply to the SE. Tight to isoclinal folds observed in individual outcrops are attributed to D2 (Mendum & Noble 2010). The S1/S2 foliation contains a strongly developed grain shape lineation (L2) that plunges gently to moderately towards the NE to ENE (Fig. 2.4). At some locations in the northern part of the Inlier, the S1/S2 foliation is folded about open-tight F3 folds with sub-vertical axial planes. F3 folds verge towards the SE (Mendum &

Noble 2010) and F3 fold hinges plunge towards the NE-ENE usually parallel to L2 mineral lineations. F4 folds also have sub-vertical axial planes but verge towards the NW (Mendum & Noble 2010). F4 fold hinges also plunge towards the NE-ENE parallel to L2 mineral lineations. Interference between F3 and F4 folds locally leads to formation of spectacular Type 3 fold interference patterns observed on joint faces oriented perpendicular to the NE-ENE plunging mineral lineations (Mendum & Noble 2010, their Fig. 3b).

Numerous veins, lenses and sheets of red-pink microgranite and granitic pegmatite cut the metamorphic rocks in the Rosemarkie Inlier. They occur as sharply bounded steeply dipping intrusions that range in thickness from less than 1 cm up to 5 m and are usually concordant or subconcordant to the NE-SW striking S1/S2 grain shape foliation. In a few outcrops these intrusive bodies cut across the S1/S2 grain shape foliation (see review by Highton 2009). Mendum & Noble (2010) refer to all these intrusive bodies as leucogranites. The leucogranites frequently display 'pinch and swell' boudinage structures in NE-SW trending strike-parallel exposures and less commonly in NW-SE trending dip-parallel exposures.

The leucogranite intrusive bodies are commonly pervasively sheared and contain internal grain shape fabrics (Fig. 2.5) that are typically parallel to the margins of the NE-SW striking planar intrusions, with sub-horizontal (NE-SW trending) to gently plunging mineral lineations on the margins of the intrusions. These linear fabric elements in the leucogranite sheets are typically sub-parallel to lineations in the surrounding gneissic metasedimentary rocks (Mendum & Noble 2010; their fig. 4). Grain shape fabrics within the leucogranites are defined by ribbons of quartz and feldspar (Mendum & Noble 2010). Quartz ribbons have clearly deformed by crystal plastic flow and dynamic recrystallization while many of the feldspar 'ribbons' may be trails of intensely fractured and fine-grained clasts. Larger feldspar grains remain as augen or porphyroclasts around which these ribbons anastomose, while some of the smaller feldspar grains appear to have crystallized during on-going penetrative deformation. Mendum & Noble (2010) regarded these microstructures as indicating strong penetrative deformation of the leucogranites under amphibolite facies conditions. In horizontal exposure surfaces feldspar augen/porphyroclasts (typically less than 1 cm in size) often have sigma or delta shaped tails of fine-grained quartz and feldspar indicating a local shear sense while in other cases the tails have a neutral geometry (Mendum & Noble 2010; Stewart 2010). Spectacular photographs of water-worn and polished horizontal exposure surfaces of a leucogranite containing asymmetric feldspar augen with sigma-shaped tails indicating a sinistral shear sense have been reported by Stewart (2010).

Isotopic dating of leucogranites and exhumation of the Rosemarkie Inlier

Mendum and Noble (2010) carried out isotopic dating analyses from the Rosemarkie Inlier on samples from two leucogranite intrusions and two samples from their surrounding metasedimentary rocks (hornblende-biotite gneisses). Zircon U-Pb data obtained by LA-MC-ICP-MS (laser ablation multi-collector inductively coupled plasma mass spectrometry) analyses from two hornblende-biotite gneisses clearly indicated a Lewisianoid affinity, with protolith ages ranging from c. 2930 Ma to 2810 Ma. It remains

unclear if these Archean ages relate to bedrock that may have been eroded to supply zircon clasts that were subsequently deposited in younger sediments (e.g., Neoproterozoic Moine rocks) or if they relate to zircon crystallization during metamorphism of the enclosing sedimentary rocks. U-Pb TIMS (thermal ionization mass spectrometry) zircon and monazite ages of 400.8 ± 2.6 Ma and 397.6 ± 2.2 Ma, respectively, were determined from the two leucogranite samples indicating a Lower Devonian (late Emsian) age for emplacement. Xenocrysts of Lewisian age zircon were also found in the leucogranite samples.

Deformation microstructures in the leucogranites, together with metamorphic mineral assemblages and fold geometries in the surrounding metasedimentary rocks are all indicative of mid-crustal conditions. Given that the crystalline rocks of the Rosemarkie Inlier are unconformably overlain by Devonian conglomerates and sandstones of late Eifelian age (Marshall et al. 2007; c. 393 Ma), this led Mendum & Noble (2010) to suggest that the metamorphic rocks of the Inlier had been exhumed from mid-crustal levels (minimum component of 12 - 15 km of vertical uplift) within a maximum of 6 million years. Mendum and Noble (2010) proposed that the Inlier had been exhumed as a 'pip within the Great Glen Fault Zone during oblique sinistral transpression and shearing parallel to the NE-NNE plunging grain shape lineation. However, while the timing and kinematics of shearing within the leucogranites have now been established, no comparable data sets were available for the metasedimentary rocks surrounding the leucogranites.

Rock sample locations, petrology, and microstructures

Nine oriented rock samples were collected from the northern segment of the Rosemarkie Inlier (Table 2.1). The map positions of these samples are shown in Figures 2.1 and 2.2, together with the locations of the leucogranite and metasedimentary rock samples isotopically dated by Mendum & Noble (2010). Eight of these samples are metasedimentary rocks, while one sample (RM-22-3) was collected from the center of a leucogranite sheet. Slabs for all samples were cut parallel to lineation and perpendicular to foliation. Foliation in all samples strikes NE-SW and dips steeply to the SE, while grain shape lineation on the foliation plunges gently-moderately (0° - 52°) to NE-ENE in these samples with sub-horizontal – gentle plunges in the more northerly sampling locations and steeper plunges in the more southerly sample locations (Table 2.1; Fig. 2.4). Oriented thin sections were prepared for all the metasedimentary rock samples. However, due to its fragile nature (and the rock saws available in the Virginia Tech Department of Geosciences) a rock billet and thin section were not prepared from the slab cut from leucogranite RM-22-3.

Leucogranite sample RM-22-3 (Fig. 2.5) was collected from the same NE-SW striking and steeply SE dipping leucogranite sheet as originally described by Stewart (2010) in his field guide to the Rosemarkie Inlier. This leucogranite sheet is located 1.25 km to the NE of the similarly oriented leucogranite sheets used by Mendum & Noble (2010) for isotopic dating – see above. The leucogranite sheet strikes parallel to gneissic foliation in the surrounding metasedimentary rocks. A grain shape lineation on the foliation surface of sample RM-22-3 pitches at 18° from the 070° strike direction, giving a lineation plunge of c. 16° towards

078°. This angle of lineation plunge is very similar to lineation plunge in the nearest metasedimentary rock samples (17° in sample RM-22-9 and 24 - 29° in sample RM-22-2), although the trend of the leucogranite lineation in RM-22-3 is more to the ENE while lineation in the metasedimentary rocks plunges closer to the NE (Fig. 2.4). In his field guide Stewart (2010, his Fig. 14.5) described asymmetric orthoclase feldspar porphyroclasts and shear bands from the leucogranite sheet and exposed on a geographically horizontal wave-polished erosion surface that viewed vertically downwards indicate a sinistral shear sense. Preparation of oriented and polished slabs from sample RM-22-3 has confirmed the observations and sinistral shear sense interpretation of Stewart (2010) and has revealed the presence of asymmetric feldspar porphyroclasts with sigma shaped wings composed of ribbons of comminuted (minutely fractured) pink feldspar and white-glassy plastically deformed quartz (Fig. 2.5).

Sample RM-22-8 is a biotite-feldspar-garnet gneiss with brick-red pleochroic biotite laths and elongate (500 x 300 micron) plagioclase and orthoclase grains defining the grain shape foliation (Fig. 2.6). Quartz probably makes up less than 5% of the rock. Both feldspar and the rare quartz grains have recrystallized by grain boundary migration (GBM). No microstructural evidence for preserved shear senses was found.

Samples RM-22-1, 2, 4, 6 & 9 (Figs. 2.7 – 2.13) are amphibole-rich gneisses composed of elongate laths of amphibole interlayered with recrystallized feldspar (plagioclase and orthoclase) and variable (but always very minor) amounts of quartz. This interlayering of amphibole and feldspar defines the grain shape foliation. The amphibole laths are pleochroic pale green to slightly bluish in color in plane polarized light and range from 2mm (2000 microns) to 4 mm (4000 microns) in length and 0.3 mm (300 microns) to 0.5 mm (500 microns) in width. The amphibole laths are presumably of hornblendic composition and are all remarkably fresh in thin sections with no signs of chemical retrogression. In some foliation parallel domains, the amphibole laths have a ‘shredded’ appearance due to localized shearing, but no obvious retrogression is observed suggesting that shearing did not occur in the presence of grain boundary fluids. Plagioclase and orthoclase grains are equant to elongate in shape with the larger grains commonly measuring 550 microns x 200 microns. Internally the plagioclase grains often display undulose extinction and tapering deformation twins indicating that they have deformed plastically. Grain boundary microstructures between adjacent feldspar grains suggests that the feldspar grains have recrystallized by GBM. No convincing microstructural shear sense indicators were found in any of these amphibole-rich gneisses. Planar extensional fractures oriented at a high angle to foliation (and lineation) with no obvious fracture-parallel offset of the grain shape foliation were recorded in thin sections from several of these gneisses and are particularly strongly developed in sample RM-22-1.

Samples RM-22-5 and RM-22-7 are quartz-rich gneisses containing smaller total amounts of feldspar (both orthoclase and plagioclase) and elongate grains (or laths) of white mica (Fig. 2.14E). Skeletal garnet is also present in sample RM-22-7. Grain shape foliation is defined by ribbon like domains of quartz and felspar, with the two minerals usually forming separate ribbons, and often separated by elongate while mica grains. Quartz ribbons are locally formed of either single grains or multiple recrystallized grains. These single and

multi-grain quartz ribbons are up to 1.1 mm (1100 microns) in length x 0.5 mm (500 microns) in width. Feldspar-ribbons are always made up of multiple feldspar grains and are up to 5–10 mm (5000 - 10,000 microns) in length x 0.5 mm (500 microns) in width in sample RM-22-7 but are smaller in sample RM-22-5. Individual feldspar grains in these ribbons are up to 500 microns in size. Asymmetric development of myrmekite patches (Fig. 2.14D; referred to as *quarter structures* – see review by Passchier & Trouw 2005, p. 150) on the edges of one of the largest rhomb-like orthoclase grains in sample RM-22-7 indicates a sinistral shear sense (NW side up to the SW / SE side down to the NE) viewed geographically downwards on the XZ thin section. This shear sense is confirmed by the geometry of asymmetric white-mica fish in sample RM-22-7 (Fig. 14E) using the geometric criteria reviewed by ten Grotenhuis et al. (2003) and Passchier & Trouw (2005, p. 142).

Quartz and feldspar grains have dynamically recrystallized by GBM and internally display a range of microstructures (undulatory extinction, tilt walls and locally blocky extinction; Figs. 2.6 - 2.14) indicating high-temperature deformation. Crystal plastic deformation of feldspar by dislocation creep (as is indicated by these microstructures) is only observed in naturally deformed rocks deformed under upper amphibolite or higher conditions (see review by Tullis 2002). Fazio et al. (2020) have estimated a minimum temperature of c. 675 °C for the onset of GBM recrystallization of feldspar in a study of forceful emplacement of a high-temperature pluton and resultant contact metamorphism and straining of wall rocks in southern Italy. Minimum temperatures for onset of recrystallization by GBM in quartz is usually assumed to be in the c. 490 - 530 °C range (see review by Law 2014). However, although the majority of microstructures, such as large scale (100s of microns) gently curving quartz and feldspar grain boundaries in samples RM-22-5 & 7 indicate recrystallization by high-temperature GBM, much smaller (20 - 40 micron) and localized bulges between adjacent feldspar and quartz grains in sample RM-22-5 indicate later and lower temperatures of at least incipient recrystallization of feldspar and quartz by grain boundary bulging (GBB), probably within the temperature ranges of 450 - 550 °C for feldspar (Passchier & Trouw 2005, p. 260; Fazio et al. 2020) and 300 - 400 °C for quartz (see review by Law et al. 2014). This all suggests that a range of feldspar and quartz microstructures have been *'frozen in'* during cooling and exhumation of the Rosemarkie rocks.

Quartz crystal fabrics from Samples RM-22-5 and RM-22-7 and their tectonic significance

The c-axis fabric of 1000 dynamically recrystallized quartz were measured in (XZ) thin sections using a Leitz optical microscope and 4-axis universal-stage, where each sample was cut parallel to the ENE plunging mineral lineation and perpendicular to foliation. S. Mulcahy (Western Washington University) developed an Excel macro that was used to collect universal stage data. N. Mancktelow (ETH, Zurich) created the Stereoplot software used to contour these fabrics. The quartz c-axis fabric data are displayed on a lower hemisphere equal-area projection in which the data have been rotated into a XZ projection plane viewed geographically downwards towards the SW (Figs. 2.15 - 2.17). Both samples are characterized by asymmetric cross-girdle c-axis fabrics that intersect macroscopic

foliation at right angles to the mineral lineation direction (Fig. 2.15), demonstrating that the lineation has developed parallel to the maximum principal stretch (X). Sample RM-22-5 was collected at no more than 100 m (see location map in Fig. 2.1) from the metasedimentary rocks and leucogranite sheets used by Mendum & Noble (2010) for isotopic dating of zircon and monazite grains. Sample RM-22-7 was collected at no more than 150 m from the leucogranite sheet described by Stewart (2010) and from which sample RM-22-3 was collected (Fig. 2.1).

Sample RM-22-5 yields a transitional Type I to Type II (Lister 1977) cross-girdle fabric (Fig. 2.16a & b) in which an approximate small circle distribution of c-axes about the foliation pole (Z) is connected by a partial great circle of c-axes passing through the sample Y direction at right angles to lineation (X). Measured in the XZ plane the C1 and C2 angles between the foliation pole and the cross-girdle fabric are unequal and indicate a sinistral shear sense, with the *leading edge* of the cross-girdle fabric making a C1 angle of 31° with the foliation pole while the *trailing edge* makes an angle of 36°. The sinistral shear sense indicated by the asymmetric c-axis fabric is consistent with a NW side up to the SW and SE side down to the NE sense of motion associated with the NE to ENE plunging mineral lineation (Fig. 2.16c & d). The opening angle (C1+C2) of the cross-girdle c-axis fabric from sample RM-22-5 indicates a deformation temperature of c. 510 °C using the linear opening angle thermometer of Faleiros et al. (2016). This inferred deformation temperature is significantly lower than the likely deformation temperature range (> 675 °C) indicated by feldspar GBM microstructures in sample RM-22-5, possibly indicating that the quartz c-axis fabric continued to evolve during cooling/exhumation with the now preserved quartz fabric reflecting only the later and cooler stages of deformation. This interpretation is consistent with the grain boundary bulging microstructures observed at the margins of some feldspar and quartz grains which indicate temperatures of less than c. 450-500 °C (see above). However pervasive shearing is unlikely to have continued significantly below c. 500 °C as the feldspar grains remain unfractured and there is no microstructural evidence for subgrain rotation recrystallization (SGR) of quartz which in nature occurs in the c. 400 - 500 °C range (see review by Law et al. 2014).

Sample RM-22-7 yields an asymmetric Type II (Lister 1977) cross-girdle fabric (Fig. 2.17a & b) formed by two planar (great circle) distributions of c-axes crossing each other close to the sample Y direction. The C1 (36°) and C2 (45°) angles between the foliation pole and the *leading* and *trailing edges* of the cross-girdle fabric indicate – as with sample RM-22-5 - a sinistral shear sense Fig. 2.16c & d). As noted above, this shear sense is also indicated by asymmetric white mica fish in RM-22-7 (Fig. 2.14E). Once again, this sinistral shear sense is consistent with a NW side up to the SW and SE side down to the NE sense of motion, but in sample RM-22-7 is associated with shearing parallel to a more steeply ENE plunging lineation. The opening angle (81°) in sample RM-22-7 is significantly larger than in RM-22-5, indicating a deformation temperature of c. 610 °C using the linear opening angle thermometer of Faleiros et al. (2016). This higher deformation temperature suggests that a greater portion of the early higher temperature history is preserved in sample RM-22-7 than in RM-22-5, although the kinematics for the two samples are very similar.

For a geothermal gradient of ~ 30°C per km (as assumed by Holdsworth et al. 2001 in their paper on shearing in the Great Glen Fault Zone), the 610 °C deformation temperature estimated for sample RM-22-7 would correspond to a crustal depth of ~ 20 km. Assuming that the fabrics in the Rosemarkie Inlier rocks did develop within the Great Glen Fault Zone and were exhumed by oblique sinistral shearing parallel to the NE-ENE plunging mineral lineation, then adopting the inclined transpression model for the Rosemarkie Inlier by Mendum & Noble (2010) which included an average plunge of 37° for the lineation, exhumation to the topographic surface from a depth of 20 km would require a horizontal displacement component of approximately 27 km.

Age of sinistral shearing in the Rosemarkie Inlier

Emplacement of the leucogranite sheets isotopically dated at 401 - 398 ± 2 Ma by Mendum and Noble (2010) using zircon and monazite is clearly of Lower Devonian age and their oblique sinistral shearing cannot be significantly younger given the unconformably overlying Middle Devonian (393 - 387 Ma) sedimentary rocks. However, although the kinematic framework for shearing of the surrounding amphibolite facies metasedimentary rocks appears to be very similar to that of the leucogranite sheets, direct isotopic dating of oblique sinistral shearing in the metasedimentary rocks remains to be achieved. This is important because it has not yet been unequivocally demonstrated that the deformation fabrics in the Rosemarkie metasedimentary rocks developed during on-going shearing in the Great Glen Fault Zone, rather than being an older fabric that predates formation of the GGFZ and has been rolled over into the GGFZ as the GGFZ began to form. In the Moine metasedimentary rocks to the west of the Rosemarkie Inlier top to the north shearing, probably at c. 450 - 440 Ma, is indicated by microstructural and quartz fabric data in the eastern part of the Northern Highland Terrane (Law et al. 2021). Passively rotating this fabric over to a steep SE dip within the NE-SW trending GGFZ in Late Silurian - Lower Devonian times would produce an apparent oblique sinistral shear sense with a NW side up to the SW and SE side down to the NE sense of motion – as is found in the Rosemarkie Inlier. Therefore, to demonstrate that these deformation fabrics in the Rosemarkie metasedimentary rocks did form during shearing on the GGFZ, their age of formation needs to be determined. If they are of late Silurian –early Devonian age (younger than say 420 Ma) it seems most probable that they did form within the GGFZ. If isotopic ages >420 Ma are found, then it is more likely that they are pre-existing deformation fabrics that have later been caught up in the GGFZ.

Dr. Calvin Mako (Arizona Geological Survey) has examined the thin sections cut from samples RM-22-1 to 9 and has identified four samples that have potential for isotopic dating. From highest to lowest potential these are: RM-22-8 (monazite); RM-22-6 (titanite and apatite); RM-22-9 (titanite) and RM-22-4 (apatite). Microprobe thin sections have been prepared from these samples and will be sent to University of California at Santa Barbara for LA-ICPMS dating.

Chapter Two - Table

Table 2.1. Location and grain shape fabric details for samples collected.

Sample #	Study Area	UK Grid Coordinates	Foliation	Lineation	Quartz c-axis Fabric?	Notes
GG-22-1	Clunes tonalite	NN 23210 91492		36>279		
GG-22-2	Clunes tonalite	NN 21411 89537		14>161		
GG-22-3A	Torcastle North	NN 13561 78983	060/75/SE			
GG-22-3B	Torcastle North	NN 13561 78983	060/75/SE			
GG-22-3C	Torcastle North	NN 13561 78983	060/75/SE			
GG-22-3D	Torcastle North	NN 13561 78983	060/75/SE	65>098	Fig. 5.9	
GG-22-7	Torcastle North	NN 13496 79124				
GG-22-4	Dalradian south of Fort William	NN 05610 67789	060/70/SE	65>098	Fig. X	
GG-22-5	Devonian(?) south of Fort William	NN 05610 67789	044/84/SE			Adjacent to loch
GG-22-6	Dalradian south of Fort William	NN 05941 68327	050/75/SE			Quartzite
GG-22-6A	Dalradian south of Fort William	NN 05941 68327	050/75/SE	74>121	Fig. 6.6	Quartzite
GG-22-8	Dalradian SE side of Loch Lochy	NN 25465 91800				
GG-22-9	Glen Garry Vein Complex	NN 27658 95804				Kilfinnan Burn
RA-22-1	Ratagain Pluton	NG 93995 19863				
RA-22-2	Ratagain Pluton	NG 94226 19862	092/24/S			
RA-22-3	Ratagain Pluton	NG 92448 19010				
RM-22-1A	Rosemarkie Inlier	NH 77278 62764	056/80/S	00>056		
RM-22-1B	Rosemarkie Inlier	NH 77268 62764	056/80/S	00>056		
RM-22-2A	Rosemarkie Inlier	NH 77268 62771	056/80/S	29>062		
RM-22-2B	Rosemarkie Inlier	NH 77268 62771	056/80/S	24>060		
RM-22-3	Rosemarkie Inlier	NH 77256 62749	070/64/SE	16>078		Sheared granite vein
RM-22-4	Rosemarkie Inlier	NH 76351 61381	056/76/SE	35>069		
RM-22-5	Rosemarkie Inlier	NH 76453 61493	042/85/SE	31>045	Fig. 2.16	
RM-22-6	Rosemarkie Inlier	NH 76792 62016	045/60/SE	36>068		
RM-22-7	Rosemarkie Inlier	NH 77103 62561	044/76/SE	51>064	Fig. 2.7	
RM-22-8	Rosemarkie Inlier	NH 77103 62561	044/76/SE	36>056		
RM-22-9	Rosemarkie Inlier	NH 77240 62723	054/70/SE	17>061		

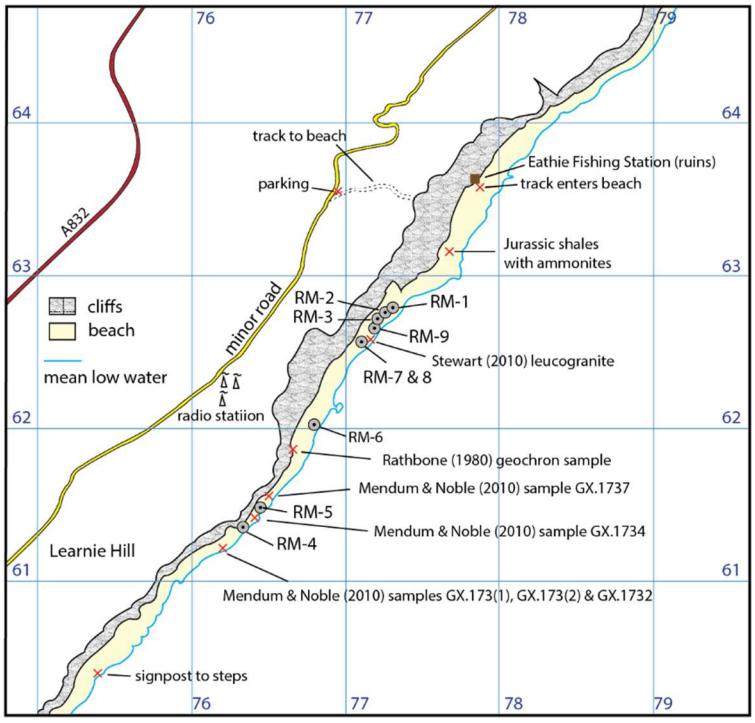

Figure 2.1. Sample locations on the northern part of the Rosemarkie coastal section.

Figure 2.2. Rosemarkie coastal section with sample locations (RM-22-1 - RM-22-9) indicated with white circles. Screenshot is taken from Google Earth.

Figure 2.3. Fault zone in the Rosemarkie Inlier containing clasts of brecciated Moine or Lewisian gneisses with sparry calcite filling original fracture porosity.

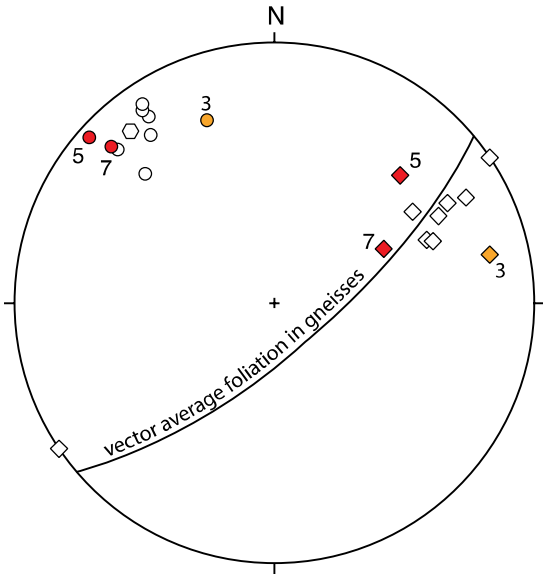

◇ Lineations in Rosemarkie samples

○ Poles to foliation in Rosemarkie samples

⬡ Vector average pole to foliation in gneisses

Figure 2.4. Grain shape fabric data for samples collected at Rosemarkie. Diamonds indicate the orientation of linear fabric elements, and in samples RM-22-5 and RM-22-7, quartz c-axis fabrics unequivocally demonstrate that these lineations are parallel to the maximum principal stretch direction (X). Sample RM-22-3 is from a sheared leucogranite sheet. Poles to grain shape foliation indicated by circles. Calculated vector average orientation of foliation in the gneissic metasedimentary rocks (but not including the sheared leucogranite sheet) is indicated.

Figure 2.5. Polished slabs of sheared leucogranite sample RM-22-3. Note rigid pink feldspar porphyroclasts around which ribbons of plastically deformed quartz and trails of comminuted feldspar fragments anastomose. Slabs cut perpendicular to mylonitic foliation and parallel to geographic horizontal.

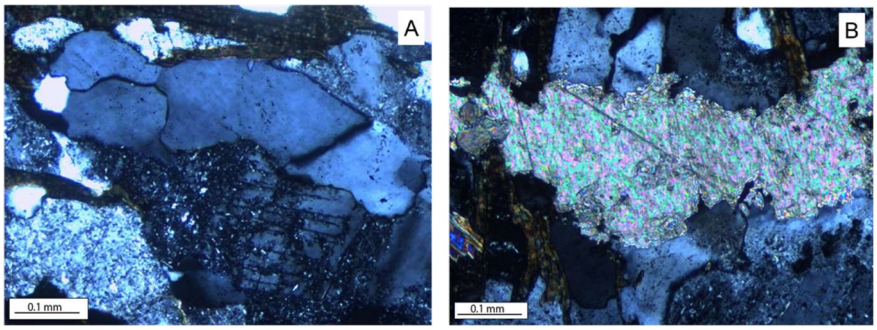

Figure 2.6. Micrographs from sample RM-22-8 containing calcite plates and microstructural evidence for plastic deformation in quartz and feldspar grains (120° grain boundaries indicating grain boundary migration). Note sericitization in feldspar grain.

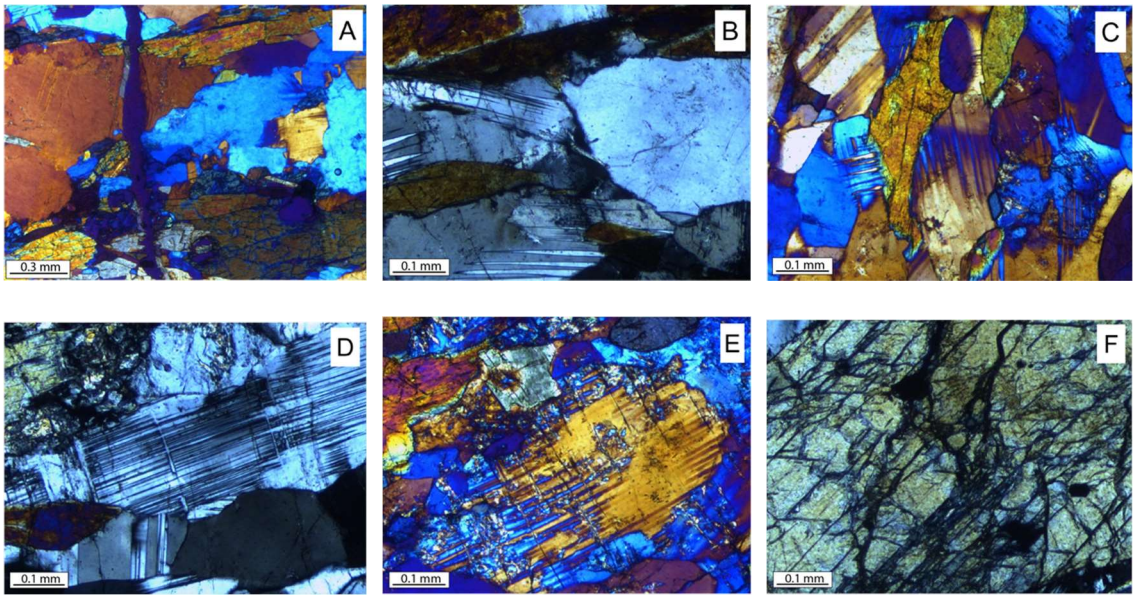

Figure 2.7. Micrographs from sample RM-22-1A contain microstructures that indicate high-temperature plastic deformation in quartz and feldspar grains. Note tapering deformation twins in plagioclase grains, lobate boundaries between quartz and feldspar grains, undulose extinction in both quartz and feldspar grains. Also note minor degrees of sericitization of feldspar grains and intense fracturing of amphibole grain.

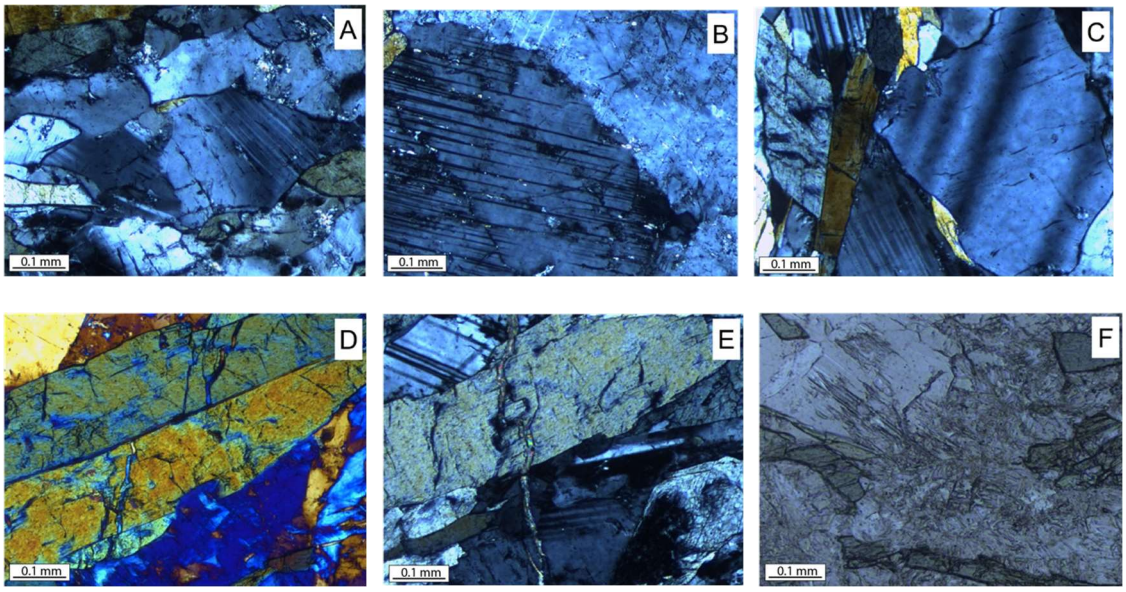

Figure 2.8. Micrographs from sample RM-22-1B contain microstructures that indicate plastic deformation overprinted by brittle deformation. Plastic deformation microstructures include deformation bands and micro-folding in quartz and feldspar grains, tapering deformation twins in plagioclase grains and sinuous boundaries between quartz and feldspar grain indicating grain boundary migration. Note growth twins and extension fractures filled with mica in amphibole grains and sericitization of feldspar.

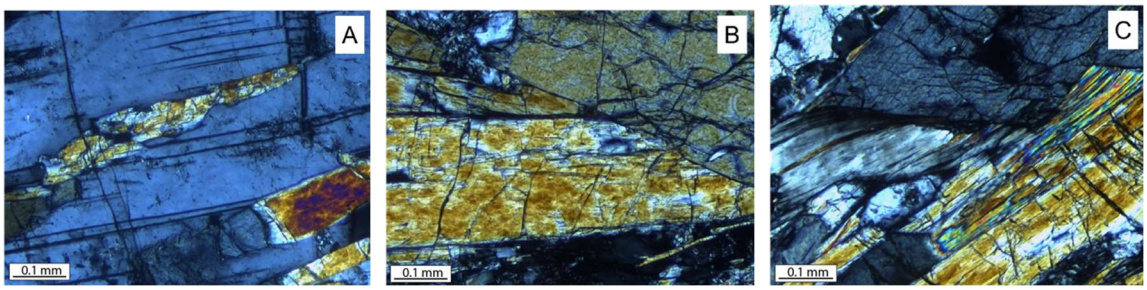

Figure 2.9. Micrographs from sample RM-22-2A contain microstructures that indicate plastic deformation (tapering deformation twins in plagioclase grain) overprinted by brittle deformation (extension microfracture filled with white mica in plagioclase grain, network of extension fractures cutting amphibole grains that in some cases that do not terminate at amphibole grain boundaries.

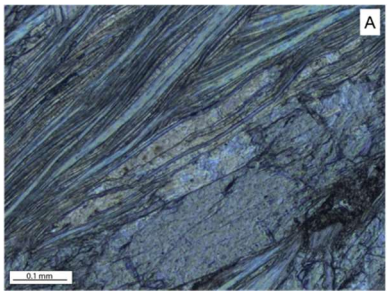

Figure 2.10. Braided white mica and amphibole grains from sample RM-22-2B, indicating penetrative shearing during plastic deformation.

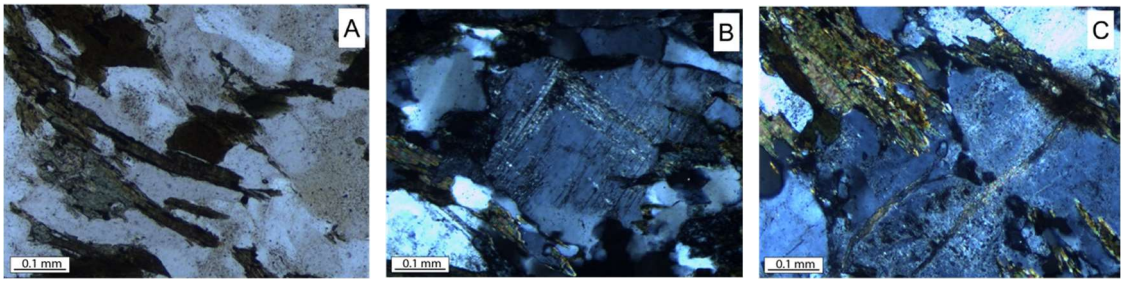

Figure 2.11. Micrographs from sample RM-22-4 containing chlorite and biotite overgrowths, as well as calcite veins that do not terminate at grain boundaries.

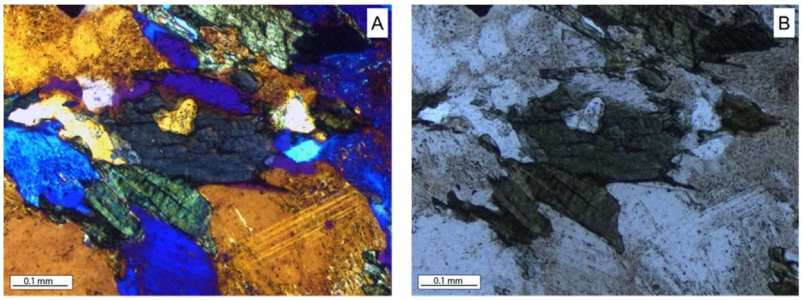

Figure 2.12. Micrographs from sample RM-22-6 containing chlorite that has grown along boundaries between feldspar grains. Note minor sericitization in feldspar grains.

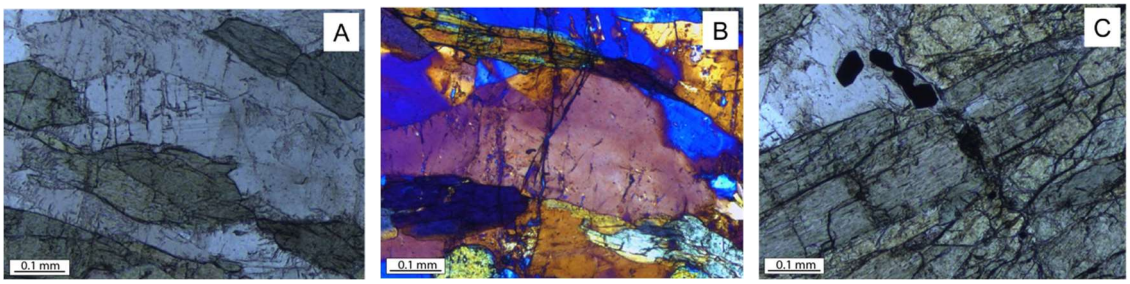

Figure 2.13. Micrographs from sample RM-22-9, containing evidence for high temperature mid-crustal plastic deformation overprinted by brittle deformation during exhumation. Microstructures include undulose extinction and deformation bands in quartz grains, alignment of quartz and elongate amphibole grains and fracturing of amphibole grains. Some fractures terminate at amphibole grain boundaries, and others are infilled with fine-grained mineral deposits.

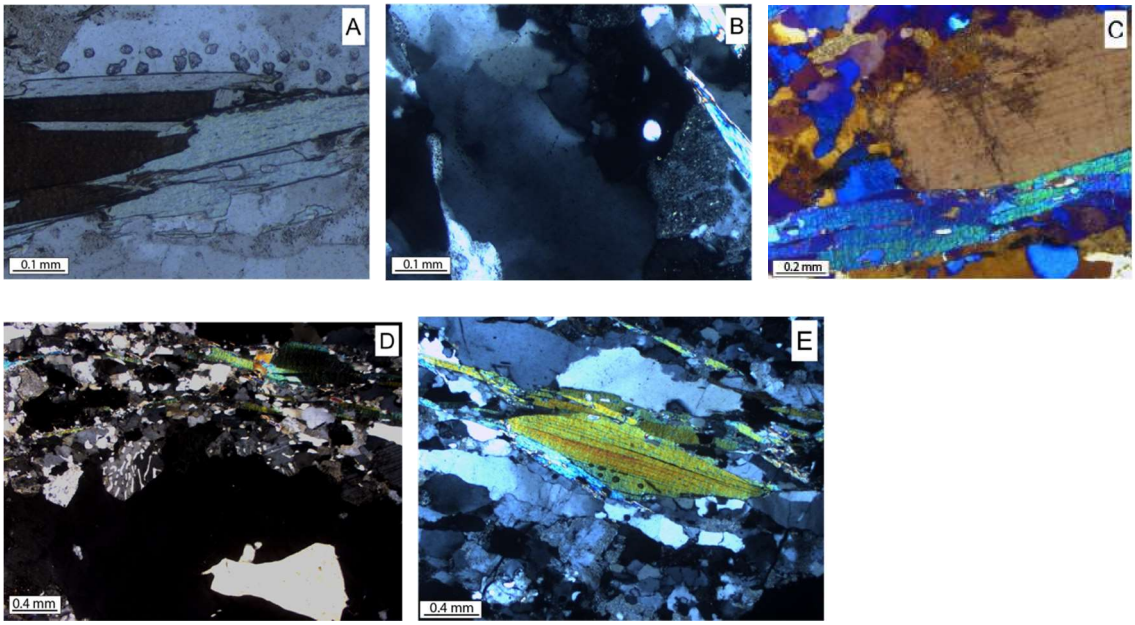

Figure 2.14. Micrographs from RM-22-7 cut perpendicular to foliation and parallel to lineation. Quartz and feldspar grains define a ribbon-like grain shape fabric. Quartz grains exhibit undulose extinction and deformation bands; feldspar grains contain myrmekite patches. Asymmetric mica fish indicates a sinistral shear sense.

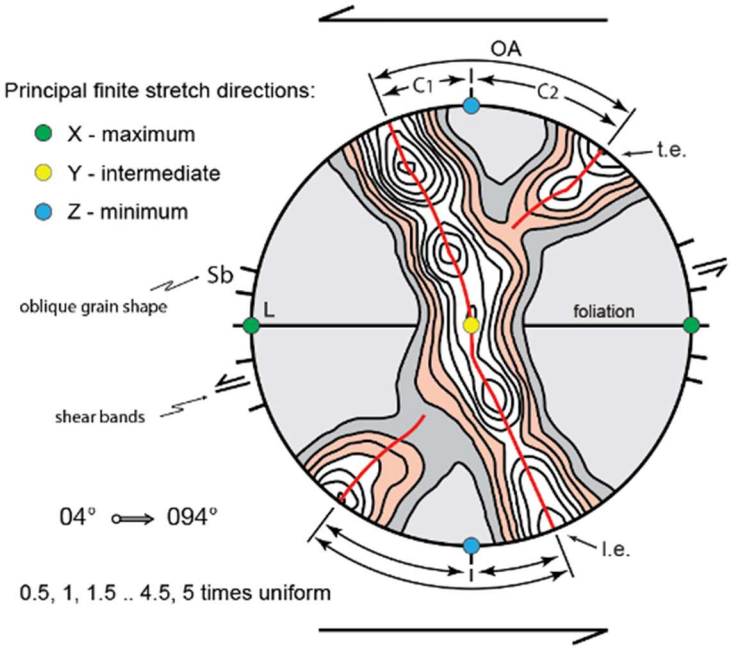

Figure 2.15. Example of a cross-girdle quartz c-axis fabric diagram, indicating angles between pole to foliation and leading and trailing edges of fabric skeleton (C1 and C2, respectively. C1<C2 indicates a sinistral shear sense. OA = opening angle (C1 + C2) between leading and trailing edges of fabric skeleton; Sb = alignment of elongate dynamically recrystallized quartz grains oblique to foliation. Note: cross-girdle fabric intersects foliation at right angle to grain shape lineation indicating that lineation developed parallel to the maximum principal stretch direction (X). Adapted from Law et al. (2021). Figure 9; pg. 17. Used with permission of Law; email and copyright agreement attached.

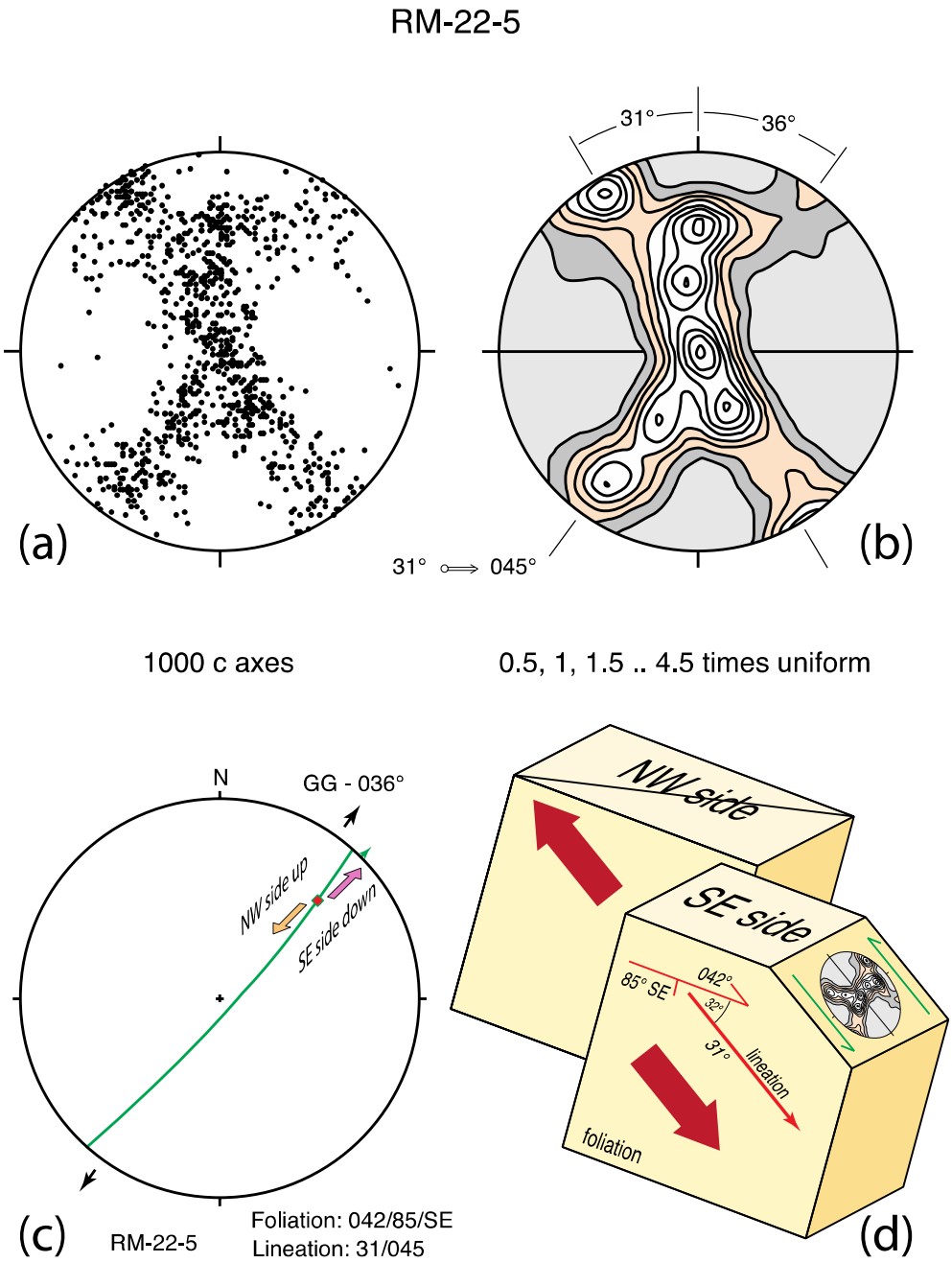

Figure 2.16. Optically measured quartz c-axis fabric from Rosemarkie sample RM-22-5 and kinematic interpretation. (a, b) Scatter and contour plots of measured fabric; plunge and trend of mineral grain shape lineation in sample indicated. An opening angle of 67° between the leading and trailing edges of fabric indicates a likely deformation temperature of c. 510 °C, although deformation microstructures in feldspar grains indicate that deformation started at higher temperatures. (c) Stereonet showing geographic orientation of foliation and lineation in sample and shear sense inferred from asymmetry of quartz fabric; local trend of Great Glen fault (GG) indicated. (d) Block diagram schematically illustrating 3D sense of shearing (NW side up to the SW and SE side down to the NE) indicated by fabric asymmetry.

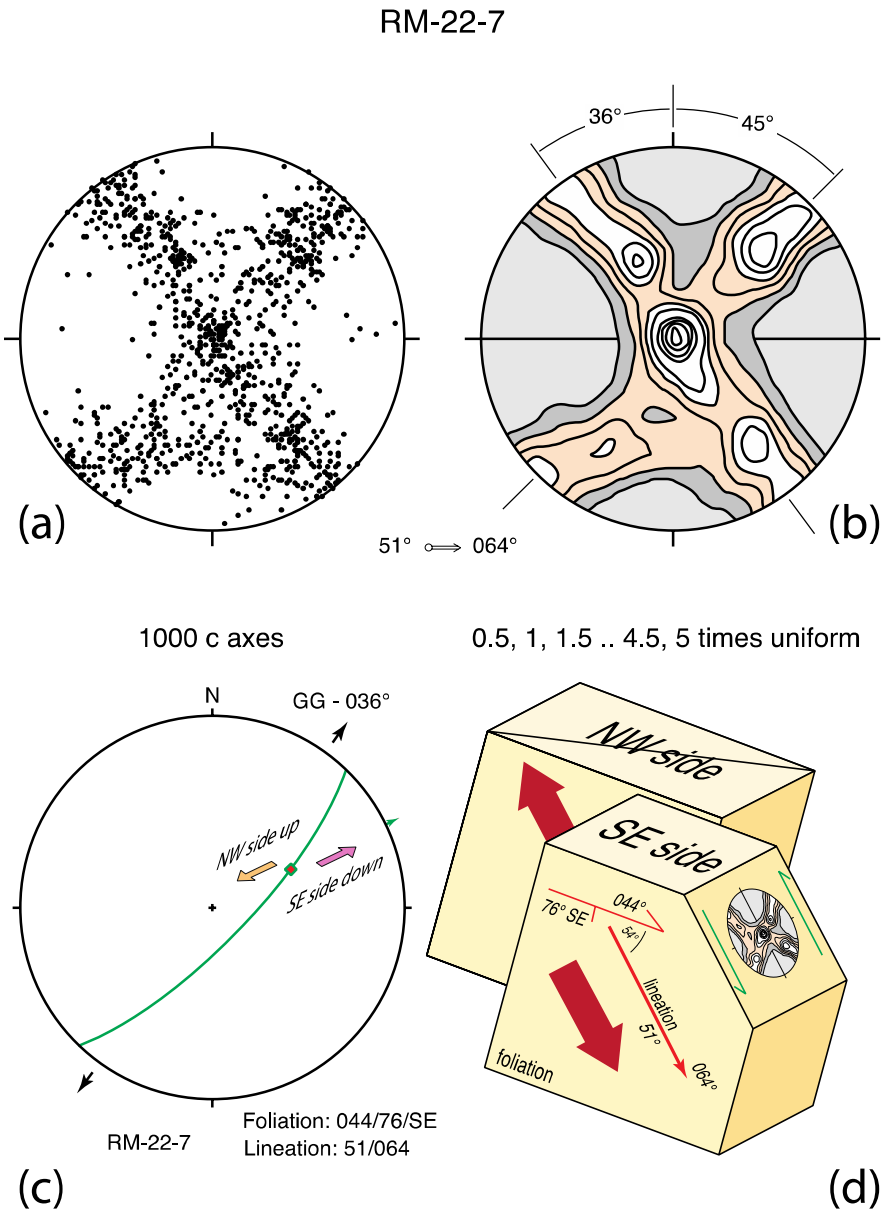

Figure 2.17. Optically measured quartz c-axis fabric from Rosemarkie sample RM-22-7 and kinematic interpretation. (a, b) Scatter and contour plots of measured fabric; plunge and trend of mineral grain shape lineation in sample indicated. An opening angle of 81° between the leading and trailing edges of the fabric indicates a likely deformation temperature of c. 610 °C. (c) Stereonet showing geographic orientation of foliation and lineation in sample and shear sense inferred from asymmetry of quartz fabric; local trend of Great Glen fault (GG) indicated. (d) Block diagram schematically illustrating 3D sense of shearing (NW side up to the SW and SE side down to the NE) indicated by fabric asymmetry.

Chapter 3: Clunes and Glen Garry Vein Complex

Sampling Area: Plutonic rocks on the NW side of the Great Glen Fault

Plutonic rocks have been sampled from two locations on the NW side of Loch Lochy. These include the Clunes tonalite exposed near the small township of Clunes and the Glen Garry Vein complex exposed approximately 7 km to the NE of the Clunes pluton in the Kilfinnan Burn near the small township of Kilfinnan (Figs. 3.1 & 3.2). The locations of both intrusive bodies are covered on UK Ordnance Survey 1:50,000 scale (Sheet 34) and 1:25,000 scale (Sheet 400) topographic maps. The Clunes pluton is shown on British Geological Survey 1:50,000 scale Sheet 62E, while the Glen Garry Vein Complex exposed in Kilfinnan Burn is shown on British Geological Survey 1:50,000 scale Sheet 63W (British Geological Survey 1975, 1995).

A geologic map of the Clunes tonalite has been published by Stewart et al. (2001) (Fig. 3.3). A field guide to the Glen Garry Vein Complex exposed in Kilfinnan Burn has been provided by Stewart (2010).

3.1 Clunes Tonalite

Tectonic setting

The Clunes tonalite was initially chosen for detailed study because it was thought to have been intruded during strike-slip shearing on the adjacent Great Glen Fault and sub-magmatic – high-temperature solid microstructures within the pluton were thought to have developed during early stages of cooling of the pluton (Stewart et al. 2001). Field evidence derived from the pluton (curving of the magmatic fabric on the pluton's SE margin towards alignment with the GGF) and from its Moine Supergroup (Glenfinnan and Loch Eil Groups) country rocks were interpreted as indicating that the pluton was intruded during sinistral shearing on the adjacent Great Glen Fault (Stewart et al. 2001). U-Pb zircon chronology yielded a crystallization age of 427.8 ± 1.9 Ma suggesting (Stewart et al. 2001) that sinistral shearing on the Great Glen Fault was ongoing by 430 Ma in mid-Silurian times. It was therefore hoped that microstructural analysis of additional samples from the SE margin of the Clunes tonalite would form a test of the original suggestion by Stewart et al. (2001) that sub-magmatic to high-temperature solid-state microstructures had developed within the pluton during the early stages of its cooling history. However, a field visit to the pluton in the summer of 2022 revealed that the exposures sampled by Stewart et al. (2001) in the mid-late 1990s were no longer accessible due to dense reforestation. Indeed, only two locations on the side of a forestry trail were now accessible.

Petrology and microstructures of samples collected

As noted above, exposures of both the interior of the Clunes tonalite and its contacts with the surrounding Moine metasedimentary rocks that were accessible in the middle-late 1990s when Martyn Stewart undertook fieldwork as part of his Ph.D. thesis (Stewart 1997,

with results subsequently published in Stewart et al. 2001) were found to be totally inaccessible in summer 2022 due to recent reforestation on the NW bank of Loch Lochy. Only two outcrops of tonalite were found (Figs. 3.2 & 3.3) – both are artificial outcrops produced by quarrying and widening of a forestry service track and or located on the SE side of the Clunes pluton adjacent to the trace of the Great Glen Fault that runs through Loch Lochy. Oriented sample GG-22-1 (UK grid reference NN 23219 91492) was collected from a small quarry on the side of a forestry track close to the eastern margin of the pluton. Oriented sample GG-22-2 (UK grid reference NN 2141189537) was collected close to the western margin of the pluton from a drainage ditch on the same forestry track. The dominant mineral assemblage in both samples consists of hornblende, orthoclase, plagioclase, and chlorite. Accessory minerals include biotite and generally less than 5% quartz and garnet. Sample GG-22-2 is dominated by fresh hornblende, while sample GG-22-1 contains altered/retrogressed hornblende.

The tonalite in sample GG-22-1 (Fig. 3.4) is cut by two orthogonal sets of planar fracture zones ranging in width from c. 2 mm down to a few tens of microns. Within the fracture zones, the feldspar grains are broken down into angular clasts (the largest measuring c. 1 mm in size) surrounded by a matrix of ultra-fine-grained black to opaque groundmass in which individual mineral fragments are too small to be resolved with the optical microscope. Elongate mats of crumpled chlorite that may define a grain shape foliation (possibly of originally magmatic origin) are crosscut by these fracture zones. Plagioclase grains are internally fractured, and their crystal lattices are gently warped with resultant sweeping extinction patterns under cross-polarized light. Some plagioclase grains also have wedge-shaped deformation twins. Quartz grains exhibit undulatory extinction and tilt walls under cross-polarized light, with deformation lamellae oriented at a high angle to the tilt walls. Hornblende grains locally exhibit blocky extinction under cross-polarized light. The microstructures observed in the feldspars indicate that at least limited plastic deformation has occurred in these grains at deformation temperatures of greater than 450-500 °C (Tullis 2002; Fazio et al. 2020), although unlike in the Rosemarkie Inlier imposed strains in the Clunes tonalite were not high enough to produce any significant grain shape foliation. Relatively high deformation temperature may also be indicated by the blocky extinction in the hornblende grains, although these microstructures could also be produced by microfracturing and rotation of blocks of the crystal lattice between these fractures. The microstructures in the quartz grains indicate the operation of plastic deformation at lower temperatures (c. 300 - 400 °C) usually associated with lower greenschist facies conditions during regional metamorphism. As the Clunes tonalite postdates penetrative deformation and regional deformation in the surrounding Moine metasedimentary rocks the observed feldspar and quartz microstructures in the Clunes tonalite most likely formed during cooling of the tonalite in response to weak far-field stresses associated with motion on the Great Glen Fault.

In sample GG-22-2 collected near the SW margin of the Clunes tonalite, very little microstructural evidence for fracturing was found (Fig. 3.5). On gently dipping (026°/20°E) joint planes at this location the tonalite contains a well-developed mineral lineation defined by elongate clusters of biotite and feldspar grains that plunges at 14° towards 163°. A grain shape lineation with this trend has previously been recognized and

mapped within the Clunes tonalite by Stewart et al. (2001, their fig. 2) and interpreted as a pre-rheologically critical melt percentage (pre-RCMP) fabric, containing aligned crystals within an undeformed matrix, formed during magmatic flow. Thin sections were cut perpendicular to these joint planes and parallel to the mineral lineation. Limited undulatory extinction is present in both orthoclase and feldspar grains in sample GG-22-2, but unlike in GG-22-1 no clear internal warping/bending of their lattice (e.g., curving plagioclase twin boundaries) was found. Quartz grains do, however, contain tilt walls and locally exhibit undulatory extinction (Fig. 3.5c) which resemble those in GG-22-1.

3.2 Glen Garry Vein Complex

Tectonic Setting

The Glen Garry Vein Complex is one of several phases of late Caledonian igneous activity intruding Loch Eil Group psammites on the NW side of the Great Glen Fault (Fettes & Macdonald 1978). The vein complex is defined by intense granodiorite veining over an area exceeding 300 square kilometers. The veins usually have no preferred orientation and are also usually undeformed with no foliation development (Fettes & Macdonald 1978) suggesting that they are very late intrusions that formed after all penetrative deformation in this part of the Northern Highlands Terrane had ceased. Close to the Great Glen Fault, however, the larger veins have a rough NE alignment (Fettes & Macdonald 1978; Stewart 2010). In the area around Kilfinnan Burn the ENE trending gneissic foliation in the Loch Eil Group psammites is rotated towards the NE-trending granodiorite veins so that a sinistral sigmoidal fabric develops suggesting that vein emplacement experienced syn-emplacement sinistral shearing on the GGF (Stewart 2010). The Glen Garry Vein Complex is undated, but the 428 Ma Clunes pluton is cut by undated felsic sheets, which are likely part of the same vein complex (Fettes & Macdonald 1978; Milne et al. 2023).

Petrology and microstructures of samples collected

Sample GG-22-9 (Fig. 3.6) (UK grid reference NN 27658 95804) was collected from extensive water-worn outcrops of pink granodiorite belonging to the Glen Garry Vein Complex and exposed in Kilfinnan Burn (Stewart 2010). No clearly defined grain shape fabric is observed in thin sections cut from Sample GG-22-9 but both quartz and feldspar (orthoclase, microcline, and plagioclase) grains internally display a range of solid-state deformation-induced microstructures. The largest tabular microcline grains measure up to 0.5 - 1.00 cm in length.

Undulose extinction is present in some quartz grains, while tilt walls oriented parallel to prism planes are present in other quartz grains indicating crystal plastic deformation by dislocation slip on basal crystallographic planes. A few quartz grains exhibit a blocky extinction pattern marked by prism plane tilt walls with less commonly observed basal plane tilt wall oriented at right angles to prism plane tilt walls, thereby dividing the grains up into rectangular – square blocks of sightly differing extinction position. This blocky extinction marked by prism and basal plane tilt walls could be equivalent to the chessboard extinction microstructure which is usually interpreted to indicate combined basal <a> and

prism <c> slip at deformation temperatures > c. 630 °C (see summary by Passchier & Trouw 2005).

Undulose extinction is also observed in some of the orthoclase, microcline, and plagioclase feldspar grains. Microcline marked by cross-hatched twinning is the dominant feldspar in terms of abundance in thin-section. Chemical alteration (to minute sericite crystals) is common in the orthoclase feldspar grains, while the microcline and plagioclase grains usually appear unaltered. No deformation twins that might be indicated by tapering twin domains were observed in thin section, although some twins do appear to be stretched. Some of the feldspar grains (particularly plagioclase) exhibit undulatory extinction suggesting at least limit crystal plastic deformation. Other plagioclase grains internally exhibit spectacular flexing, sinuous bending, and locally more angular kinking of twin domains (Fig. 3.6), together with internal displacement of twins on isolated curving fractures that are only developed within the interior of the plagioclase grains. These microstructures also indicate at least limited crystal plastic deformation of feldspar at temperatures > c. 500 °C, although the magnitude of strain produced is very small and certainly not enough to produce a new solid-stage grain shape foliation.

Quartz-quartz grain boundaries have small (25 micron) bulges (Fig. 3.6I) suggesting localized recrystallization by grain boundary bulging (GBB). However, some of the larger quartz grains contain smaller inclusions of quartz with identical extinction positions suggesting that in 3D they form parts of a larger single grain. These *island microstructures* (Passchier & Trouw 2005; also referred to as *dissection* or *left-over* microstructures; Urai et al. 1986; Stipp et al. 2002a, b) indicate the importance of grain boundary migration (GBM) recrystallization of quartz that formed at higher temperatures (> c. 500 °C) and presumably earlier than the grain GBB microstructures (c. 300 - 400 °C; see review by Law 2014). Adjacent orthoclase-plagioclase grains and quartz-plagioclase grains locally display small (c. 25 micron) lobate/bulging microstructures also indicating incipient relatively high temperature (> c. 450 - 500 °C; Tullis 2002; Fazio et al. 2020) solid state deformation.

Granodiorite sample GG-22-9 is cut by late fractures of two types. Many of the feldspar grains are cut by networks of thin fractures that rarely extend outside of individual grains. These fractures are typically 30 - 50 microns in width and often infilled with either calcite, white mica (Fig. 3.6) or fine-grained opaque material of uncertain origin. They appear to be extension fractures with little or no obvious offset of microstructures such as twin boundaries traced along their length. These apparent extension fractures in the feldspar grains do not extend into adjacent quartz grains but terminate at feldspar-quartz grain boundaries. This suggests that while the feldspar grains were undergoing fracture, adjacent quartz grains were deforming plastically. The second type of fracture in sample GG-22-9 is marked by fairly planar zones of intense fracturing, measuring up to 1.5 mm (1500 microns) in width, that cut across both feldspar and quartz grains. Within these fracture zones both the feldspar and quartz grains have been ground down into angular fragments set in a fine-grained ground mass in which individual fragments cannot be resolved with the optical microscope.

As outlined above for samples from the Clunes tonalite, all these microstructures indicate that grain-scale deformation in granodiorite sample GG-22-9 from the Glen Garry Vein Complex occurred at temperatures ranging from c. 630 °C down to 300 - 400 °C. As the vein complex postdates regional metamorphism and formation of grain shape fabrics (foliation) in the surrounding Moine metasedimentary rocks, this suggests that these deformation microstructures were produced during cooling of the veins to background temperatures after regional scale metamorphism and deformation had ceased. Although still undated isotopically, the Glen Garry Vein Complex likely post-dates intrusion of the 427.8 ± 1.9 Ma Clunes tonalite (Fettes & Macdonald 1978; Stewart et al. 2001) and is therefore likely to be of Late Silurian age. Sample GG-22-9 from the Glen Garry Vein Complex exposed in Kilfinnan Burn is located at no more than 500 m from the axis of Loch Lochy which presumably also marks the central core of the Great Glen fault system. The observed feldspar and quartz microstructures in the granodiorite vein complex exposed in Kilfinnan Burn therefore most likely formed during cooling (from c. 630 – 300°C) of the granodiorite in response to weak far-field stresses associated with shearing on the adjacent Great Glen fault.

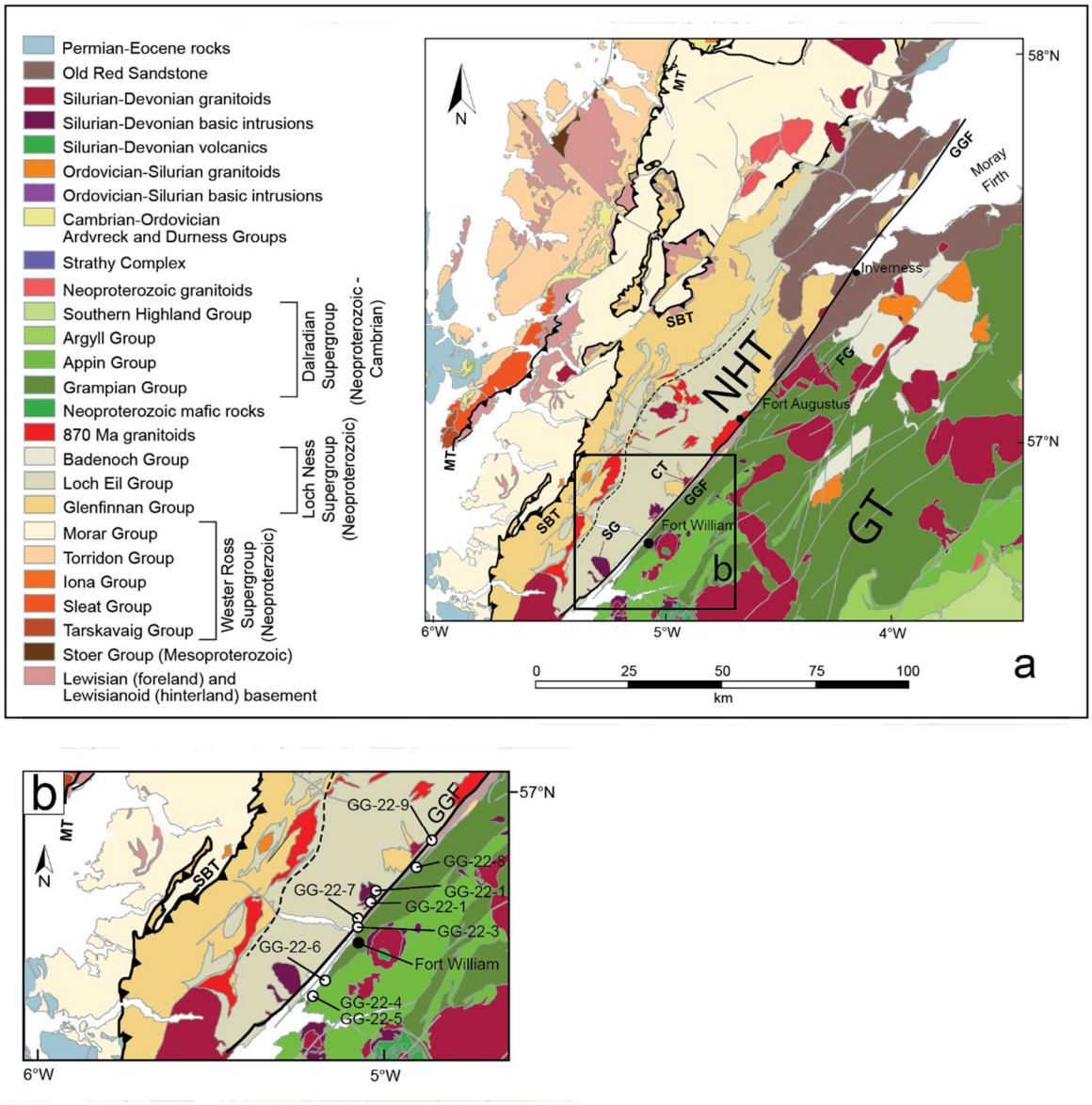

Figure 3.1. (a) Geologic map of the part of the Scottish Highlands, with groupings of sample locations indicated by black boxes; modified from Law et al. (in review; Figure 8.2). (b) Sample locations in the southern part of the Great Glen near Fort William; including Clunes samples GG-22-1 & 2, and Glen Garry Vein Complex sample GG-22-9. NHT = Northern Highlands Terrane, GT = Grampian Terrane, SG = Strontian Granite, CT = Clunes Tonalite, FG = Foyers Granite, GGF = Great Glen Fault, MT = Moine Thrust, SBT = Sgurr Beag Thrust.

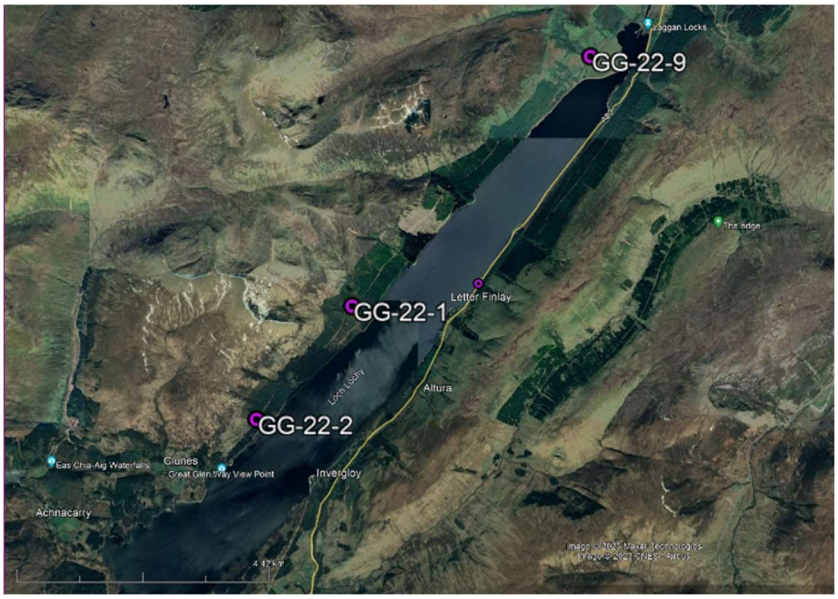

Figure 3.2. Sample locations (GG-22-1 & GG-22-2 from SE part of the Clunes tonalite; GG-22-9 from Glen Garry Vein Complex). Screenshot is taken from Google Earth.

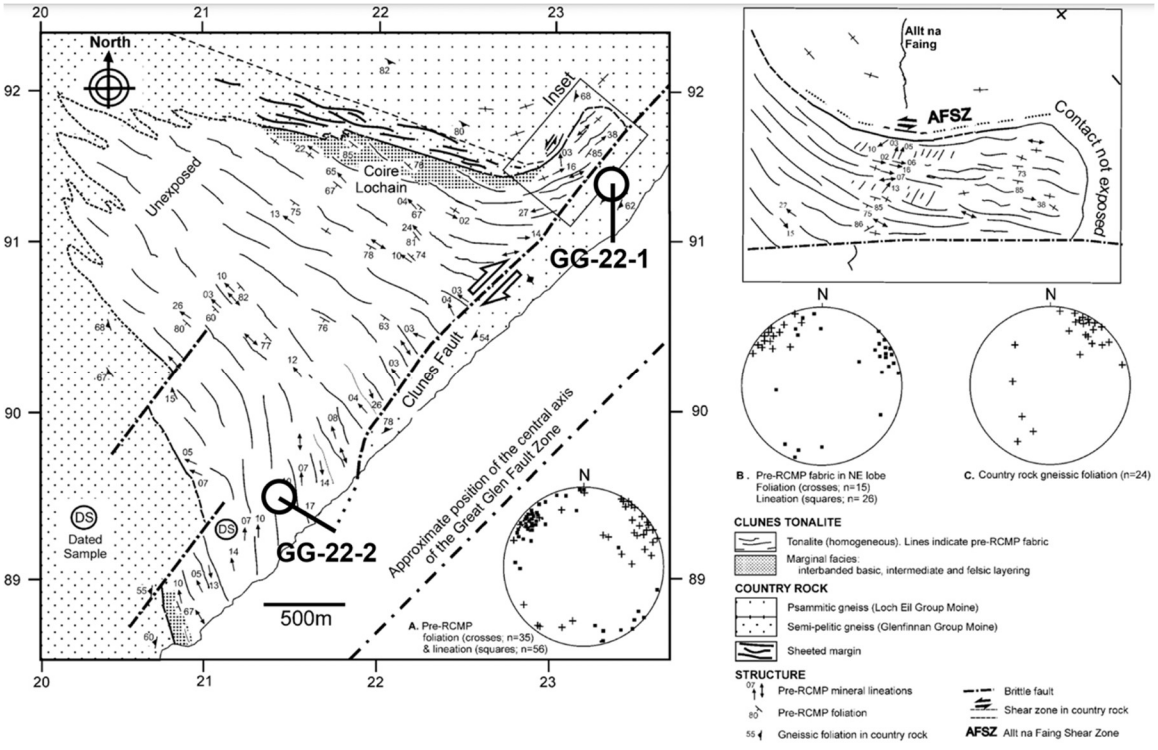

Figure 3.3. Structural map of the Clunes tonalite pluton adjacent to the Great Glen Fault Zone (GGFZ). Figure from Stewart et al. (2001). Figure 2; pg. 823. Fair Use determination attached.

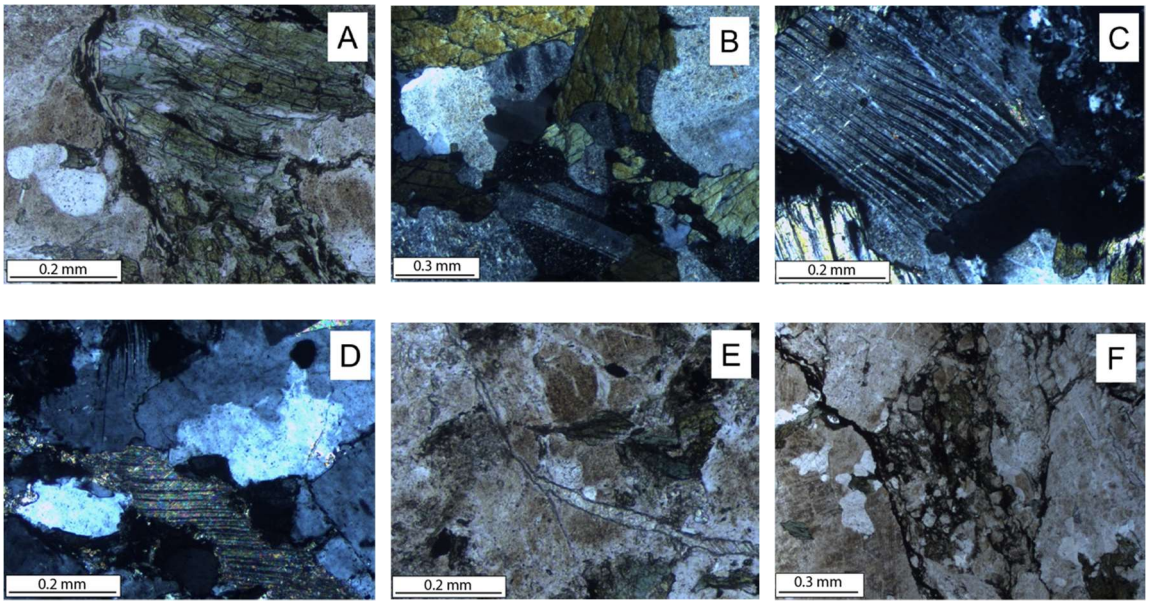

Figure 3.4. Micrographs from sample GG-22-1 from the Clunes tonalite. Microstructures locally indicate high temperature solid state plastic deformation (flexed/kinked tapering deformation twins in plagioclase; sinuous quartz and feldspar grain boundaries indicated grain boundary migration recrystallization; flexed twins in calcite grains, and later brittle deformation (extension fractures filled with fibrous calcite; breccia zones containing fine-grained clasts of feldspar surrounded by ultra-fine-grained opaque fault gouge).

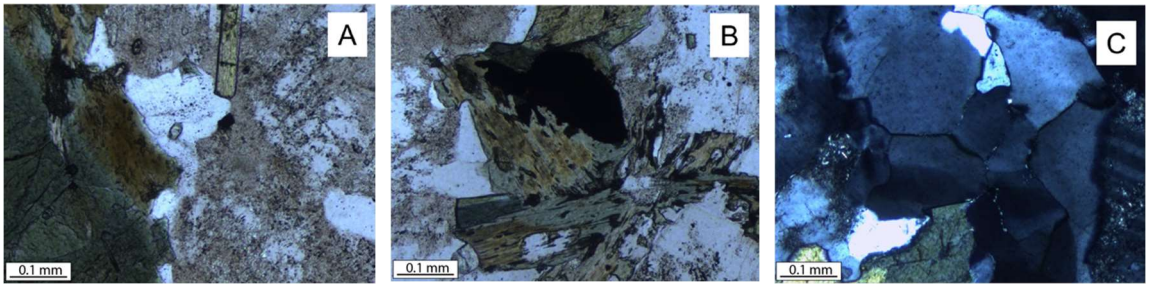

Figure 3.5. Micrographs from sample GG-22-2 from the Clunes tonalite. Microstructures locally indicate high temperature solid state plastic deformation (undulose extinction in quartz and feldspar grains; sinuous quartz and feldspar grain boundaries - some with 120° intersections - indicated grain boundary migration) as well as late-stage alteration processes (biotite altered to chlorite; minor sericitization of feldspar).

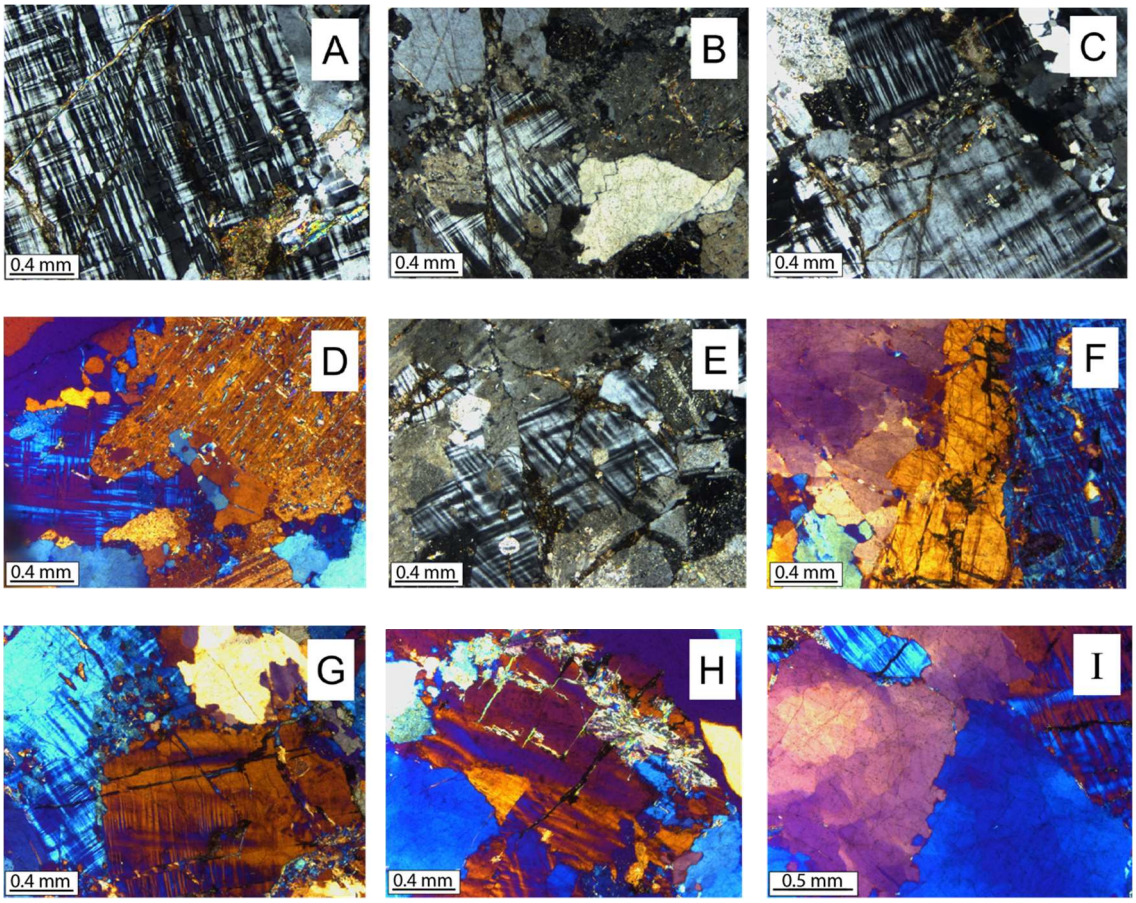

Figure 3.6. Micrographs from sample GG-22-9 from the Glen Garry Vein Complex in Kilfinnan Burn. Microstructures locally indicate high temperature solid state plastic deformation (blocky / chessboard extinction in quartz grains; undulose extinction, tartan twinning and tapering deformation twins in plagioclase; island grains in quartz and feldspar suggested extreme grain boundary migration recrystallization. Lower temperature plastic deformation indicated by smaller scale highly lobate/bulging boundaries between quartz grains in turn indicating localized grain boundary bulging recrystallization. Late brittle deformation indicated by fractures (including extension fractures infilled with fibrous calcite) that cut across earlier higher temperature crystal-plastic microstructures.

Chapter 4. Ratagain Pluton

Tectonic setting

The Strathconnon fault is one of a series of NE-SW trending strike-slip faults in the Northern Highlands Terrane (Fig. 4.1) that are sub-parallel to the Great Glen Fault and are thought to have been contemporaneous with strike-slip motion on the Great Glen (see reviews by Watson 1984; Strachan et al. 2002). Net sinistral movement of about 6 km on the Strathconnon Fault is indicated by the offset of both micro-diorites belonging to the Silurian age Ratagain intrusive suite and Lower Devonian acid porphyrites and felsites; this offset predates intrusion of camptonites of Permo-Carboniferous age (Ramsay 1955; May et al. 1993).

Hutton and McErlean (1991) argued that sinistral shear along the Strathconnon Fault (Fig. 4.1) accompanied the emplacement of the adjacent 425 ± 3 Ma Ratagain pluton (Rogers & Dunning 1991) in Late Silurian times. This interpretation of syn-emplacement shearing by Hutton and McErlean (1991) was based on the counterclockwise swing in the map view of *pre-full crystallization* magmatic fabrics in the Ratagain pluton from a NW-SE trend in the interior of the pluton to a NE-SW trend adjacent to the similarly trending Strathconnon fault located on the SE side of the pluton. The pluton is composed of different magma batches ranging in composition from monazite and quartz monzonite through diorite and quartz monzodiorite to late intrusions of granite (see summary by Lawrence et al. 2022). From combined anisotropy of magnetic susceptibility (AMS) data and thin-section-based petrographic analyses, Lawrence et al. (2023) have argued that magmatic fabrics are preserved throughout the Ratagain pluton with only weakly developed solid-state deformation microstructures (including quartz with bulging or sutured grain boundaries, myrmekite, kinked plagioclase twins and cleavage traces in biotite, quartz subgrains) locally overprinting magmatic grain shape fabrics – particularly in the NE corner of the pluton. Within analytical error, the Ratagain pluton and the Clunes tonalite (427.8 ± 1.9 Ma; Stewart et al. 2001) have overlapping intrusion ages. As the Clunes tonalite was also argued to be emplaced during sinistral on the adjacent Great Glen fault (Stewart et al. 2001; see Chapter 3) this by extension suggests that Late Silurian sinistral displacements on the Great Glen and Strathconnon faults were contemporaneous.

Rock sample locations and macroscopic structures

The area surrounding the Ratagain pluton is covered by UK Ordnance Survey 1:50,000 scale (Sheet 33) and 1:25,000 scale (Sheet 413) topographic maps. The Ratagain pluton is shown on the British Geological Survey 1:50,000 scale Sheets 71E and 72 W (British Geological Survey 1976, 1984). Petrologic descriptions, together with geologic maps, of the pluton, have been published by Peach et al. (1910), Nicholls (1951); Hutton & McErlean (1991); Hutton et al. (1993); McErlean (1993) and Lawrence et al. (2022). A detailed account of the geologic evolution of the surrounding area before the intrusion of the pluton, together with the supporting map, has been provided by Krabbendam et al. (2017).

Two oriented samples were collected from the SE margin of the Ratagain pluton adjacent to the Strathconnon Fault (Figs. 4.2 & 4.3) to determine if any magmatic or solid-state microstructures were present. Both samples are from the quartz monzonite/ monzonite unit of the pluton as mapped by Lawrence et al. (2022) and are located within 100 m of the mapped position of the Strathconnon Fault. Sample RA-22-1 (UK Ordnance Survey grid reference NN 93996 19860; see Table 2.1) was collected from a roadcut on the south side of the A.87 road approximately 200 m to the NNE of the Kintail Lodge Hotel. Sample RA-22-3 (grid reference NN 92448 19010) was collected 1.6 km to the WSW of sample RA-22-1 from a stream section at the junction of minor roads leading to Ratagain and Glenelg. An oriented sample (RA-22-2) of foliated and intensely lineated Moine metasedimentary rock (grid reference NN 94226 19862) located between the SE margin of the pluton and the mapped position of the Strathconnon Fault on the hillside to the NE of Kintail Lodge Hotel was also collected to determine any microstructural evidence for shearing associated with motion on the adjacent fault.

Microscopic rock sample descriptions

Sample RA-22-1 (Fig. 4.4) is composed of megacrysts of internally zoned orthoclase and plagioclases feldspar (ranging from 2 to >4 mm in size) set in a much finer-grained (100 - 500 micron) matrix of orthoclase, plagioclase, and interstitial quartz grains. Quartz grains display ubiquitous undulatory extinction and common development of prism plane tilt walls/deformation bands. Basal plane tilt walls are less commonly observed, but where both sets of tilt walls are developed an incipient blocky extinction pattern is formed. Some of the larger interstitial quartz grains have recrystallized to aggregates of smaller (200 - 300 micron) more rounded grains which may have formed by transition grain boundary migration (GBM) to subgrain rotation (SGR) recrystallization mechanisms. Grain boundaries between adjacent quartz grains are usually gently curving suggesting the dominance of GBM recrystallization in quartz, although some more localized lobate microstructures (20 - 40 microns in amplitude) on these grain boundaries suggests the at least local operation of grain boundary bulging (GBB) processes. Both orthoclase and plagioclase grains exhibit a small amount of undulatory extinction, but unlike samples from the Clunes pluton and the Glen Garry Vein Complex adjacent to the Great Glen Fault (see Chapter 3) feldspar grains in Sample RA-22-1 do not contain tapering deformation twins or exhibit any internal folding or kinking of twin planes. Grain boundaries between adjacent feldspar grains and between adjacent feldspar and quartz grains are generally straight to only slightly curving with no obvious deformation microstructures such as grain boundary bulges. No microstructures associated with fracturing were found in sample RA-22-1.

Microstructures in sample RA-22-3 (Figure 4.5) are similar to those in RA-22-1, although feldspar megacrysts are larger, ranging up to 1 cm in length. Quartz grains have pronounced undulatory extinction and prism plane tilt walls. Undulatory extinction in the feldspar grains is more pronounced than in sample RA-22-1, but as in sample RA-22-1, no deformation twins or folding or kinking of twin planes within the feldspar grains has been observed. Discreet planar fractures measuring up to 30 microns in width and locally filled

with either quartz or mica are present in sample RA-22-3. No obvious offset of microstructures is seen along these planar fractures that appear to be of extensional rather than shearing origin. The fractures have only been observed in the feldspar grains and do not appear to extend into the adjacent quartz grains but terminate at feldspar-quartz grain boundaries. Very similar microstructures were observed in sample GG-22-9 from the Glen Gary Vein Complex (see Chapter 3) where they were interpreted as indicating that while the feldspar grains were undergoing fracture, adjacent quartz grains were deforming plastically.

Summary of deformation conditions

Quartz and feldspar microstructures in samples RA-22-1 and RA-22-3 (Figs. 4.4 & 4.5) from the SE edge of the Ratagain pluton indicate the operation of incipient solid-state deformation at temperatures ranging from c. 450 - 500 °C (indicated by very limited plasticity of feldspar) down to c. 300 - 400 °C (grain boundary bulging between adjacent quartz grains, fracturing of feldspar, and contemporaneous plastic flow in adjacent quartz grains). As was found with sample GG-22-9 from the Glen Garry Vein Complex, strain magnitudes associated with this solid-state deformation were very low, and no obvious solid-state grain shape fabrics were formed. The solid-state deformation microstructures are likely to have formed in response to weak far-field stresses associated with shearing on the adjacent Strathconnon fault. However, whether this occurred before the pluton cooled to background temperatures or if it was a discreet event after pluton emplacement and cooling is more difficult to determine without knowing the local background temperature during shearing on the Strathconnon fault.

Sample RA-22-2 from deformed psammites located between Rogart pluton sample RA-22-1 and the Strathconnon Fault and mapped as part of the Morar Group of the Moine Supergroup (May et al. 1993; Krabbendam et al. 2017, their figure 4), is an LS tectonite with foliation striking 092° and dipping at 24° S and a grain shape lineation plunging at 20° towards 213°. In thin sections cut parallel to lineation and perpendicular to foliation, macroscopic foliation is defined by the alignment of elongate plastically deformed quartz and feldspar (both orthoclase and plagioclase) grains surrounded by anastomosing trails of interlayered biotite and white mica laths with local retrogression of these mica trails to chlorite (Figure 4.6). Shear bands that offset this grain shape foliation and are inclined at c. 20° to the foliation indicate a top to the NNE shear sense. Deformation and metamorphism associated with the formation of this LS grain shape fabric within the Morar Group metasedimentary rocks could be of Scandian (Silurian), Grampian (Ordovician), or even older age. The grain shape foliation is cut at a high angle by planar to irregularly shaped fractures ranging from 25 to 500 microns in width. The thinner planar fractures are filled with brownish (in planar polarized light) fine-grained mineral deposits, while the thicker more irregular fracture zones are filled with brecciated quartz, feldspar, and mica. All the fracture zones cut across both quartz and feldspar grains indicating that both minerals were behaving rigidly at the time of fracturing. This in turn suggests that the Moine rocks were fractured while at a lower temperature than the fracturing of feldspar (but not quartz) that occurred in quartz monzonite sample RA-22-3. Assuming that fracturing recorded in the two samples is of at least similar age, this may indicate that late-

stage fracturing recorded in sample RA-22-3 occurred before the SE margin of Ratagain pluton had cooled to background temperatures, and the higher temperature deformation microstructures recorded in quartz monzonite samples RA-22-1 and 3 would have formed during the earlier stages of pluton cooling. If this line of reasoning is appropriate, the microstructural data from samples RA-22-1, 2, and 3 would in combination support the proposal by Hutton & McErlean (1991) that the Ratagain pluton was intruded and then cooled during shearing on the adjacent Strathconnon Fault.

Chapter 4 - Figures

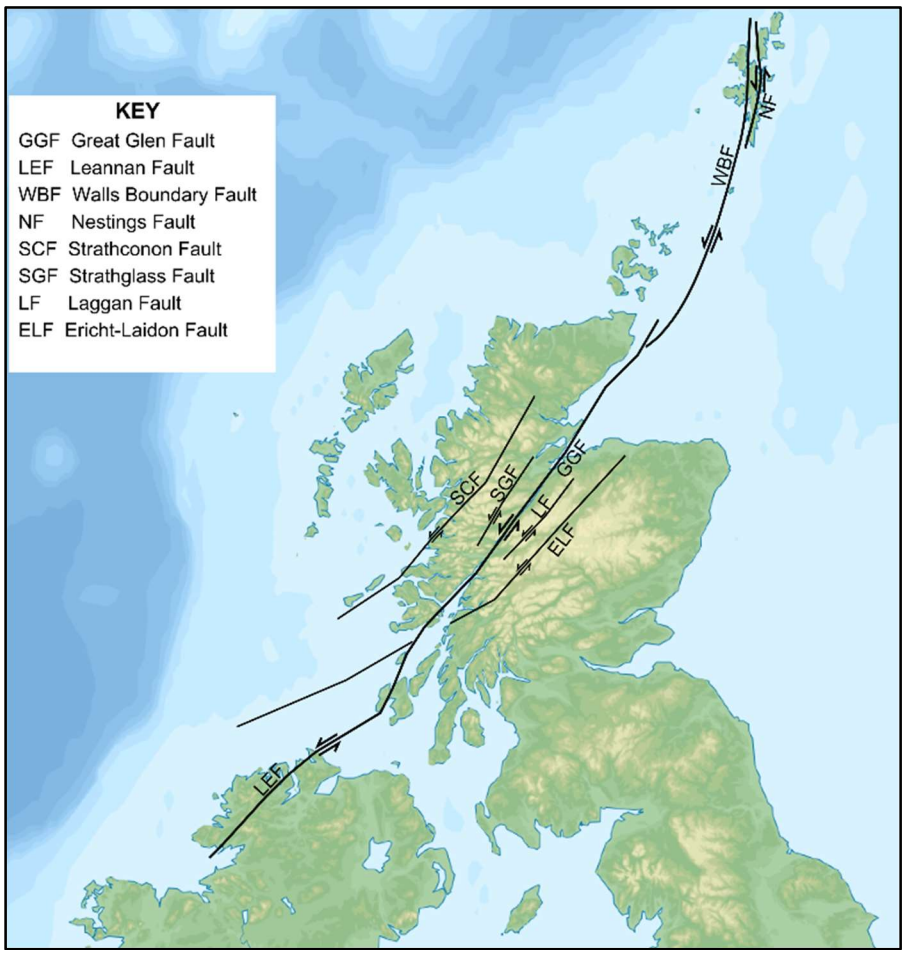

Figure 4.1. Simplified map of major Caledonian age strike-slip fault zones crosscutting northern mainland Scotland, Shetland, and Ireland. GGF = Great Glen Fault, LEF = Leannan Fault, WBF = Walls Boundary Fault, NF = Nestings Fault, SCF = Strathconnon Fault, SGF = Strathglass Fault, LF = Laggan Fault, ELF = Ericht-Laidon Fault. Figure by Mike Norton (2018; unmodified) adapted from Hellerick. https://commons.wikimedia.org/wiki/File:Great_Glen_Fault_map.png. Creative Commons (CC BY-SA 4.0) agreement attached.

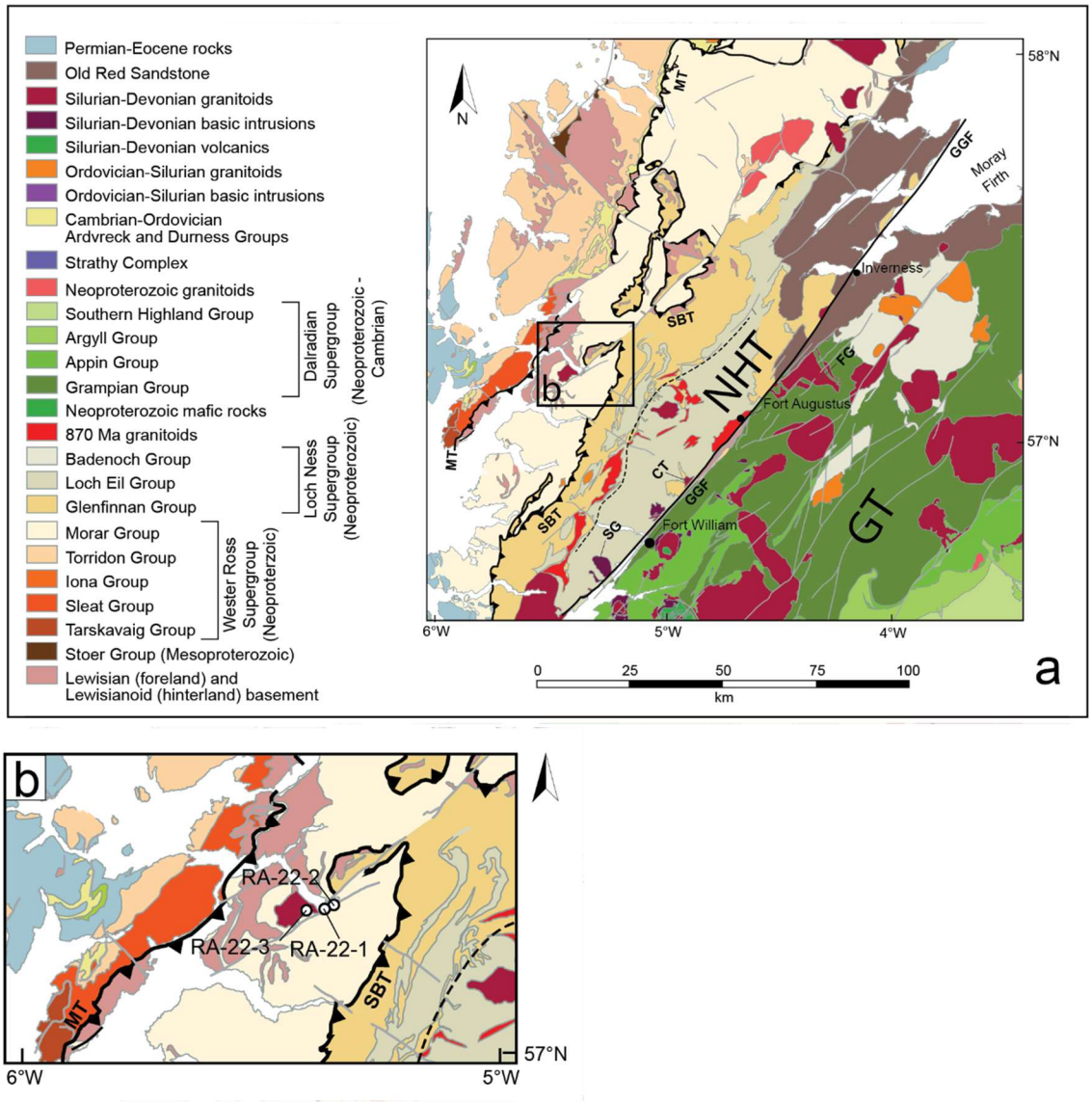

Figure 4.2. (*a*) Geologic map of the part of the Scottish Highlands, with groupings of sample locations indicated by black boxes; modified from Law et al. (in review; Figure 8.2). (*b*) Location of samples RA-22-1 and RA-22-3 from the Ratagain pluton and sample RA-22-2 from mylonitic Moine metasedimentary rocks located between the SE margin of the pluton and the Strathconnon Fault. NHT = Northern Highlands Terrane, GT = Grampian Terrane, SG = Strontian Granite, CT = Clunes Tonalite, FG = Foyers Granite, GGF = Great Glen Fault, MT = Moine Thrust, SBT = Sgurr Beag Thrust.

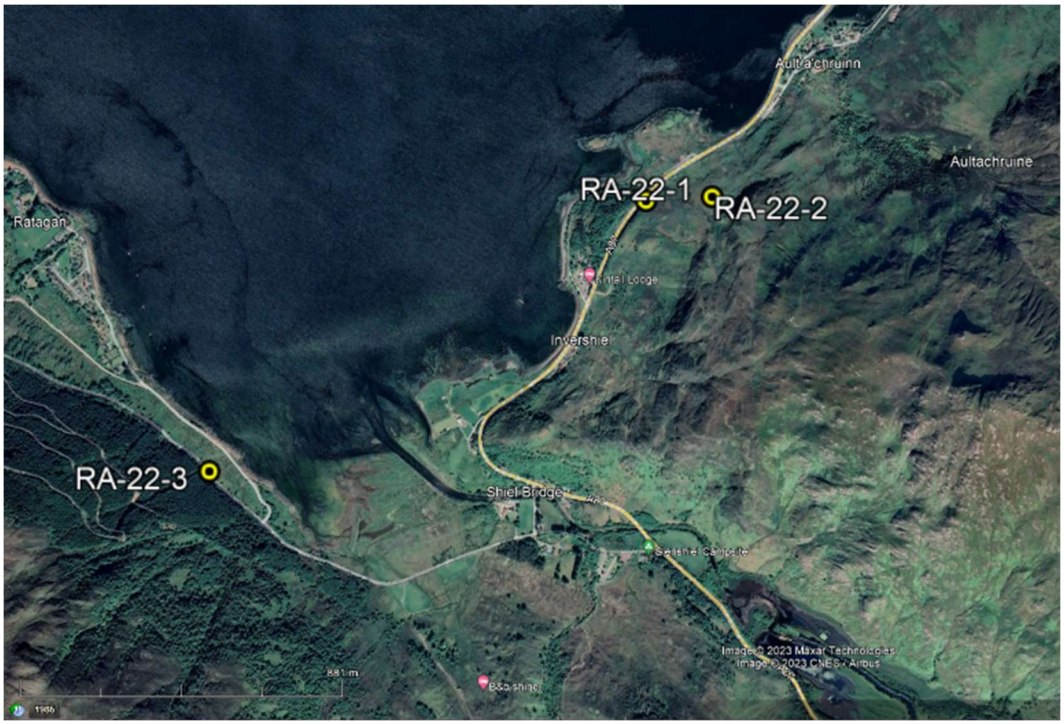

Figure 4.3. Sample locations (RA-22-1 and RA-22-3) in the SE part of the Ratagain pluton and sample RA-22-2 from mylonitic Moine metasedimentary rocks located between the SE margin of the pluton and the Strathconnon Fault. Sample locations indicated with yellow circles. Image compiled from aerial photographs. Screenshot is taken from Google Earth.

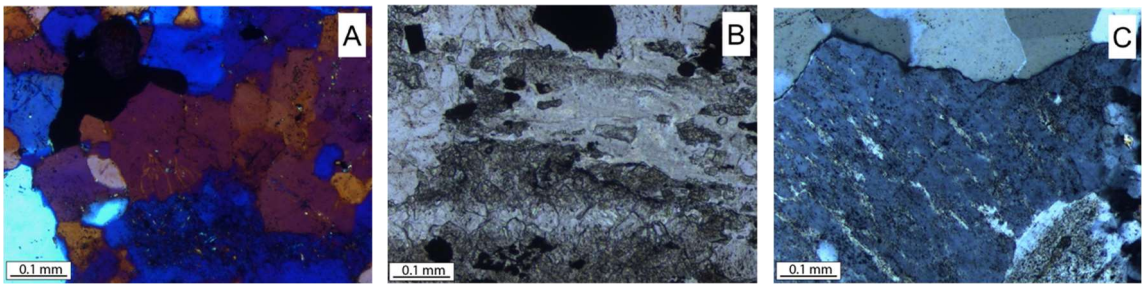

Figure 4.4. Micrographs from sample RA-22-1 from the Ratagain pluton. Microstructures locally indicate high temperature solid state plastic deformation (sinuous quartz and feldspar grain boundaries indicate grain boundary migration recrystallization). Locally intense sericitization of feldspar.

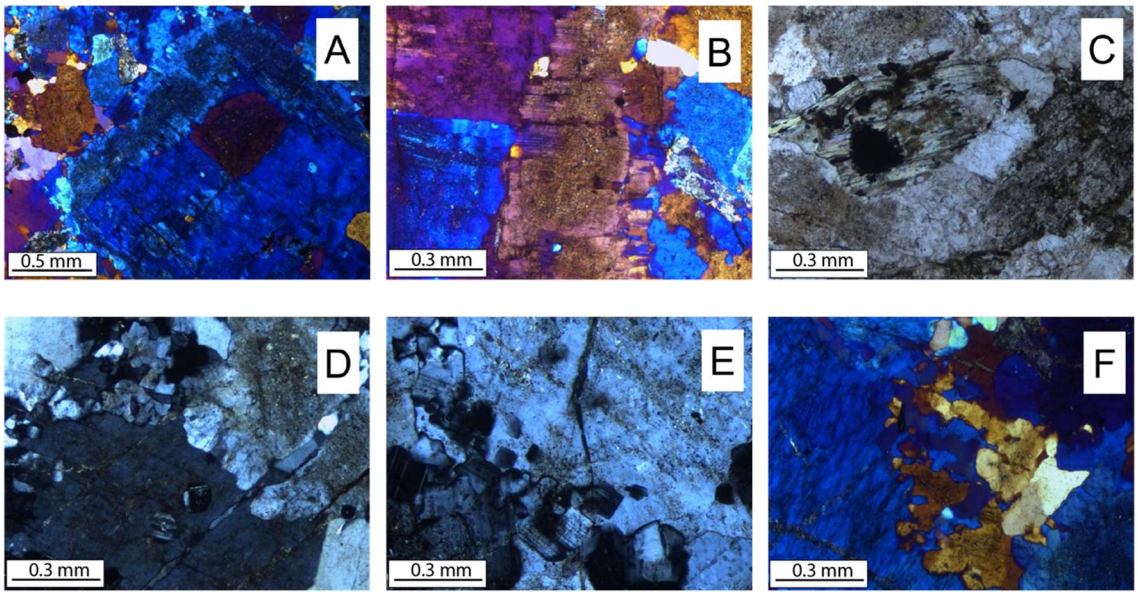

Figure 4.5. Micrographs from sample RA-22-3 from the Ratagain pluton. Microstructures locally indicate high temperature solid state plastic deformation (deformation twins in feldspar grains; sinuous quartz and feldspar grain boundaries indicate grain boundary migration recrystallization). Lower temperature plastic deformation indicated by smaller scale highly lobate/bulging boundaries between quartz grains in turn indicating localized grain boundary bulging recrystallization. Multiple stages of crystal growth may be indicated by feldspar zoning and incorporation of feldspar grains into larger grains. Note late-stage fractures with fine-grained mineral fills and local sericitization of feldspar grains.

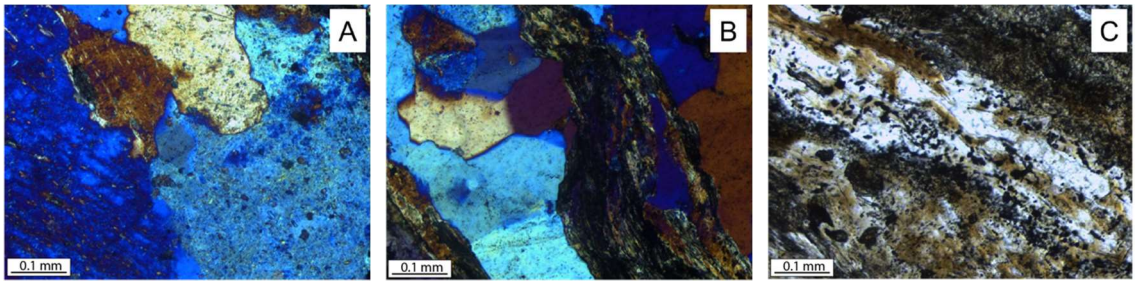

Figure 4.6. Micrographs from sample RA-22-2 from sheared Moine metasedimentary rocks located between the Ratagain pluton and the Strathconnon Fault. Microstructures locally indicate high temperature plastic deformation (sinuous quartz and feldspar grain boundaries indicate grain boundary migration recrystallization). Note late-stage alteration of feldspar grains.

Chapter 5: Torcastle

Sampling area

The Torcastle sampling area is located ~ 3 km to the NE of Fort William in the central part of the Great Glen (Fig. 5.1). Bedrock in the sampling area is exposed on both the NW and SE banks of River Lochy that drains to the SW from Loch Lochy to Loch Linnhe. These exposures are clearly shown on UK Ordinance Survey 1:50,000 scale (Sheet 41) and 1:25,000 scale (Sheet 399) topographic maps. The geology of the area is summarized on British Geological Survey 1:50,000 scale Sheet 62E (British Geological Survey 1975).

Detailed geologic maps together with lithological and structural descriptions of the Torcastle riverbank exposures – referred to as Torcastle North and Torcastle South - have been published by Stewart et al. (1997, 1999, 2000). A field guide to the Torcastle exposures, together with color versions of the geologic maps for Torcastle North and Torcastle South, have been provided by Stewart (2010). Due to high water levels on River Lochy during summer 2022 fieldwork, samples have only been collected from the Torcastle North exposures. Sample locations are shown in Figures 5.2 & 5.3 using the geologic map of Stewart (2010) as a base.

Tectonic setting

Exposures of bedrock on the banks of River Lochy in the Torcastle sampling area are located within a 500 m wide band of highly deformed rocks mapped as *'mylonite'* on BGS Sheet 62E that strikes NE-SW (052° - 232°) and extends for 11 km from Loch Lochy to Loch Linnhe. Bedrock exposures are in the center of this mapped *'mylonite'* unit at ~ 200 - 250 m from the NE-SW striking faults (presumed to be sub-vertical) that bound the *'mylonite'* unit and also mark (at least in terms of map units) the margins of the Great Glen Fault Zone. Zones of bedrock 'crushing' are shown on BGS Sheet 62E as extending for a further 1 km in map view on the NW and SE sides of the GGFZ. Rocks on the NW side of the GGFS are mapped as psammites with subordinate pelites belonging to the Moinian (Moine Supergroup) on BGS Sheet 62E, while rocks on the SE side are mapped as quartz-feldspar 'granulites' of either Moinian or uncertain stratigraphic origin which are interlayered with and succeeded to the SE by mica schists, quartzites, limestones and slates ascribed to the Dalradian succession.

Remapping of the Moine succession in the Northern Highland Terrane to the NW of the GGFZ has placed rocks adjacent to the GGFZ near the Torcastle exposures within the Loch Eil Division (e.g., Strachan 1985; British Geological Survey 2007a, b; Mendum 2009; Strachan et al. 2010; Krabbendam et al. 2021) of the Moine Supergroup. No comparable stratigraphic remapping appears to have been done on the SE side of the GGFZ where the metamorphic rocks adjacent to the GGFZ are informally referred to as 'Dalradian' (e.g., Krabbendam et al. 2022) although they have also been ascribed to the Grampian Group of the Dalradian Supergroup (British Geological Survey 2007b; Stephenson et al. 2013).

The rocks in the Torcastle river-side exposures are composed of NE-SW striking psammitic gneisses and quartzites dipping steeply (~70 - 80°) to the SE and interlayered with micaceous/pelitic units, rare garnetiferous amphibolites and retrogressed intrusions of metabasite and lamprophyre (Fig. 5.3). Stewart et al. (2000) regarded this assemblage as lithologically most similar to the Glenfinnan Group (Moine Supergroup) of the Northern Highland Terrane which stratigraphically (and structurally) underlies the younger Loch Eil Group rocks of the Moine Supergroup mapped on the adjacent NW side of the GGFZ at Torcastle. This may indicate that the Torcastle rocks have been brought up from greater structural depths within the GGFZ (Stewart et al. 2000). Glenfinnan Group rocks are exposed at current ground level on the NW side of the GGFZ adjacent to the Strontian Granite at 55 km to the SW of Torcastle (British Geological Survey 2007; Mendum 2009) and the presence of Glenfinnan Group rocks within the GGFZ at Torcastle could alternatively be explained by 10s of km scale sinistral strike slip faulting. Equally however in this type of scenario Glenfinnan Group rocks are also exposed at current ground level on the NW side of the GGFZ at 10 and 45 km to the NE of Torcastle (e.g. Strachan 1985; British Geological Survey 2007a,b; Mendum 2009; Strachan et al. 2010) and the presence of Glenfinnan Group rocks within the GGFZ at Torcastle could also be explained by 10s of km scale dextral offset and strike slip faulting.

Brittle fractures are pervasively developed throughout the water-worn and polished Torcastle river-side exposures. These fractures anastomose around lenses of both relatively undeformed feldspar and quartz grains that exhibit microstructural evidence for earlier crystal plastic deformation. Sheared white mica and chlorite grains are locally present within zones of concentrated brittle shearing. Rarely exposed mineral lineations (composed mainly of comminuted quartz and phyllosilicates) within these brittle shear zones are sub-horizontal to gently plunging suggesting strike-slip shearing. Based on detailed outcrop-scale mapping Stewart et al. (1997, 1999, 2000) and Stewart (2010) recognized two main sets of steeply dipping shear zones (ranging from a few mm to a meter or more in width) within which brittle fracturing of quartz and feldspar grains is particularly concentrated. One set of shear zones strike ~ NE-SW sub-parallel to the local trend of the GGFZ. Rare shear sense indicators such as truncated folds suggest a sinistral shear sense (Stewart et al. 2000). The second set of shear zones strike ~ WNW-ESE and contain rare dextral shear sense indicators. Stewart et al. (1997, 1999, 2000) regarded the two sets of brittle shear zones as being broadly contemporaneous although the WNW trending dextral shear zones generally curve (counterclockwise in map view) into the NE-SW trending shear zones rather than displacing them. Stewart et al. (1997, 1999, 2000) considered that all these structural observations were consistent with bulk sinistral strike slip deformation within the Torcastle segment of the GGFZ.

Stewart et al. (1997, 1999) noted that while feldspar grains were only fractured and exhibited no microstructural evidence for plastic deformation, adjacent quartz grains exhibited microstructures (deformation bands and lamellae, undulose extinction, and highly serrated grain boundaries) indicative of at least limited crystal plastic deformation and dynamic recrystallization by grain boundary migration processes. No quantitative examples of potential kinematic indicators or mechanisms of dynamic recrystallization associated with plastic deformation (e.g., crystal fabrics or microstructures corresponding

to the three quartz recrystallization regimes proposed by Hirth & Tullis 1992 with increasing deformation temperatures and decreasing strain rates) were given for the Torcastle rocks. Nonetheless, Stewart et al. (1997, 1999, 2000) and particularly Holdsworth et al. (2001) were able to use all these observations to argue that the rock exposed at Torcastle (and also on the SE side of the Great Glen near Torcastle) had commenced shearing within the GGFZ while below the regional brittle-ductile transition zone and had then been progressively exhumed to higher structural levels with early crystal plastic microstructures being overprinted by brittle fracturing of both quartz and feldspar during ongoing sinistral strike slip shearing on the GGFZ. Stewart et al. (1997) reasoned that early shearing occurred at temperatures greater than c. 250 - 300 °C and less than c. 450 - 500 °C given the then-available consensus on minimum temperatures for the onset of crystal plasticity in quartz and feldspar, respectively. They also argued that because of the dominantly brittle deformation of phyllosilicates (white mica and chlorite) this early shearing probably occurred at the lower end of this likely temperature range suggesting a crustal depth of at least 10 km assuming normal geothermal gradients.

Rock sample locations and macroscopic structures

Five oriented rock samples were collected from the Torcastle North river-side exposures. The map positions of these samples are shown in Figures 5.1 – 5.3. All samples are quartz-rich psammites containing variable amounts of feldspar and white mica and are informally referred to in this thesis as quartzites. Sample GG-22-7 was collected from flat-lying waterworn and polished outcrops on the north side of River Lochy at UK Ordnance Survey grid reference NN 13496 79124 (see Table 1). Samples GG-22-3A – D were collected from a prominent 1 meter-wide almost vertical rib of quartzite exposed on the south side of the river at grid reference NN 13561 78983 (see Table 2.1).

North side of the river*:* Fracturing is spectacularly well-exposed at the mesoscopic scale in the polished and flat-lying exposures on the north side of the river. Fracturing is pervasively developed at the cm to 10s of cm scales dissecting the original quartzite into angular clasts (Fig. 5.4). Thin (mm scale) dark blue-gray zones of intensely comminuted quartz in which the rock has been ground down into a fine-grained lithified paste can be traced from 10s of centimeters across the flat-lying outcrops and generally strike WNW-ESE (Fig. 5.4). These fine-grained WNW-ESE shear zones cut across an earlier more pervasively developed 'WSW-ENE to SW-NE striking cataclastic banding'. All these structures are in turn cut across by a sub-vertical NE-SW (054° - 234°) fracture zone that traced along strike to the SW progressively changes from a single fault surface to a 10 cm wide zone of intense brecciation (Fig. 5.4).

South-side of the river*:* Fracturing is on first inspection less obviously developed at outcrop in the quartzite rib on the south side of the river, although careful examination of the oriented samples collected reveals that they are in fact cut by fractures developed at the cm-scale of spacing. A weakly developed foliation within this quartzite rib strikes ~ 060° and dips at ~ 75° SE and at least in map view appears to be sub-parallel to the contacts with the surrounding easily eroded micaceous layers. As noted above the GGFZ (as marked by the 500 m wide band of mylonites shown on BGS Sheet 62E) strikes NE-SW (052° - 232°)

in the Torcastle area. In sample GG-22-3B the external foliation surface has a polished appearance with a 'slickenside' mineral lineation composed of fine-grained comminuted quartz and probably phyllosilicate grains pitching at ~70° from the 060° strike direction. A stereonet-based calculation indicates that this equates to the slickenside lineation plunging at ~ 65° towards 095°. In sample GG-22-3D a very weakly developed lineation defined by elongate quartz (and some pink feldspar) grains pitches at ~ 70° from the 060° strike direction (plunging at ~ 65° towards 097°). This grain shape lineation appears to be more pervasively developed throughout the hand sample rather than a surface feature.

Microscopic rock sample descriptions

Oriented thin sections have been prepared for all samples collected from the Torcastle outcrops.

North side of river*:* In sample GG-22-7 from the north side of the river a vertically dipping NNW-SSE striking thin section was prepared (Figure 5.5). The sample is composed of quartz, orthoclase, and plagioclase feldspar grains with rare laths of white mica. The feldspar grains are often fractured and twins in some of the plagioclase grains are kinked, but otherwise have no other microstructural indicators for internal deformation. Both the orthoclase and plagioclase grains range from 4000 – 400 microns (4.0 – 0.4 mm) in size, are variably altered to sericite, and many are probably fracture clasts. Quartz grains exhibit undulose to blocky extinction indicating the operation of crystal plastic deformation. Quartz grains range from elongate to equant in cross section with grain sizes ranging from 500 – 100 microns. Local blocky extinction suggests that subgrain rotation recrystallization (SGR) has occurred, while gently curving quartz-quartz grain boundaries suggest an important component of grain boundary migration (GBM) recrystallization – possibly at earlier higher temperatures. Much smaller (tens of micron scale) indentations in quartz-quartz grain boundaries suggests that grain boundary bulging (GBB) has locally occurred – possibly with falling deformation temperatures. Microstructural domains with similarly oriented quartz grains locally define a vague grain shape foliation and these domains are separated by fracture zones. Some fractures are confined to individual feldspar clasts while other larger fractures cut across multiple feldspars as well as the intervening matrix of recrystallized quartz. Within the orthoclase feldspar clasts, the wider fractures are often infilled with feldspar that is in optical continuity with the host feldspar grain. Calcite is present as large (2000 – 1000 micron) grains that are often arranged in trails that may have crystallized along fractures. The calcite grains exhibit well-defined multiple sets of pencil-thin deformation twins.

South side of river – *Microstructures in thin sections cut parallel to geographic horizontal:* In samples GG-22-3A to C (Figs. 5.6, 5.7 & 5.8) oriented thin sections were cut parallel to the geographic horizontal to image any microstructures that might be associated with strike-slip shearing. In contrast to sample GG-22-7 collected on the north side of the river, samples GG-22-3A to C collected 120 m further to the south appear to be almost unfractured in the horizontally oriented thin sections. Widely spaced planar fractures measuring only a few microns in width do cross the whole thin section in these samples and exhibit two main orientations – with one set of fractures striking 110 - 290°

and the more variably oriented set have strikes ranging between 150 - 330 and 175 - 355°. Recrystallized quartz between these isolated fractures defines in thin section an easily recognizable grain shape foliation that is parallel to the 060° striking macroscopic foliation observed at the hand sample scale. This grain shape foliation is itself defined by a parallel alignment of ribbon-like relic quartz grains which have internally recrystallized into equant to slightly elongate new grains of closely similar crystal orientation, together with the parallel alignment of the more elongate new grains. A few elongated laths of white mica and chlorite are also aligned sub-parallel to this foliation. Very little apparent offset of the relic grains is seen along the fracture sets, suggesting that they are dominantly of extensional rather than strike-slip origin.

The equant to slightly elongate recrystallized quartz grain shapes and their development within the much larger ribbon-like relic grains unequivocally indicated that subgrain rotation is the dominant recrystallization regime experienced by quartz, most notably in samples GG-22-3A to C located on the south side of the river. Relic ribbon quartz grains are typically 1000 microns (1 mm) in width but commonly vary in length from 2000 to 5000 (2 - 5 mm) traced parallel to the grain shape foliation. Some of the less internally recrystallized relic ribbons exhibit deformation bands oriented sub-parallel to the grain shape foliation. Recrystallized quartz grains and quartz subgrains typically range from 125 - 100 microns in size. Rectangular highly altered orthoclase and plagioclase feldspar grains measuring from 250 - 750 microns in length are scattered throughout the dynamically recrystallized quartz matrix. The long axes of these feldspar grains range from parallel to perpendicular to the foliation defined by deformed and recrystallized quartz grains. The feldspar grains are intensely altered and overprinted by minute sericite grains. No microstructural evidence for plastic deformation (e.g., undulose extinction) or significant fracturing was found in these feldspar grains.

South side of river – *Microstructures in thin sections cut parallel to steeply plunging lineation:* In samples GG-22-3D (Fig. 5.9) a thin section was cut perpendicular to macroscopic foliation and parallel to the weakly defined and steeply plunging quartz grain shape lineation observed in hand sample. A block diagram explaining the orientation of this thin section relative to geographic and sample coordinates is presented in Figure 5.9. Basic microstructures observed in this lineation-parallel thin section resemble thin sections cut parallel to the geographic horizontal with rectangular feldspar grains dispersed in a matrix of quartz grains dominated by subgrain rotation recrystallization microstructures. However, feldspars range up to 1500 - 3000 microns (1.5 - 3.0 mm) in length. Foliation is primarily defined by elongate laths of white mica and chlorite and occasional development of white mica ‘fish’. Fractures are more commonly observed in this lineation parallel thin section – some are trans-granular fractures traversing the entire thin section while many smaller fractures are typically confined to single feldspar grains.

Kinematically the most important difference with the geographic horizontal thin sections is that in the thin section cut parallel to the steeply plunging lineation dynamically recrystallized quartz grains (typically 100 - 150 microns in size) define foliation-parallel ribbon-like aggregates in which the orientation of the long axes of the more elongate dynamically recrystallized grains are oriented oblique to foliation. Such oblique

dynamically recrystallized grains shape alignments have been widely reported in both experimentally deformed analogue materials (e.g., Means 1981) and naturally deformed quartzites (see reviews by Lister and Snoke 1984, Passchier & Trouw 2005) and form reliable and widely accepted shear sense indicators. Viewed towards the SW the oblique grain shape alignment in the lineation-parallel thin section cut from sample GG-22-3D indicates a NW side-up and SE side-down sense of shear. This shear sense interpretation is supported by asymmetrical rare white mica fish in the same thin section (Fig. 5.9C) and using the microstructural criteria proposed by Grotenhuis et al. (2003) – see also review by Passchier & Trouw (2005, p. 141 - 149).

South side of river –*Quartz crystal fabric measured in thin section cut parallel to steeply plunging lineation:* The c-axis fabric of 1000 dynamically recrystallized quartz were measured in (XZ) thin sections using a Leitz optical microscope and 4-axis universal-stage, where each sample was cut parallel to the ENE plunging mineral lineation and perpendicular to foliation. S. Mulcahy (Western Washington University) developed an Excel macro which was used to collect universal stage data. N. Mancktelow (ETH, Zurich) created the Stereoplot software used to contour these fabrics. The quartz c-axis fabric data are displayed on a lower hemisphere equal-area projection in which the data has been rotated into a projection plane viewed towards the SW (Fig. 5.10a & b) using the Stereonet software package. The measured quartz c-axes define a transitional Type I to II (Lister 1977) cross-girdle fabric in which the central segment crosses the foliation almost exactly perpendicular (± 1 - 2°) to the macroscopic quartz grain shape lineation. By analogy with numerical modelling of quartz c-axis fabric development (e.g. Lister & Williams 1979; Lister & Hobbs 1980) and both uniaxial compression and split-cylinder experimental plastic deformation of quartzites (e.g. Tullis 1977; Heilbronner & Tullis 2002, 2006) this relationship between grain shape lineation and the crossing of the foliation at right angles to lineation by the cross-girdle c-axis fabric (Fig. 2.15) unequivocally indicates that the steeply plunging quartz grain shape lineation has developed parallel to the maximum principal stretch direction (X) during on-going crystal plastic deformation and dynamic recrystallization. Also, numerical and experimental studies, such cross-girdle fabrics, are known to develop under close to plane strain (k=1) conditions. Additionally, the unequal inclination of the two girdles to the pole to foliation measured in the XZ plane (C1 and C2 angles in Fig. 5.10b) also unequivocally indicates a NW side-up and SE side-down shear sense. As noted above, this shear sense is also indicated by the alignment of elongate dynamic recrystallized quartz grains oblique to foliation and white mica ‘fish’ observed in the same thin section.

The measured quartz c-axis fabric in sample GG-22-3D also provides potential information on temperatures under which crystal plastic deformation has occurred as the fabric opening angle (combined C1 and C2 angles in Fig. 5.10b) increases with increasing deformation temperature, positively correlated with hydrolytic weakening and decreasing strain rate (see review by Law 2014). Using the linear opening angle thermometer of Faleiros et al. (2016) the combined C1 and C2 opening angle (68°) in the cross-girdle fabric from sample GG-22-3D would indicate a deformation temperature of ~ 515 °C.

Summary of deformation conditions for Torcastle North quartzites

Microstructural analysis of thin sections cut from the Torcastle North samples clearly indicate that the quartzites have undergone an early phase of crystal plastic deformation and dynamic recrystallization.

Sample GG-22-7 is dominated by subgrain rotation (SGR) recrystallization with some grain boundary migration (GBM) recrystallization of quartz which could be broadly contemporaneous with or earlier than SGR recrystallization. Stipp et al. (2002a, b) have demonstrated for the Tonale Line in the Italian Alps that GBM in quartz occurs at temperatures greater than ~ 500 °C while SGR occurs at temperatures of ~ 400 - 500 °C with a transition from GMB-SGR at ~ 490 - 525 °C. Assuming comparable strain rates and degree of hydrolytic weakening for the Tonale Line and Torcastle quartzites (see review by Law 2014) the GBM microstructures in sample GG-22-7 would suggest maximum deformation temperatures of ~ 490 - 525 °C. The lack of any significant plastic deformation (apart from occasional kinking of twins in the feldspar grains) suggests that deformation temperature probably did not significantly exceed these values indicated by the quartz recrystallization microstructures as minimum upper greenschist facies to lower amphibolite facies conditions are necessary to initiate crystal plastic creep in feldspars (Tullis 2002; Passchier & Trouw 2005, p. 58 and 260).

Samples GG-22-3A-D located ~ 120 m to the south of sample GG-22-7 is dominated by SGR quartz recrystallization microstructures possibly suggesting slightly lower deformation temperatures However, the opening angle for the quartz c-axis fabric from sample GG-22-3D indicates a deformation temperature of ~ 515 °C which is at the high end of the range of deformation temperatures (400 - 500 °C) usually associated with SGR recrystallization. The lack of any obvious microstructural evidence for crystal plastic deformation of feldspar in sample GG-22-3D also indicates that deformation temperatures did not significantly exceed ~ 500 °C. Assuming a geothermal gradient of ~ 30°C per km (as assumed by Holdsworth et al. 2001 in their paper on shearing in the Great Glen Fault Zone) this correspondence to a maximum depth of ~ 16 km.

Both microstructures (dynamically recrystallized grain shape alignments oblique to foliation, white mica fish) and the asymmetric cross-girdle fabric recorded in sample GG-22-3D unequivocally a NW side-up and SE side-down shear sense associated with the steeply plunging grain shape lineation (Fig. 5.10c & d). In present-day map view, this corresponds to an oblique sinistral sense of shear. The cross-girdle fabric also unequivocally demonstrates that this steeply plunging (65° towards 098°) grain shape lineation is a maximum principal stretch direction (X) associated with approximately plane strain deformation conditions. The small-circle component of c-axes in this fabric however may indicate deformation slightly within the flattening field but close to the plane strain (k=1) line (Lister & Hobbs 1980; Schmid & Casey 1986).

All these deformation features are compatible with a tectonic model involving exhumation of the Torcastle quartzites from below the brittle-ductile transition zone during ongoing sinistral shearing and transpression on the GGFZ. Assuming that fabric elements in the

Torcastle samples are still in close to their original orientations, the steeply plunging maximum principal stretch direction would indicate a steeply oriented ascent of the quartzites from beneath the brittle-ductile transition zone. As the quartzites ascended through the brittle-ductile transition zone they would, of course, have been overprinted by the brittle fault zones and fractures associated with strike-slip shearing that dominate the quartzites at the outcrop and hand sample scales.

Chapter 5 - Figures

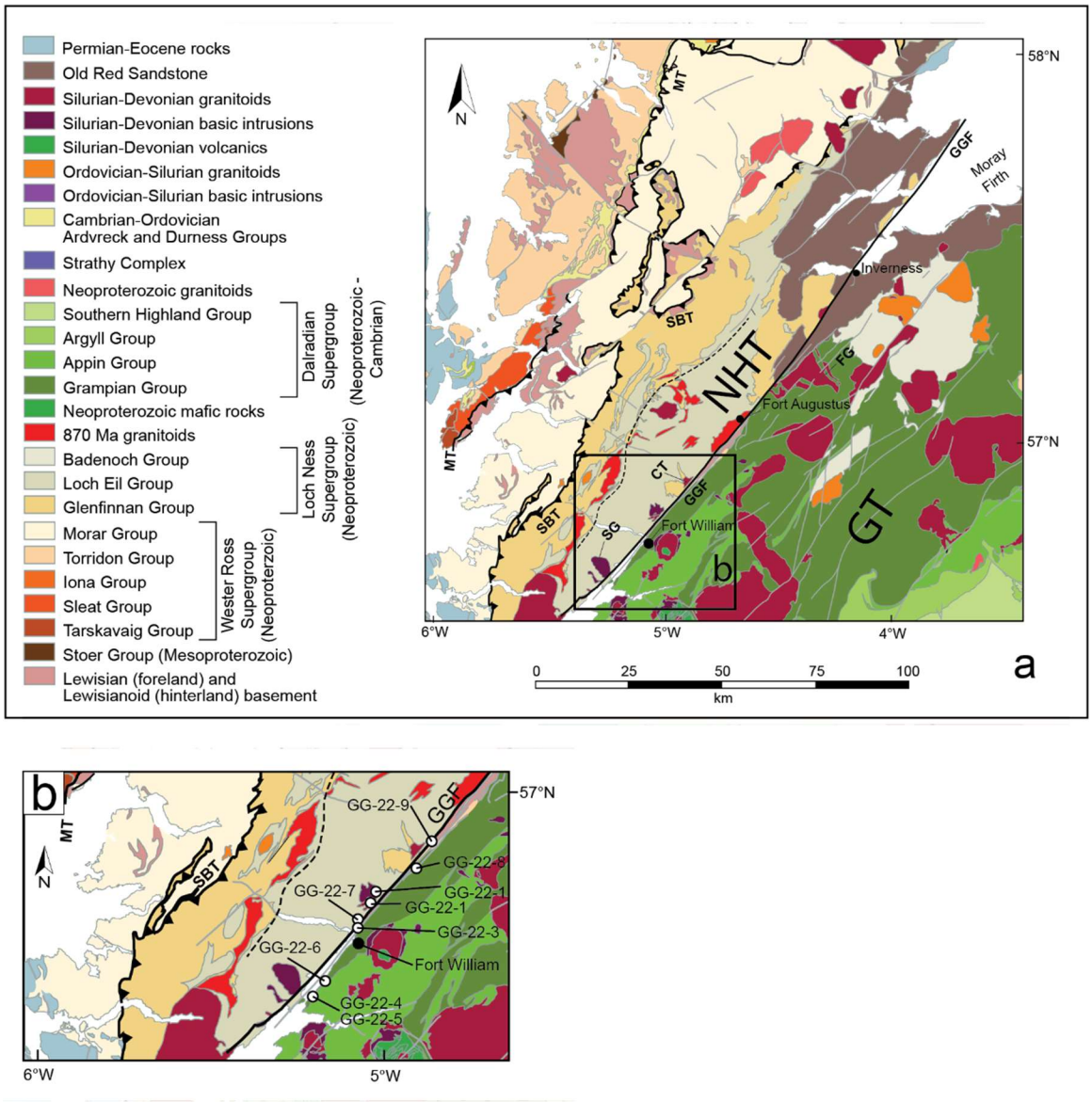

Figure 5.1. (a) Geologic map of the part of the Scottish Highlands, with groupings of sample locations indicated by black boxes; modified from Law et al. (in review; Figure 8.2). (b) Sample locations in the southern part of the Great Glen near Fort William; including Torcastle North samples GG-22-3 and GG-22-7.

Figure 5.2. Torcastle North sample locations (GG-22-3 and GG-22-7) from the SW and NW banks, respectively, of River Lochy. Sample locations indicated with purple circles. Image compiled from aerial photographs. Screenshot is taken from Google Earth.

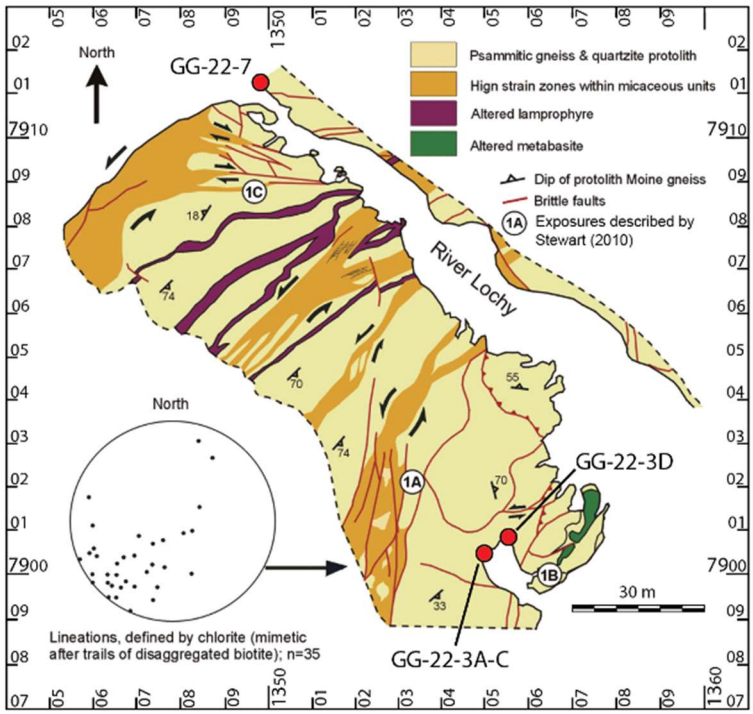

Figure 5.3. Geologic map of the Torcastle North riverside exposures with locations of samples GG-22-3A-C and GG-22-3D from the south bank of River Lochy and sample GG-22-7 from the north bank. UK Ordinance Survey grid coordinates are indicated. Adapted from the original geologic map of Stewart (2010). Figure 14.2; pg. 269. Used with permission from the Edinburgh Geological Society; email attached.

Figure 5.4. Water-worn and polished exposures of shattered quartzites near sample GG-22-7 on the north bank of River Lochy. Note extension fracture infilled with fracture fragments of quartzite surrounded by finer grained and darker cataclastic matrix.

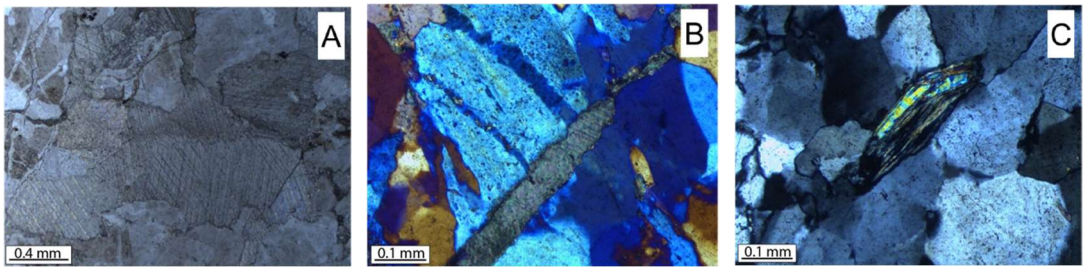

Figure 5.5. Micrographs from Torcastle North quartzite sample GG-22-7. Microstructures locally indicate high temperature plastic deformation (sinuous quartz grain boundaries indicate at least a minor component of grain boundary migration recrystallization). Lower temperature plastic deformation indicated by smaller scale highly lobate/bulging boundaries between quartz grains in turn indicating localized grain boundary bulging recrystallization. Lower temperature deformation also indicated by thin deformation twins in both large matrix calcite grains and calcite-fills in extension fractures cutting both feldspar and quartz grains.

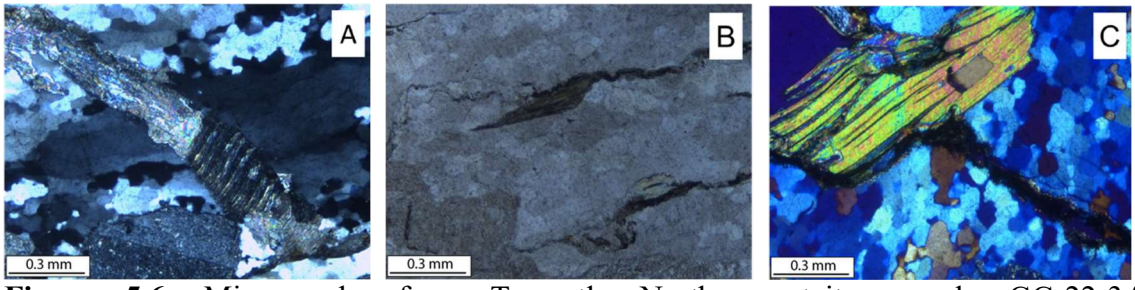

Figure 5.6. Micrographs from Torcastle North quartzite sample GG-22-3A. Microstructures indicate medium temperature plastic deformation (equant – slightly elongate quartz subgrains and new grains within larger host quartz grains) in turn indicating subgrain rotation recrystallization of quartz). Later lower temperature deformation indicated by calcite-filled extension fractures cutting across earlier microstructures. Note

late kinked white mica that overgrows fracture and apparent stylolite seams in plane polarized light micrograph.

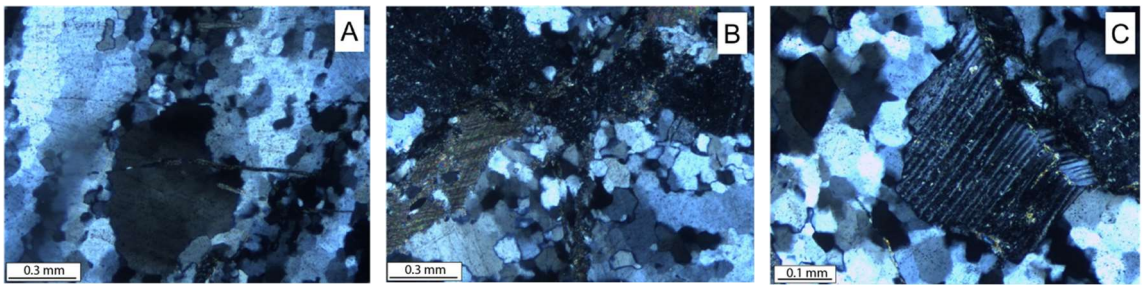

Figure 5.7. Micrographs from Torcastle North quartzite sample GG-22-3B. Microstructures indicate medium temperature plastic deformation (equant – slightly elongate quartz subgrains and new grains within larger elongate to ribbon-like host quartz grains) in turn indicating subgrain rotation recrystallization of quartz). Lower temperature plastic deformation is indicated by thin deformation twins in calcite grains and small highly lobate/bulging boundaries between quartz grains in turn indicating localized grain boundary bulging recrystallization. Note undulose extinction and bending of white mica grain. Bending of twin boundaries in feldspar clast could indicate either earlier higher temperature deformation of quartzite or older and unrelated protolith history of sedimentary feldspar clast.

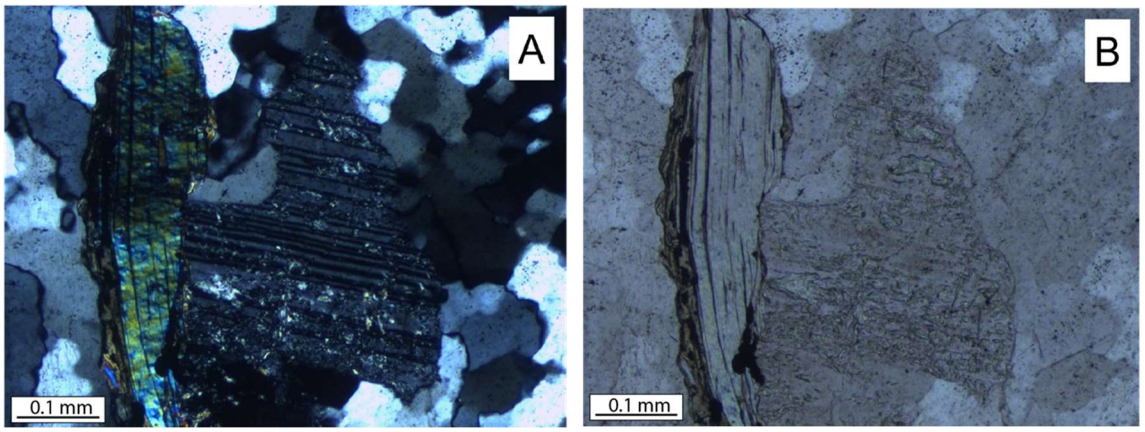

Figure 5.8. Micrographs from Torcastle North quartzite sample GG-22-3C taken in cross-polarized and plane polarized light of kinked white mica adjacent to plagioclase grain.

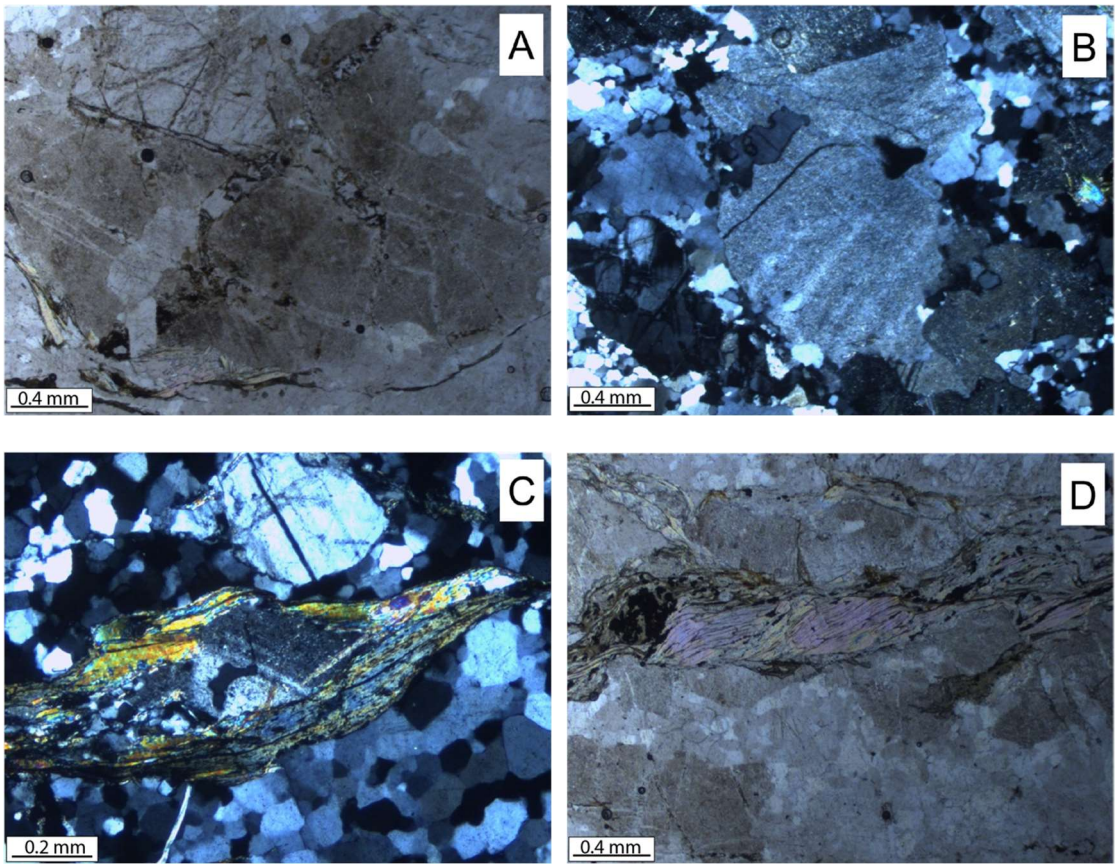

Figure 5.9. Micrographs from Torcastle North quartzite sample GG-22-3D. Note domains of feldspar grains surrounded by domains of finer grained quartz that has recrystallized by a combination of subgrain rotation and minor amounts of grain boundary migration. Note bending/kinking and fracturing of white mica grains and local interlayering of white mica and chlorite laths, some of which wrap around feldspar aggregates.

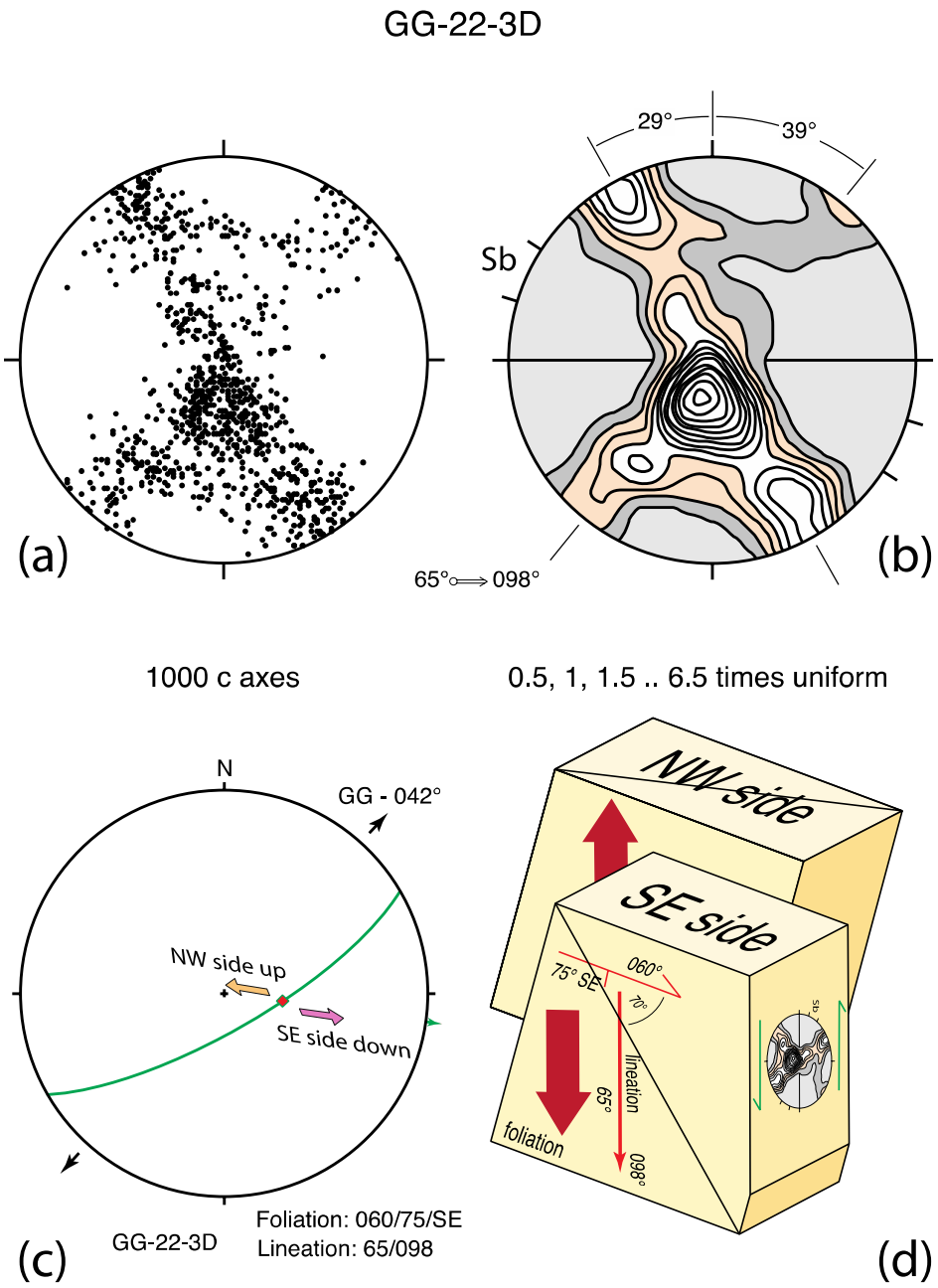

Figure 5.10. Optically measured quartz c-axis fabric from Torcastle North sample GG-22-3D and kinematic interpretation. (a, b) Scatter and contour plots of measured fabric; plunge and trend of mineral grain shape lineation in sample indicated. An opening angle of 68° between the leading and trailing edges of fabric indicates a likely deformation temperature of c. 515 °C. Sb – alignment of elongate dynamically recrystallized quartz grains. (c) Stereonet showing geographic orientation of foliation and lineation in sample and shear sense inferred from asymmetry of quartz fabric; local trend of Great Glen fault (GG) indicated. (d) Block diagram schematically illustrating 3D sense of shearing (NW side up to the SW and SE side down to the NE) indicated by fabric asymmetry and oblique grain shape alignment (Sb).

Chapter 6: Southeast Side of the Great Glen Fault

Sampling areas and tectonic setting

Three samples were collected on the SE side of the Great Glen Fault; all three samples are from roadcuts on the side of A82 road. Sample locations are shown in Figures 6.1 and 6.2, and traced from NE to SW, include GG-22-8, GG-22-6, and GG-22-4.

Sample GG-22-8 was collected on the SE side of Loch Lochy opposite a large well-marked parking layby on the A82 and on the SW side of a prominent waterfall (UK Ordnance Survey grid reference NN 2546591800; see Table 1). The location is almost due east of sample GG-22-1 collected within the Clunes tonalite on the opposite side of Loch Lochy (see Chapter 3) and is covered by UK Ordinance Survey 1:50,000 scale (Sheet 33) and 1:25,000 scale (Sheet 400) topographic maps. The location is also covered by British Geological Survey 1:50,000 scale Sheet 62E (British Geological Survey 1975) where it is placed within a map unit of *"Quartz-feldspar granulite of probable Moinian"* stratigraphic origin which is interlayered with and succeeded to the SE by mica schists, quartzites, limestones, and slates ascribed to the Dalradian succession. More recently these rocks exposed on the SE side of Loch Lochy have been ascribed to the Grampian Group of the Dalradian Supergroup (British Geological Survey 2007; Stephenson et al. 2013) or simply marked as 'Dalradian' (e.g., Krabbendam et al. 2022). The sampling location for GG-22-8 has been described in the field guide by Stewart (2010, his location 14.4) who regarded them as being microstructurally unlike any of the Grampian/Dalradian rocks exposed locally. Stewart (2010) suggested that the microstructures in these rocks (including coarse-grained crystals surrounding subgrains, as well as sutured grain boundaries) were more typical of the Moine metasedimentary rocks exposed on the NW side of the Great Glen or possibly gneissic basement rocks beneath the Grampian terrane (Badenoch Group), uplifted adjacent to the GGF as a result of transpressional displacements. The sampling location is c. 600 m from the NE-SW axis of Loch Lochy which presumably also marks the central core of the Great Glen Fault Zone.

Samples GG-22-6 and GG-22-4 (UK grid references NN 05941 68327 and NN 05610 67789, respectively) were collected on the SE side of Loch Linnhe, with sample GG-22-4 collected 550 m to the SW of GG-22-6. Both sampling locations are covered by UK Ordnance Survey 1:50,000 scale (Sheet 41) and 1:25,000 scale (Sheet 392) topographic maps. The locations are also covered by British Geological Survey 1:63,360 scale Sheet 53 (British Geological Survey 1985) and British Geological Survey 1:50,000 scale Sheet 53W (British Geological Survey 2007a). On BGS Sheet 53, the white-yellow quartzites at the sampling location for GG-22-6 are placed within the *Linnhe Quartzites* map unit at the base of the Dalradian succession of metasedimentary rocks, while on the more recent BGS Sheet 53W, the quartzites are included in the *Linnhe Psammite Member* of the Fort William Formation/Grampian Group of the Dalradian Supergroup. On BGS Sheet 53, the pale green psammites at the sampling location for GG-22-4 are also placed within the *Linnhe Quartzites*, while on the more recent BGS Sheet 53W, the psammites are placed in the stratigraphically younger *Linnhe Semipelite Member* of the Fort William Formation/Grampian Group. Subsequent publications (British Geological Survey 2007b;

Stephenson et al. 2013) have placed all the quartzites and psammites exposed along the SE shoreline of Loch Linnhe in the Grampian Group. No previously published geologic descriptions or field guides for these locations have been found, although the sedimentology of the Grampian Group metasedimentary rocks exposed along the SE side of Loch Linnhe has been discussed by Glover (1993). Stewart et al. (1999) and Holdsworth et al. (2001) have described phyllonitic and cataclastic fault zones trending NE-SW on the SE shoreline of Loch Linnhe approximately 3 km to the NE of the location for sample GG-22-6, but these exposures are now overgrown and obscured. Both sampling locations are c. 600 m from the NE-SW trending axis of Loch Linnhe, which is further to the SE, coincides with the mapped position of the Great Glen Fault on BGS Sheet 53W between Corran and Sallachan Point (British Geological Survey 2007a).

Microstructures and crystal fabrics

Unoriented ***Sample GG-22-8*** (Fig. 6.3) is a banded gneiss composed of alternating pink and pale green bands ranging from 1 to 2 cm in width. The pink bands are composed of sericitized orthoclase and plagioclase feldspar grains measuring up to 500 microns in size with interstitial irregularly shaped quartz grains ranging from 250 - 500 microns in size. The pale green bands are dominated by large quartz grains measuring up to 5 mm in size with subsidiary highly sericitized orthoclase and plagioclase grains up to 2.5 mm in size, all wrapped around by an anastomosing network of chlorite and white mica laths with the larger white mica grains measuring up to 750 microns in length. Particularly in the pale green bands the large quartz grains are highly strained internally, forming lozenge to elliptical grains shapes with long axes aligned sub-parallel to the compositional banding.

Quartz grains display undulose extinction, deformation bands, and basal plane tilt walls with deformation lamellae oriented perpendicular to the tilt walls and indicating basal <a> crystal plastic slip. Quartz-quartz grain boundaries are marked by 30 - 120-micron grain boundary bulges suggesting at least incipient grain boundary bulging (GBB) recrystallization. These microstructures are very similar to quartz microstructures described by Derez et al. (2015) and Singleton et al. (2020) in quartzites naturally deformed under lowermost greenschist facies (chlorite grade) conditions at temperatures of approximately 300 °C – i.e., in the transition zone between epizonal and greenschist conditions. The crystal lattices of the larger (c. 100 - 200 micron) white mica grains are internally kinked and exhibit sweeping/blocky extinction. The more rectangular elongated feldspar grains are aligned with their long axes parallel to the compositional banding. Internally the feldspar grains exhibit either no, or at most very weakly developed, undulose extinction. A few plagioclase grains exhibit very gently flexed twin planes. The feldspar grains are commonly fractured with some of the larger (100-micron width) cracks filled with either quartz or fibrous white mica and sericite oriented perpendicular to the crack walls. Some of these cracks terminate at feldspar-quartz grain boundaries while a few pass on into the adjacent quartz grains. Trails of white mica and sericite/chlorite anastomose between the quartz and feldspar grains probably indicate diffusive mass transfer (pressure solution) processes. Most of these quartz and feldspar microstructures indicate penetrative deformation under lowermost greenschist facies conditions with dislocation glide in quartz, brittle cracking in feldspar, and diffusive mass transfer/pressure solution operating between

the mineral grains and leading to reprecipitation of quartz and mica in the dilatant cracks. The weakly developed undulatory extinction in the feldspar grains could indicate earlier higher temperature deformation but can also be explained by incipient fracturing and healing of microcracks in the feldspar crystal lattice leading to slightly different extinction positions between fracture blocks (Tullis & Yund 1992; McLaren & Pryer 2001; Stünitz et al. 2003; Hentschel et al. 2019).

Oriented ***Sample GG-22-6*** (Figs. 6.4 & 6.5) is a strongly foliated and lineated pale green/yellowish quartzite. Foliation strikes 050° and dips at 75° SE and the grain shape lineation pitches at 85°on the foliation and plunges at 74° towards 121° (Fig. 6.6d). This steep angle of lineation pitch on a NE-SW striking foliation is similar to that in sample GG-22-3 from the Torcastle quartzites in the center of the Great Glen Fault Zone (Chapter 5; Fig. 5.10). In thin-section, macroscopic foliation is defined by trails of highly elongated white mica grains.

In thin sections cut perpendicular to foliation and parallel to lineation recrystallized quartz grains vary from equant (c. 250 microns) to highly elongated (up to 750 x 125 microns) in shape with their long axes typically aligned at 10 - 30° to the macroscopic foliation and defining an oblique grain shape alignment (Sb; See Fig 6.4). As outlined above for the Torcastle area (Chapter 5), such oblique dynamically recrystallized grains shape alignments have been widely reported in both experimentally deformed analog materials (e.g., Means 1981) and naturally deformed quartzites (see reviews by Lister and Snoke 1984, Passchier & Trouw 2005) and form reliable and widely accepted shear sense indicators. Viewed towards the SW, the oblique grain shape alignment in the lineation-parallel thin section cut from sample GG-22-6 indicates a NW side-down and SE up-down sense of shear (Fig. 6.6c, d).

Internally quartz grains exhibit undulose extinction, deformation bands, and prism plane tilt walls with deformation bands, commonly oriented sub-parallel to the oblique grain shape alignment (Sb). Such oblique grain shape alignments are usually observed in quartzites dominated by subgrain rotation (SGR) recrystallization (e.g., Means 1981), although subgrains are only occasionally observed within the smaller quartz grains in sample GG-22-6. Trails of minute (a few microns) white mica laths aligned sub-parallel to the macroscopic foliation are found within the larger quartz grains suggesting that recrystallization of quartz has been dominantly by grain boundary migration (GBM) in which the small micas have not acted as barriers to migrating grain boundaries. This has been referred to as GBM II recrystallization by Stipp et al. (2002a, b). Quartz-quartz grain boundaries range from gently curving, suggesting that GBM recrystallization is dominant, to highly lobate indicating the at least local importance of grain boundary bulging. Quartz recrystallization in GG-22-6 undoubtedly started in the high-temperature GBM II regime and with the progressive exhumation and cooling transitioned through first the transitional GMB-SGR regime (at temperatures of c. 500 °C) and then rapidly through the SGR regime (as few subgrains seem to have been formed or preserved) and finally into the lower temperature (300 - 400 °C) regime where late-stage grain boundary bulging was dominant.

A few orthoclase and plagioclase feldspar grains (measuring up to 750 - 1000 microns) are observed scattered throughout the matrix of dynamically recrystallized quartz grains in sample GG-22-6. The feldspar grains are often lozenge shaped with their long axes oriented sub-parallel to the quartz grain shape alignment (Sb). The larger felspar grains exhibit no undulose extinction but are internally fractured with individual cracks (up to 75 microns in width) infilled with either quartz or white mica. These cracks typically terminate at the edges of the feldspar grains. Smaller feldspar grains have clearer undulatory extinction suggesting at least a minor component of crystal plastic deformation.

In thin sections cut perpendicular to foliation and parallel to the foliation strike direction in sample GG-22-6, recrystallized quartz grains range in shape from equant to elongate, but unlike in the XZ thin sections cut parallel to lineation, in these approximately YZ sections, the elongate quartz grains have long axes parallel to the macroscopic foliation. Internally the quartz grains demonstrate similar microstructures to those seen in the XZ thin sections although subgrain formation and trails of white mica inclusions are more clearly seen within the larger quartz grains. Plagioclase grains also exhibit more clearly defined undulose extinction and tapering deformation twins.

The c-axes of 1000 quartz grains were measured in the XZ thin section using an optical microscope and universal stage. Analytical details for such fabric analyses have previously been given in Chapter 2 for the Rosemarkie area. The measured quartz c-axes (Fig. 6.6a, b) define a transitional Type I to II (Lister 1977) cross-girdle fabric in which the central fabric segment crosses the foliation almost exactly perpendicular (± 1 - 2°) to the macroscopic quartz grain shape lineation, unequivocally indicating that the steeply plunging quartz grain shape lineation has developed parallel to the maximum principal stretch direction (X) during on-going crystal plastic deformation and dynamic recrystallization. The unequal inclination of the two girdles to the pole to foliation measured in the XZ plane (C1 and C2 angles) also unequivocally indicates a NW side-down and SE side-up shear sense (Fig. 6.6c, d). As noted above, this shear sense is also indicated by the alignment (Sb) of elongate dynamic recrystallized quartz grains oblique to macroscopic foliation in the same thin section. Using the Faleiros et al. (2016) linear opening angle thermometer, the combined C1 and C2 opening angle (64°) in the cross-girdle fabric from sample GG-22-6 would indicate a deformation temperature of ~ 490 °C.

Oriented ***Sample GG-22-4*** is a dark green psammite with foliation oriented parallel to color banding (strike 036° dipping at 70° SE) and a weakly developed mineral grain shape lineation that plunges approximately down the dip of the foliation. Thin sections (Fig. 6.7) were cut perpendicular to the foliation and parallel to the dip direction of the foliation. Grain size is much smaller than in sample GG-22-6 collected 550 m along strike to the NE.

Quartz grains range in shape from equant (up to 100 microns in diameter) to elongate with long:short axial ratios rarely exceeding 3:1 and maximum grains sizes of 150 microns x 50 microns. Orthoclase and plagioclase feldspar grains are of similar aspect ratios and sizes, and the long axes of both the quartz and feldspar grains are aligned parallel to the foliation trace. The quartz and feldspar grains are wrapped by an anastomosing network of white mica and chlorite which helps to define the macroscopic foliation in thin section. Different

proportions of chlorite relative to the other mineral grains result in the macroscopic color banding seen in hand sample. The larger quartz grains have well-developed subgrain microstructures (typically measuring 50 - 60 microns) and have clearly recrystallized by subgrain rotation (SGR) mechanisms. The feldspar grains appear to have retained their original detrital grain shapes and are internally undeformed.

The grain shape foliation defined by quartz, feldspar, white mica, and chlorite grains is cut across at 25° by a 1250 micron (1.25 mm) wide shear zone that can be traced across the entire thin section and hand sample. The shear zone appears to strike subparallel to the foliation but dips more steeply at 85° to the NW. The shear zone is filled with dynamically recrystallized quartz with a few elongated grains of calcite. Quartz grains within the shear zone are elongated (c. 200 x 100 microns) and define a grain shape foliation that is slightly oblique (c. 3 - 5 ° maximum) to the shear zone margins. Subgrains (typically measuring 50 microns in size) are well developed in the larger elongated quartz grains. Insertion of an analyzer plate demonstrates that the quartz grains in the shear zone have an intense crystal-preferred orientation that would indicate a NW side up and SE side down shear sense along the steeply SE plunging mineral lineation (Fig. 6.8e, f).

Late sub-horizontal and NW-dipping fractures (measuring up to 75 microns in width and filled with calcite) cut across both the grain shape foliation and the later shear zone. Some of the larger calcite grains display well-developed twin sets inclined at 120° to each other.

The c-axes of 1000 matrix quartz grains were measured in the XZ thin section using an optical microscope and universal stage. Analytical details for such fabric analyses have previously been given in Chapter 2 for the Rosemarkie area. The measured quartz c-axes (Fig. 6.8a, b) define a transitional Type I to II (Lister 1977) cross-girdle fabric in which the central fabric segment crosses the foliation almost exactly perpendicular (± 1 - 2°) to the macroscopic quartz grain shape lineation, unequivocally indicating that the steeply plunging quartz grain shape lineation has developed parallel to the maximum principal stretch direction (X) during on-going crystal plastic deformation and dynamic recrystallization. The unequal inclination of the two girdles to the pole to foliation measured in the XZ plane (C1 and C2 angles) also unequivocally indicates a NW side-up and SE side-down shear sense (Fig. 6.8e, f). The opening angle (C1 + C2) between the leading and trailing edges of the cross-girdle fabric (Fig. 6.8b) indicates a deformation temperature of ~ 540 °C using the linear opening angle thermometer of Faleiros et al. (2016).

The c-axes of 500 quartz grains were also measured within the crosscutting shear zone in sample GG-22-4 (Fig. 6.8c-d). The measured c-axes define a dominant single girdle fabric also intersecting the matrix foliation at 90° to lineation in the hand sample and strongly indicating that the shearing which produced both the matrix grain shape fabric /crystal fabric and the shear zone fabrics are kinematically linked as they share a common intermediate principle stretch direction (Y) which plunges at 5° towards 214°. A few of the quartz grains within the shear zone begin to define a trailing edge girdle. The leading-edge single girdle c-axis fabric is inclined at 86° to the shear zone margins and this sense of obliquity is consistent with NW side-up and SE side-down shear sense (Fig. 6.8e-f). as also

indicates by both the orientation of elongate dynamically recrystallized quartz grains (Sb) within the shear zone and c-axis fabric asymmetry in the surrounding matrix quartz grains outside the shear zone. This shear sense for sample GG-22-4 is the opposite of that indicated by the quartz microstructures and c-axis fabric in sample GG-22-6 at 550 m along strike to the NE, but the same shear sense as that found in sample GG-22-3 from the core of the Great Glen Fault Zone at Torcastle (Chapter 5).

Chapter 6 - Figures

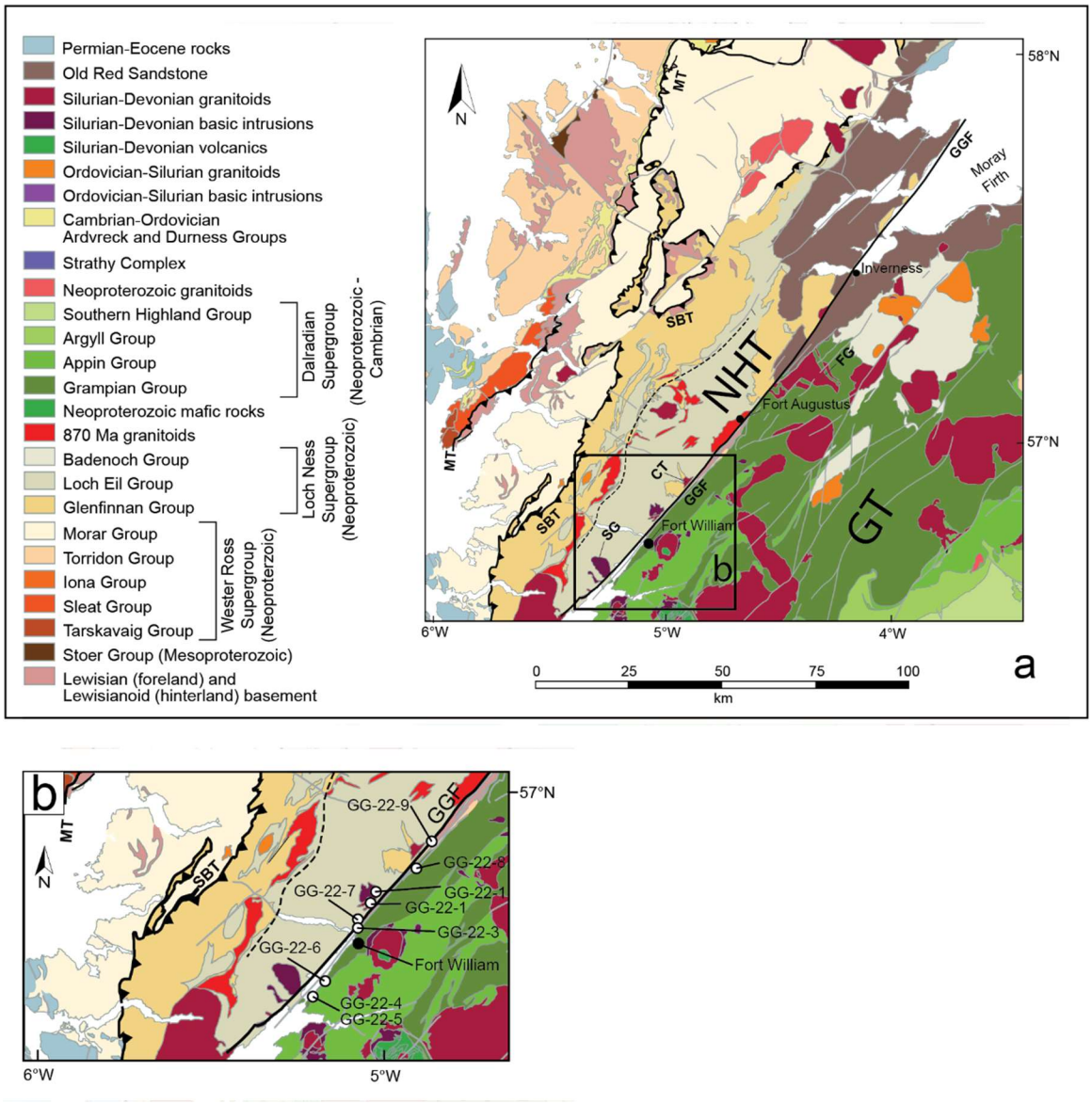

Figure 6.1. (a) Geologic map of the part of the Scottish Highlands, with groupings of sample locations indicated by black boxes; modified from Law et al. (in review; Figure 8.2). (b) Sample locations in the southern part of the Great Glen near to Fort William; including sample GG-22-8 collected from basal Dalradian on the SE side of the fault zone to the NE of Fort William and samples GG-22-4 and GG-22-6 collected from Dalradian

quartzites on the SE side of the fault zone to the SW of Fort William. NHT = Northern Highlands Terrane, GT = Grampian Terrane, SG = Strontian Granite, CT = Clunes Tonalite, FG = Foyers Granite, GGF = Great Glen Fault, MT = Moine Thrust, SBT = Sgurr Beag Thrust.

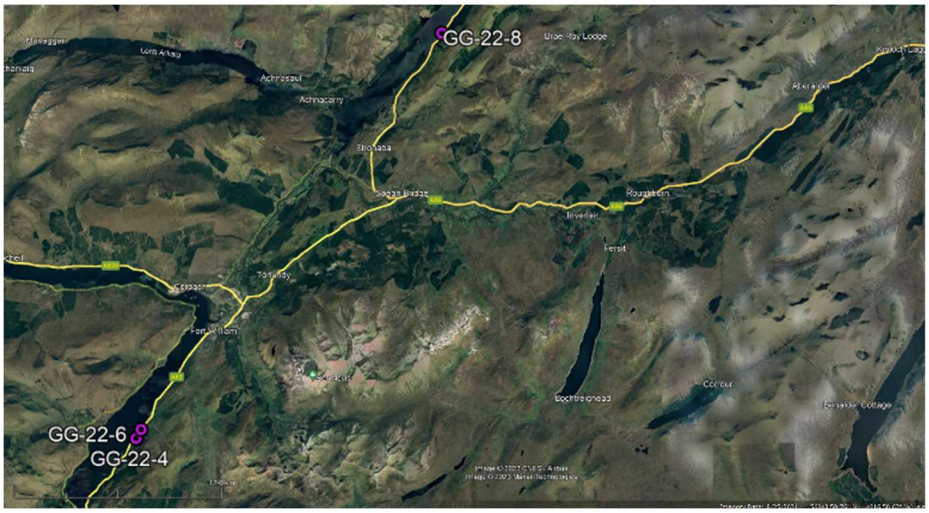

Figure 6.2. Sampling locations (GG-22-8, GG-22-4 and GG-22-6) on the SE side of the Great Glen fault Zone. GG-22-8 to NE of Fort William and GG-22-4 and GG-22-6 to the SW of Fort William. Sample locations indicated with purple circles. Image compiled from aerial photographs. Screenshot is taken from Google Earth.

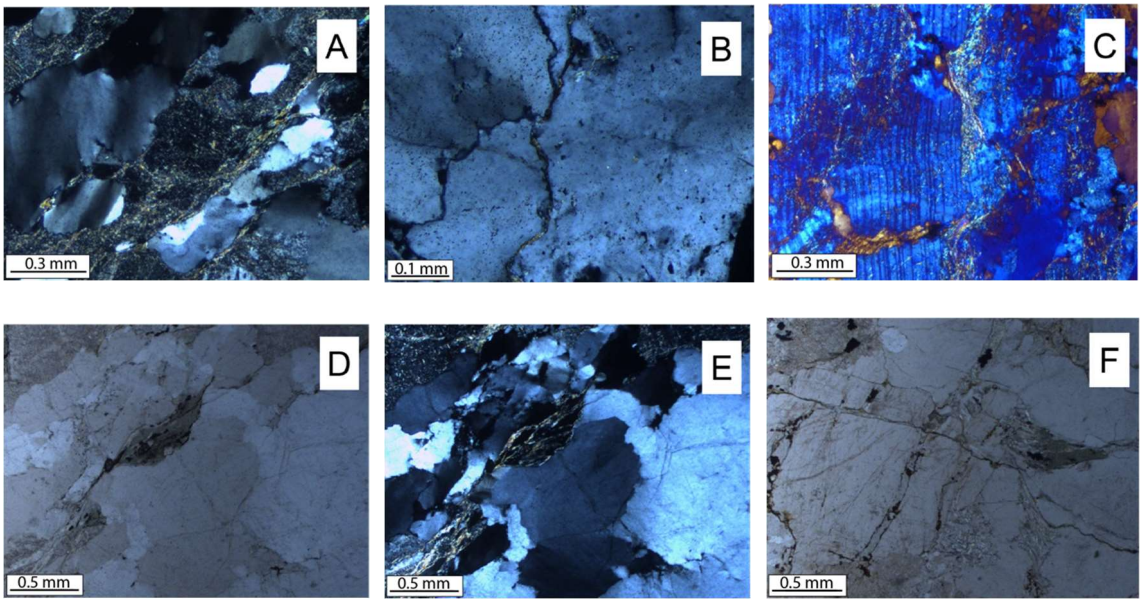

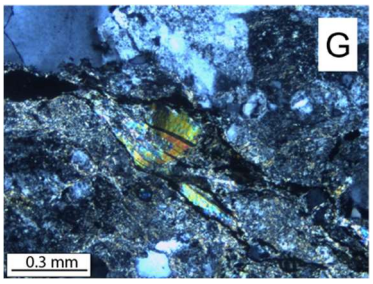

Figure 6.3. Micrographs from basal Dalradian sample GG-22-8. Microstructures indicating relatively low temperature plastic deformation of quartz include small highly lobate/bulging boundaries between quartz grains in turn indicating localized grain boundary bulging recrystallization; patchy and undulose extinction in quartz grains; kinking of white mica grains. Potentially earlier and higher temperature deformation is indicated by plagioclase grains with flexed/kinked twin planes. Late brittle deformation indicated by extension fractures infilled with white mica or calcite and locally offsetting twins in plagioclase grains. Note intense sericitization of some feldspar grains.

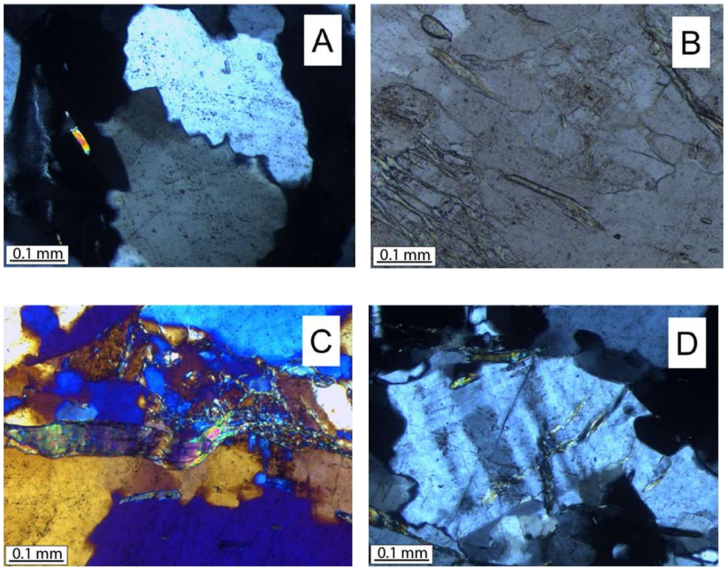

Figure 6.4. Micrographs from basal Dalradian quartzite sample GG-22-6A; section cut perpendicular to mylonitic foliation and parallel to steeply plunging grain shape lineation. Microstructures indicating relatively high temperature plastic deformation include kinking/flexing of twin planes within plagioclase grains; alignment of small white mica laths within much larger quartz grains; and gently curving quartz-quartz grain boundaries suggesting grain boundary migration recrystallization. Microstructures indicating relatively low temperature plastic deformation include small highly lobate/bulging boundaries between quartz grains in turn indicating localized grain boundary bulging recrystallization; extension cracks infilled with white mica within feldspar grains.

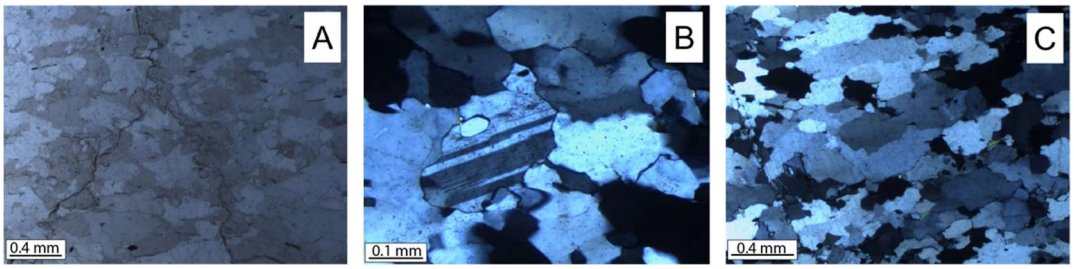

Figure 6.5. Micrographs from basal Dalradian quartzite sample GG-22-6B; section cut perpendicular to mylonitic foliation and parallel to geographic horizontal. Possible early high temperature plastic deformation of quartz and feldspar indicated by gently curving quartz-feldspar grain boundaries suggesting grain boundary migration recrystallization. Relatively low temperature plastic deformation indicated by small, highly lobate/bulging boundaries between quartz grains in turn indicating localized grain boundary bulging recrystallization – with local development of island grain microstructures. Late fractures cut across plastically deformed grains.

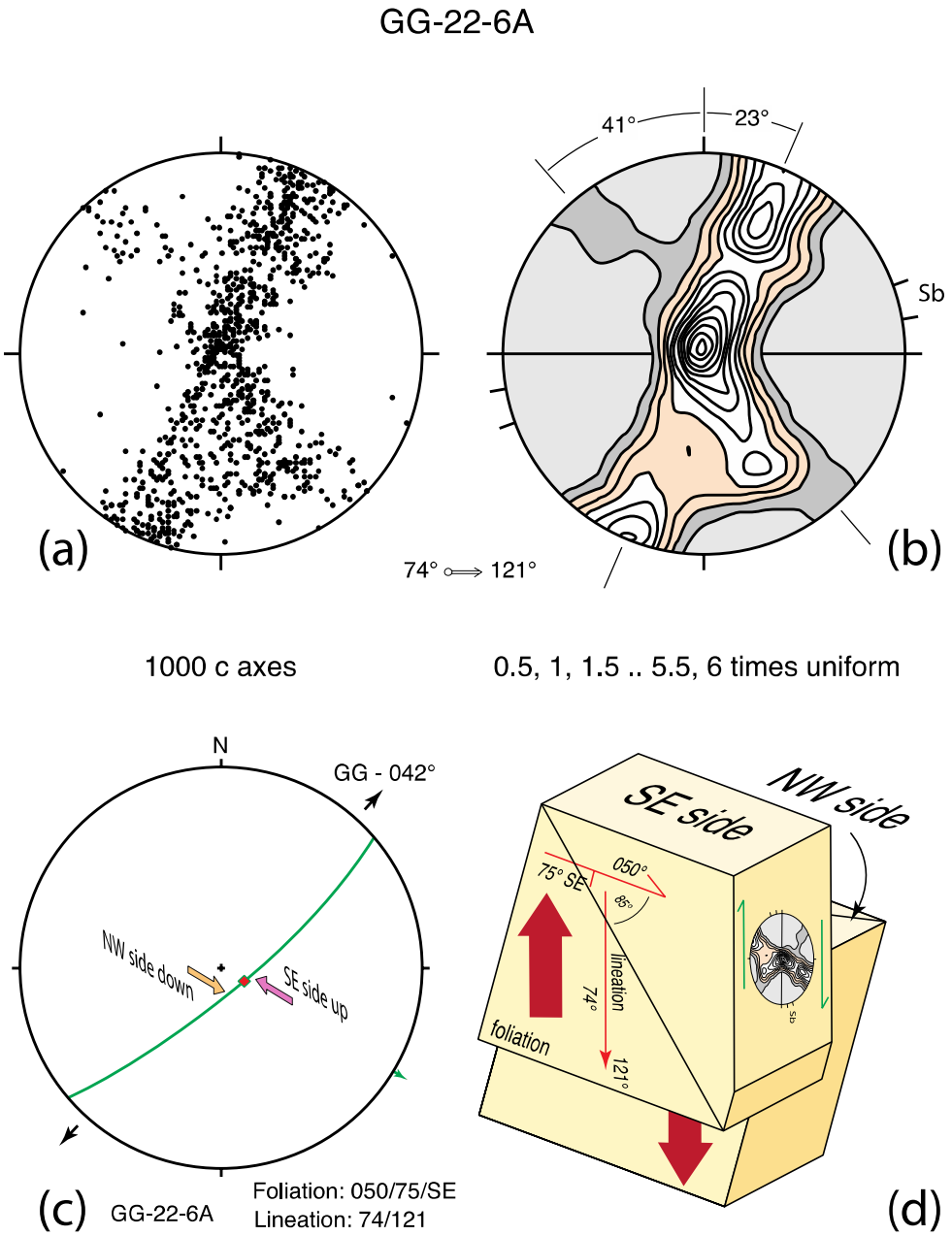

Figure 6.6. Optically measured quartz c-axis fabric from Dalradian quartzite sample GG-22-6A and kinematic interpretation. (a, b) Scatter and contour plots of measured fabric; plunge and trend of mineral grain shape lineation in sample indicated. An opening angle of 64° between the leading and trailing edges of fabric indicates a likely deformation temperature of c. 490 °C. Sb – alignment of elongate dynamically recrystallized quartz grains. (c) Stereonet showing geographic orientation of foliation and lineation in sample and shear sense inferred from asymmetry of quartz fabric; local trend of Great Glen fault (GG) indicated. (d) Block diagram schematically illustrating 3D sense of shearing (NW side down to the NE and SE side up to the SW) indicated by fabric asymmetry and oblique grain shape alignment (Sb).

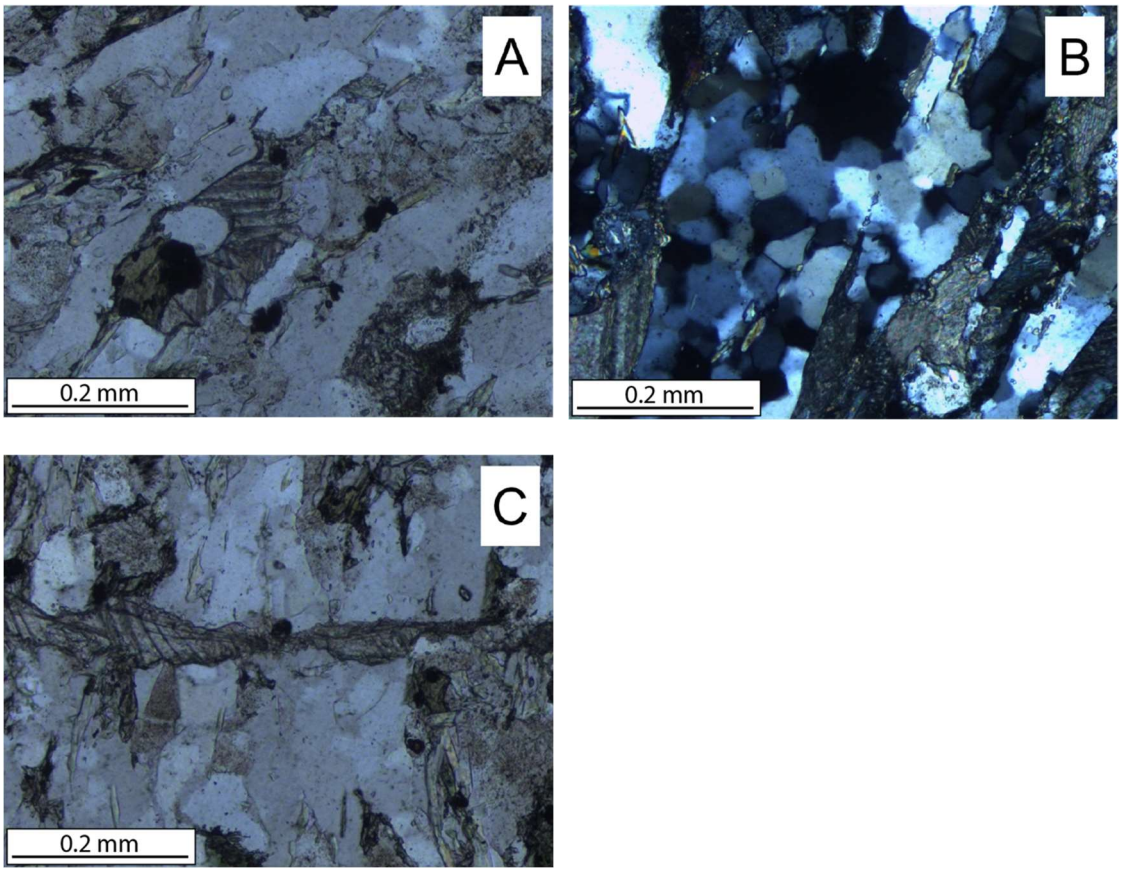

Figure 6.7. Micrographs from basal Dalradian quartzite sample GG-22-4; section cut perpendicular to mylonitic foliation and parallel to geographic horizontal. Larger quartz grains have well developed subgrain microstructures indicating plastic deformation and dynamic recrystallization by subgrain rotation. Late extensional fractures filled with calcite crosscut grain shape fabric defined by plastically deformed quartz grains. Micrographs from basal Dalradian quartzite sample GG-22-6A; section cut perpendicular to mylonitic foliation and parallel to geographic horizontal.

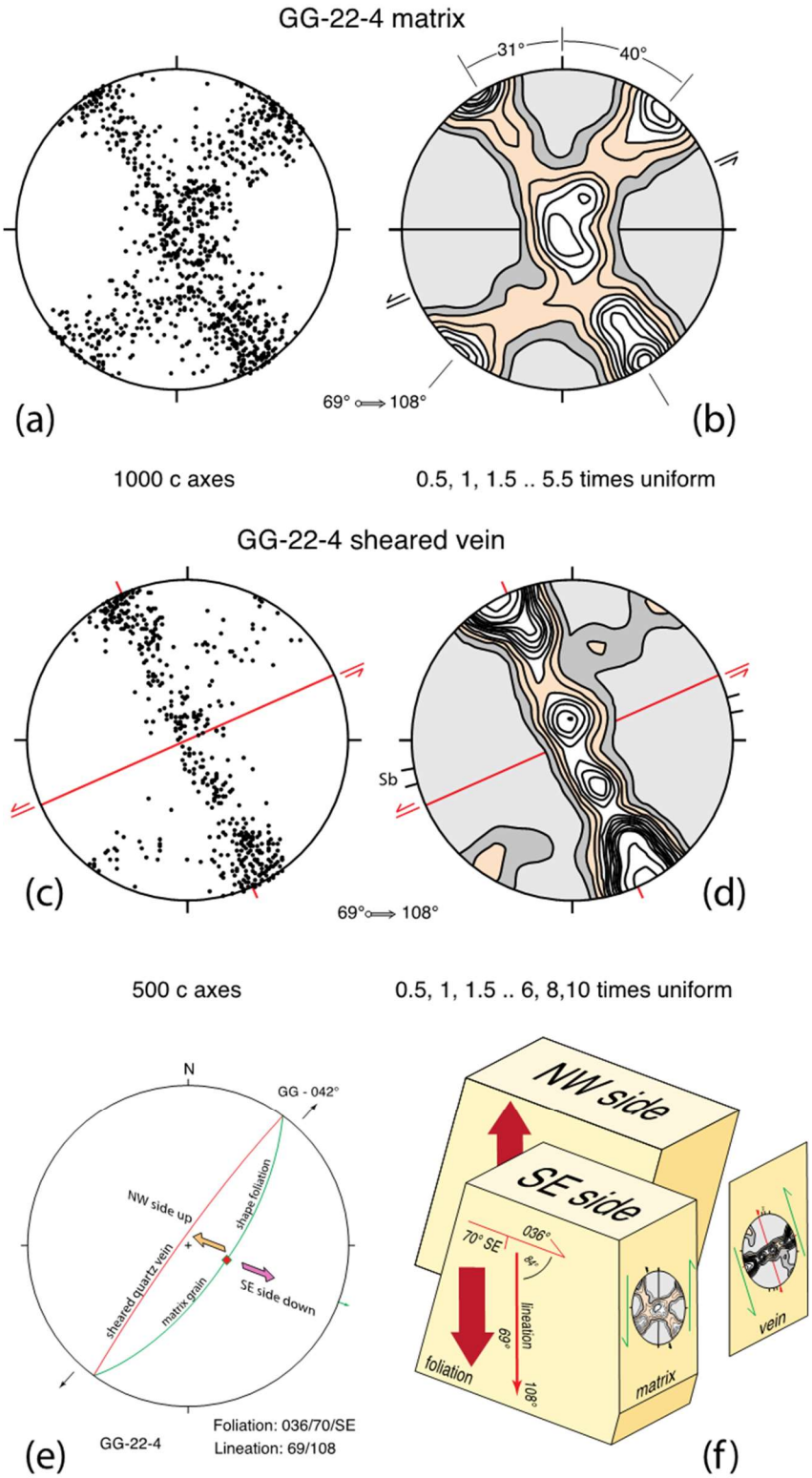

Figure 6.8. Optically measured quartz c-axis fabric from Dalradian quartzite sample GG-22-4 and kinematic interpretation. (a, b) Scatter and contour plots of measured fabric in matric quartz grains; plunge and trend of mineral grain shape lineation in sample indicated. An opening angle of 71° between the leading and trailing edges of fabric indicates a likely deformation temperature of c. 540 °C. (c, d) Scatter and contour plots of measured fabric

from quartz grains in sheared quartz vein cutting across matrix grain shape foliation. An opening angle of 62° between the strongly defined leading edge and the poorly defined trailing edge of fabric indicates a likely deformation temperature of c. 480 °C. Sb – alignment of elongate dynamically recrystallized quartz grains within vein/shear zone. (e) Stereonet showing geographic orientation of matrix foliation/lineation and crosscutting quartz vein in sample and shear sense inferred from asymmetry of quartz fabrics in both matrix and vein; local trend of Great Glen fault (GG) indicated. (f) Block diagram schematically illustrating 3D sense of shearing (NW side up to the NSW and SE side down to the SE) indicated by fabric asymmetries and oblique grain shape alignment (Sb) in both matrix quartz grains and crosscutting sheared quartz vein.

Chapter 7: Summary of Results

The Great Glen Fault (GGF) is a fundamental crustal-scale structure in northern mainland Scotland separating two Caledonian terranes (the Northern Highland and Grampian terranes to the NW and SE of the fault zone) with different Ordovician – Silurian tectonic histories. Although brittle deformation features associated with motion on the GGF at crustal levels above the brittle-ductile transition zone have been documented over the last two or three decades, crystal plastic deformation features developed deeper in the crust below the transition zone are rarely exposed and, therefore, less frequently documented. An important exception here is the documentation of quartz crystal plastic deformation microstructures from the center of the fault zone in the Torcastle area by Stewart et al. (1999, 2000). However, no kinematic interpretations (e.g., shear senses) were advanced with these published descriptions, and no assessment was made of the likely range of deformation temperatures over which these microstructures may have formed.

To address this issue, I collected suites of oriented rock samples from field areas adjacent to the GGF where evidence for crystal plastic deformation has not been completely overprinted by later brittle deformation. From NE to SW these areas include a) the Rosemarkie coastal section on the NW side of the fault zone and located on the Black Island to the north of Inverness; b) the Torcastle area in the center of the fault zone approximately 3 km to the north of Fort William and c) roadside exposures on the SE side of the fault zone to the south of Fort William.

Strike-slip motion on the GGF (and associated parallel trending faults such as the Strathconnon Fault) is traditionally thought of as beginning in late Silurian times with a phase of sinistral shearing (e.g., Watson 1984). This traditional view has been supported by field and microstructural studies of radiometrically dated plutons (428 ± 2 Ma Clunes tonalite on NW side of the GGF; 425 ± 3 Ma Ratagain pluton on NW side of the Strathconnon Fault) indicating that the plutons were intruded and cooled during sinistral motion on the adjacent faults (Hutton & McErlean 1991; Stewart et al. 2000). This view has been challenged by Searle (2021) who argued that there was no compelling evidence for these plutons being intruded during shearing on the adjacent faults, but that strike-slip motion may post-date intrusion.

To address this second issue, I collected oriented rock samples from the Clunes tonalite and the Glen Garry Vein Complex on the NW side of the GGF and from the Ratagain pluton on the NW side of the Strathconnon Fault.

Deformation conditions and kinematics of plastic deformation in metasedimentary rocks adjacent to the GGFZ

In all five samples analyzed, the quartz c-axis fabrics obtained by optical microscopy and universal stage work demonstrate that the NE to E plunging grain shape lineation has developed parallel to the maximum principal stretch direction (X). A major difference between the Rosemarkie samples on the NW side of the fault zone and samples further to the south in the center and on the SE side of the fault zone is that while lineation at

Rosemarkie plunges moderately (0 - 50°) to the NE to ENE, lineations in the south plunge steeply (65 - 74°) to the E to ESE (Fig. 7.1). Additionally, while early high deformation temperatures (> c. 675 °C) are indicated by grain boundary migration recrystallization of feldspar in the Rosemarkie samples, microstructural evidence for plastic deformation of feldspar in the more southerly positioned samples is extremely limited. Microstructures and c-axis fabrics in four of the five samples (the exception being one of the samples – GG-22-6 – from the SE side of the fault zone) indicate an oblique sinistral NW side up to the SW and SE side down to the NE sense of shearing.

Rosemarkie coastal section on NW side of GGFZ: Moine / Lewisian samples from Rosemarkie are dominantly composed of feldspar and amphibole grains which define the grain shape foliation and lineation. Feldspar (both orthoclase and plagioclase) has been recrystallized by grain boundary migration (GBM) suggesting minimum deformation temperatures of c. 675 °C. Only two of the collected samples (RM-22-5 and 7) contained significant proportions of quartz and both samples yielded strongly developed asymmetric cross-girdle c-axis fabrics demonstrating: 1) an oblique sinistral shear sense that the NE to ENE plunging mineral lineation is the maximum principal stretch direction (X) with a NW side up to the SW and SE side down to the NE sense of motion. The quartz c-axis fabric opening angle from sample RM-22-5 indicates a deformation temperature of c. 510 °C, possibly indicating that the fabric continued to evolve during cooling and exhumation, although shearing was likely minimal below c. 500 °C as the feldspar grains are not fractured, and the quartz grains do not contain subgrain rotation (SGR) microstructures that typically form at 400 - 500 °C. Sample RM-22-7 has a significantly larger opening angle than RM-22-5, indicating a deformation temperature of c. 610 °C and, for an assumed geothermal gradient of 30 °C per km, representing an estimated crustal depth of ~ 20 km. Assuming that the fabrics in the Rosemarkie Inlier rocks developed within the Great Glen Fault Zone and were exhumed by oblique sinistral shearing along a lineation plunging at 37° towards the NE (Mendum & Noble 2010), then exhumation from a depth of 20 km would require approximately 27 km of horizontal displacement.

It remains to be unequivocally demonstrated that the grain shape and crystal fabrics in the Rosemarkie samples did form with the Great Glen Fault Zone itself during oblique strike-slip shearing, rather than being older fabrics belonging to the Northern Highland Terrane (NHT) that have been rolled over to the SE into the GGFZ when shearing commenced within the fault zone. Law et al. (2021) have documented fabrics associated with a top to the N sense of shearing in the Moine metasedimentary rocks of the eastern part of the NHT (tentatively dated at 450 - 440 Ma) that if passively rolled over into the fault zone would give the same sense of shear (NW side up to the SW and SE side down to the NE) as documented in the Rosemarkie samples. Mendum and Noble (2010) have dated sheared leucogranite sheets from the Rosemarkie section that have identical kinematics and very similar foliation/lineation orientations to those in the surrounding metasedimentary rocks at 401 - 398 ± 2 Ma (Lower Devonian). This strongly indicates that the leucogranites have been sinistrally sheared within the GGFZ. Isotopic dating is still needed, however, for the deformation fabrics in the metasedimentary rocks. If these deformation fabrics are of late Silurian –early Devonian age (younger than say 420 Ma) it seems most probable that they

did form within the GGFZ. If isotopic ages >420 Ma are found, then it is more likely that they are pre-existing deformation fabrics that have later been caught up in the GGFZ.

Torcastle area in center of GGFZ: The quartz-rich metasedimentary rocks exposed at Torcastle have been tentatively correlated by Stewart et al. (2020) with the Glenfinnan Group (Moine Supergroup) of the NHT on the NW side of the fault zone. Although generally intensely fractured in fault zones associated with dominant sinistral strike-slip motion on the GGFZ (Stewart 2010 and references therein), a series of oriented samples were collected where fracturing is minimal and earlier microstructures associated with crystal plastic deformation and dynamic recrystallization are preserved. Grain shape lineation in these samples plunges at 65° towards 098°, while in the Rosemarkie samples lineation plunged more gently towards the NE to ENE (compare lineation and foliation orientation data for the different sampling areas summarized in Fig. 7.1). Quartz has dynamically recrystallized by subgrain rotation and alignment of more elongate grains oblique to macroscopic foliation indicates a NW side up and SE side down shear sense – as previously documented for the Rosemarkie samples. This shear sense is confirmed by the asymmetric cross-girdle c-axis fabric in sample GG-22-3D. The opening angle of this cross-girdle fabric indicates a deformation temperature of c. 515 °C, which is at the upper end of the likely range of deformation temperatures indicated by the SGR microstructures (400 - 500 °C). Unlike at Rosemarkie, no microstructural evidence for plastic deformation was found in the feldspar grains, suggesting that maximum deformation temperatures did not exceed these values inferred from the quartz microstructural and crystal fabrics. As with the Rosemarkie samples, although the observed microstructures and crystal fabrics are consistent with exhumation-related deformation from below the brittle-ductile transition zone during ongoing oblique sinistral shearing within the GGFZ, it remains to be unequivocally demonstrated that these microstructures and fabrics did form during shearing within the fault zone, rather than being earlier structures later caught up in the fault zone.

Roadside exposures on SE side of GGFZ: Three samples have been analyzed from the SE side of the fault zone. Traced from NE to SW these include GG-22-8, GG-22-6 and GG-22-4. All three samples are probably derived from basal parts of the Dalradian succession of the Grampian Highlands.

Unoriented sample GG-22-8 from the SE side of Loch Lochy contains quartz and feldspar microstructures indicating deformation under lowermost greenschist facies conditions, with dislocation glide and grain boundary bulging in quartz, brittle cracking in feldspar, and diffusive mass transfer/pressure solution operating between the mineral grains and leading to reprecipitation of quartz and mica in the dilatant cracks. Deformation temperatures are estimated at approximately 300 °C – i.e., in the transition zone between epizonal and chlorite grade greenschist facies conditions, perhaps with some earlier higher-temperature deformation in individual feldspar grains.

Quartz microstructures in sample GG-22-6 from the SE side of Loch Linnhe indicate that quartz recrystallization started in the high-temperature (> c. 550 °C) GBM II regime and with the progressive exhumation and cooling transitioned through first the transitional

GMB-SGR regime (at temperatures of c. 500 °C) and then rapidly through the SGR regime (as few subgrains seem to have been formed or preserved) and finally into the lower temperature (300-400 °C) regime where late stage grain boundary bulging was dominant. Feldspar grains are rare in this quartzite and contain fractures which terminate at feldspar-quartz grain boundaries indicating that while feldspar grains were deforming by fracture surrounding quartz grains were flowing plastically. A deformation temperature of c. 490 °C is indicated by the opening angle of the cross-girdle c-axis fabric for sample GG-22-6, and both the asymmetry of this cross-girdle fabric and quartz microstructures indicate a NW side-down and SE side-up about the steeply plunging lineation.

Quartz grains in sample GG-22-4 from the SE side of Loch Linnhe have deformed and recrystallized in the SGR (400 - 500 °C) regime, while the opening angle of the associated cross-girdle c-axis fabric indicates a deformation temperature of 540 °C suggesting that deformation may have started in the GBM regime and progressed into the lower temperature SGR regime. Feldspar grains appear to be internally undeformed suggesting that maximum deformation temperature was not significantly above 500 °C. The asymmetry of the cross-girdle fabric indicates a NW side-up and SE side down sense of shear about the steeply plunging lineation. The grain shape fabric in GG-22-4 is cut by a quartz-rich shear zone in which microstructures and an asymmetric single girdle c-axis fabric also indicate a NW side-up and SE side down sense of shear. This is the same shear sense as recorded for sample GG-22-3 from the center of the Great Glen fault zone at Torcastle (and the Rosemarkie samples) but opposite to the shear sense obtained along strike to the NE in sample GG-22-6.

Deformation conditions in plutonic rocks adjacent to the GGFZ and Strathconnon Fault

Within the limited number of samples collected from the Clunes Tonalite and Glen Gary Vein Complex adjacent to the GGFZ, and from the Ratagain pluton adjacent to the Strathconnon Fault, no compelling microstructural evidence was found for sub-solidus deformation. Considerable evidence was found, however, for relatively high temperature solid-state deformation in quartz and feldspar grains. As these c. 430-425 Ma intrusive bodies post-date regional deformation and metamorphism in the surrounding Moine metasedimentary country rocks, the high temperature solid-state deformation microstructures in the quartz and feldspar grains most probably formed in response to far field stresses associated with motion on the adjacent fault zones as the intrusive complexes cooled towards background country rock temperatures. Strains associated with these solid-state deformation microstructures are low, however, and magmatic grain shape fabrics are preserved.

High temperature solid-state deformation microstructures are most clearly preserved in granodiorite sample GG-22-9 from the Glen Garry Vein Complex. These microstructures include: blocky extinction in quartz grains parallel to prism and basal planes suggesting at least limited prism <c> slip at deformation temperatures > c. 630 °C; island microstructures in quartz grains indicating extensive grain boundary migration between quartz grains at temperatures > c. 500 °C; undulose extinction and spectacular flexing and bending of twin

boundaries in plagioclase grains, and localized grain boundary bulging between adjacent feldspar grains also indicating deformation at temperatures > c. 500 °C. Many of the feldspar grains are cut by extension fractures that do not extend into adjacent quartz grains suggesting that deformation continued to lower temperatures during cooling when feldspar deformed by fracturing while adjacent quartz grains continued to flow plastically.

Some of these relatively high temperature solid-state microstructures were also found in samples RA-22-1 and RA-22-3 from the SE edge of the Ratagain pluton, and to a lesser extent the SE margin of the Clunes pluton.

All of these microstructural observations are at least consistent with the long-held view that shearing on the Great Glen Fault Zone was on-going during intrusion of these plutonic complexes at 430-425 Ma.

Chapter 7 - Figures

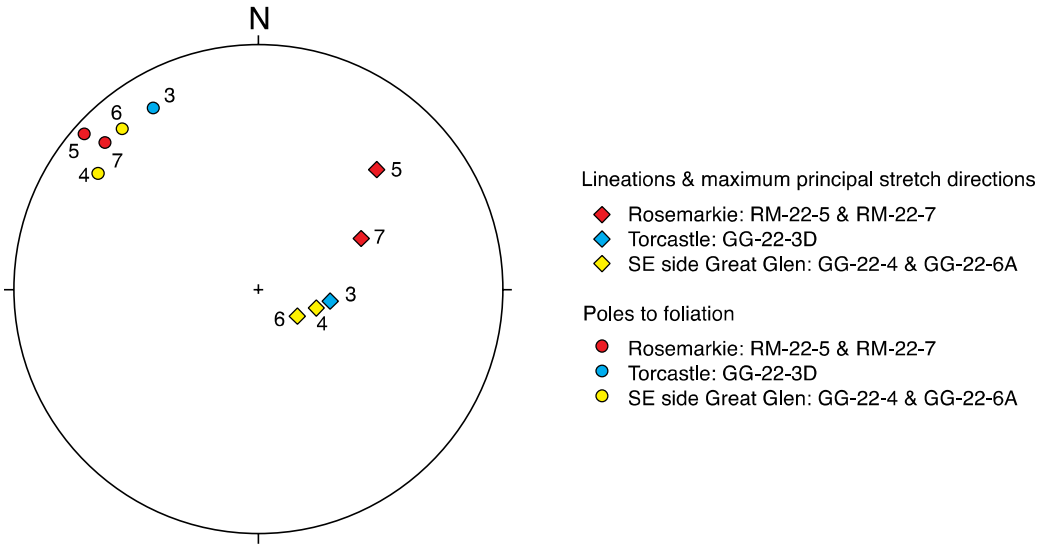

Figure 7.1. Summary of grain shape fabric data for samples from the Rosemarkie (RM-22-5 and RM-22-7), Torcastle (GG-22-3D) and SE side of Great Glen to south of Fort William (GG-22-6 and GG-22-6A) for which quartz c-axis fabrics have been obtained and demonstrate that the grain shape lineations are parallel to the maximum principal stretch direction (X). Note: 1) similar orientations of foliation in all three area, but markedly different lineation orientations for Rosemarkie samples on NW side of Great Glen compared with samples from the Torcastle area in the center of the Great Glen Fault Zone and samples from SE side of Great Glen to south of Fort William.

Chapter 8: Synthesis of Results

Results at multiple study sites along the Great Glen Fault Zone (GGFZ) and related Strathconnon Fault (SCF) provide microstructural evidence for brittle and lower-temperature plastic deformation overprinting earlier higher-temperature microstructures. In metasedimentary rocks adjacent to and within the GGFZ (Rosemarkie coastal section on NW side, Torcastle in the center of the fault zone, and roadside exposures south of Fort William on SE side) quartz grains exhibit a range of high to low temperature (c. 600 - 300 °C) microstructures associated with crystal plastic deformation that are locally overprinted by brittle microstructures. High temperature (> 600 °C) crystal plastic deformation of feldspar is largely confined to the Rosemarkie samples where the associated feldspar microstructures are locally overprinted by brittle fracturing. In contrast, feldspar clasts in the Torcastle samples display no microstructural evidence for high temperature plastic deformation while samples from the SE side of the fault zone display only occasional microstructural hints of an earlier phase of high temperature deformation. The range of deformation temperatures indicated by these microstructures is fully consistent with ongoing penetrative deformation during exhumation within the fault zone through the brittle ductile transition zone from middle to upper crustal levels.

Quartz c-axis fabrics of four oriented samples (RM-22-5 & RM-22-7 from the Rosemarkie section on the NW side of the fault zone, GG-22-3D from Torcastle in the center of the fault zone, and GG-22-4 from the SE side of the fault zone) indicate an oblique sinistral shear sense with the NW side of the sample moving up to the SW relative to the SE side of the sample, with maximum deformation temperatures ranging from 610 °C (RM-22-7; see Chapter 3) down to 480 °C (GG-22-4, see Chapter 6). This shear sense is confirmed by microstructures such as asymmetric mica fish, shear bands and alignment of elongate dynamically recrystallized quartz grains oblique to macroscopic foliation. The opposite shear sense is indicated in sample GG-22-6 from the SE side of the fault zone, with the SE side of the sample moving up to the SW relative to the NW side of the sample. Maximum principal stretch directions and mineral grain shape lineations associated with these crystal fabrics plunge gently-moderately to the NE in the Rosemarkie coastal section on the NW side of the fault zone, but more steeply to the E in the samples from the center and SE side of the fault zone.

It needs to be kept in mind that these conclusions are based on only a handful of samples collected along a 100 km long section of the Great Glen Fault Zone. Exposures of bedrock within the fault zone are very rare with most the fault zone buried beneath either lochs or glacial drift deposits. To what extent these samples are representative of the entire fault zone cannot therefore be determined.

Quartz and feldspar microstructures from c. 430 - 425 Ma plutons and magmatic vein complexes intruded along the NW sides of the Great Glen and Strathconnon faults (Clunes, Ratagain, Glen Garry Vein Complex) indicate that these magmatic rocks were internally undergoing at least a small amount of solid-state deformation during cooling from c. 630 - 300 °C. As the plutons are thought to have been intruded after regional deformation and metamorphism ceased in the surrounding Moine metasedimentary rocks, this is interpreted

as indicating that the adjacent fault zones were active during cooling of the plutonic rocks towards background temperatures at c. 430 - 425 Ma.

It remains to be demonstrated, however, that the deformation microstructures and crystal fabrics in the metasedimentary rocks collected from the NW, center and SE sides of the Great Glen Fault Zone developed during shearing on the fault zone and are not older deformation fabrics that were later rolled into the fault zone. Previous studies indicate that regional deformation and metamorphism of the Moine metasedimentary rocks on the NW side of the fault zone is likely of Scandian age (c. 430 Ma or older) while regional deformation and metamorphism of Dalradian metasedimentary rocks on the SE side of the fault zone is of Grampian age (c. 470 - 460 Ma). Dr Calvin Mako (Arizona Geological Survey) has identified four samples from the Rosemarkie coastal section (RM-22-4, RM-22-6, RM-22-8, and RM-22-9) that have potential (using monazite, xenotime, apatite and titanite) for isotopically dating formation of the penetrative deformation fabrics associated with oblique sinistral shearing. If late Silurian to Early Devonian ages are obtained this would be compelling evidence that the deformation fabrics did form within the fault zone. On the other hand, if older ages are obtained, this would suggest that the deformation fabrics are pre-existing structures that have later been incorporated within the younger Great Glen Fault Zone. Microprobe thin sections have been prepared from these samples and LA-ICPMS dating at University of California at Santa Barbara has been scheduled for June 2023.

Bibliography

Alsop, G.I. 1992. Late Caledonian sinistral strike-slip displacement across the Leannan Fault system, northwest Ireland. *Geological Journal,* **27**, 119-125, https://doi.org/10.1002/gj.3350270203

Andrews, I. 1985. The deep structure of the Moine Thrust, southwest of Shetland. *Scottish Journal of Geology*, **21**, 213–217, https://doi.org/10.1080/1023624021000019333.

Armitage, T.B., Watts, L.M., Holdsworth, R.E. & Strachan, R.A. 2021. Late Carboniferous dextral transpressional reactivation of the crustal-scale Walls Boundary Fault, Shetland: the role of preexisting structures and lithological heterogeneities. *Journal of the Geological Society, London*, **178**, https://doi.org/10.1144/jgs2020-078

Atherton, M. P. & Ghani, A. A. 2002. Slab breakoff: a model for Caledonian, Late Granite syn-collisional magmatism in the orthotectonic (metamorphic) zone of Scotland and Donegal, Ireland. *Lithos*, **62**, 65-85, https://doi.org/10.1016/S0024-4937(02)00111-1

Banks, C. J.; Smith, M.; Winchester, J. A.; Horstwood, M. S. A.; Noble, S. R. & Ottley, C. J. 2007. Provenance of intra-Rodinian basin-fills: The lower Dalradian Supergroup, Scotland. *Precambrian Research*, **153**, 46-64, https://doi.org/10.1016/j.precamres.2006.11.004

Bird, T.J., Bell, A., Gibbs, A.D. & Nicholson, J. 1987. Aspects of strike-slip tectonics in the Inner Moray Firth Basin, offshore Scotland. *Norsk Geologisk Tidsskrift*, **67**, 353-369.

British Geological Survey. 1958. *Nairn, Scotland Sheet 84, Solid Edition. 1:50 000 Geology Series*. British Geological Survey, Keyworth, Nottingham, U.K.

British Geological Survey. 1973. *Cromarty, Scotland Sheet 94, Solid Edition. 1:50 000 Geology Series*. British Geological Survey, Keyworth, Nottingham, U.K.

British Geological Survey. 1975. *Loch Lochy, Scotland Sheet 62E, Solid Edition. 1:50 000 Geology Series*. British Geological Survey, Keyworth, Nottingham, U.K.

British Geological Survey. 1976. *Kyle of Lochalsh, Scotland Sheet 71E, Solid and Drift Edition. 1:50 000 Geology Series*. British Geological Survey, Keyworth, Nottingham, U.K.

British Geological Survey. 1984. *Kintail, Scotland Sheet 72W, Solid Edition. 1:50 000 Geology Series*. British Geological Survey, Keyworth, Nottingham, U.K.

British Geological Survey. 1985.*Ben Nevis, Scotland Sheet 53, Solid & Drift Edition. 1:63 360 Geology Series*. British Geological Survey, Keyworth, Nottingham, U.K.

British Geological Survey. 1995.*Glen Roy, Scotland Sheet 63W, Solid Edition. 1:50 000 Geology Series*. British Geological Survey, Keyworth, Nottingham, U.K.

British Geological Survey. 1997.*Fortrose, Scotland Sheet 84W, Solid & Drift Edition. 1:50 000 Geology Series*. British Geological Survey, Keyworth, Nottingham, U.K.

British Geological Survey. 2007a. *Ardgour, Scotland Sheet 62E, Solid Edition. 1:50 000 Geology Series*. British Geological Survey, Keyworth, Nottingham, U.K.

British Geological Survey. 2007b. *Bedrock Geology UK North, 1:625 000 Scale, 5th Edition.* British Geological Survey, Keyworth, Nottingham.

Canning, J.C., Henney, P.J., Morrison, M.A. & Gaskarth, J.W. 1996. Geochemistry of late Caledonian minettes from Northern Britain; implications for the Caledonian sub-continental lithospheric mantle. *Mineralogical Magazine*, **60**, 221–236, https://doi.org/10.1180/minmag.1996.060.398.15

Canning, J.C., Henney, P.J., Morrison, M.A., Van Calsteren, P.W., Gaskarth, J.W. & Swarbrick, A. 1998. The Great Glen fault: A major lithospheric boundary. *Journal of the Geological Society, London*, **155**, 424-427, https://doi.org/10.1144/gsjgs.155.3.0425

Coward M.P., Enfield M.A. & Fisher M.W. 1989. Devonian basins of Northern Scotland: extension and inversion related to Late Caledonian-Variscan tectonics. *In:* Cooper, M.A. & Williams (G.D. (eds) *Inversion Tectonics*, Geological Society of London, Special Publications, **44**, 275-308, https://doi.org/10.1144/GSL.SP.1989.044.01.16

Dalziel, I.W.D. & Dewey, J.F. 2018. The classic Wilson cycle revisited. *In:* Wilson, R.W., Houseman, G.A., McCaffrey, K.J.W., Doré, A.G. & Buiter, S.J.H. (eds) *Fifty Years of the Wilson Cycle Concept in Plate Tectonics*. Geological Society, London, Special Publications, **470**, https://doi.org/10.1144/SP470.1

Derez, T., Pennock, G., Drury, M. & Sintubin, M. 2015. Low-temperature intracrystalline deformation microstructures in quartz. *Journal of Structural Geology*, **71**, 3–23, https://doi.org/10.1016/j.jsg.2014.07.015

Dewey, J.F. & Strachan, R.A. 2003. Changing Silurian-Devonian relative plate motion in the Caledonides: sinistral transpression to sinistral transtension. *Journal of the Geological Society, London*, **160**, 219–229, https://doi.org/10.1144/0016-764902-085

Dewey, J.F. & Ryan, P.D. 2022. Discussion of Searle, 'Tectonic evolution of the Caledonian orogeny in Scotland: a review based on the timing of magmatism, metamorphism and deformation'. *Geological Magazine*, **159**, 1833-1836, https://doi.org/10.1017/S0016756822000553

Dewey, J.F., Dalziel, I.W.D., Reavy, R.J. & Strachan, R.A. 2015. The Neoproterozoic to Mid-Devonian evolution of Scotland: a review and unresolved issues. *Scottish Journal of Geology*, **51**, 5–30, https://doi.org/10.1144/sjg2014-007

Dichiarante, A.M., Holdsworth, R.E., Dempsey, E.D., Selby, D., McCaffrey, K.J.W., Michie, U.McL., Morgan, G. & Bonniface, J. 2016. New structural and Re-Os geochronological evidence constraining the age of faulting and associated mineralization in the Devonian Orcadian Basin, Scotland. *Journal of the Geological Society, London*, **173**, 457–473, https://doi.org/10.1144/jgs2015-118

Dichiarante, A.M., Holdsworth, R.E., Dempsey, E.D., McCaffrey, K.J.W. & Utley, T.A.G. 2020. Outcrop-scale manifestations of reactivation during multiple superimposed rifting and basin inversion events: the Devonian Orcadian Basin, northern Scotland. *Journal of the Geological Society, London*, **178,** https://doi.org/10.1144/jgs2020-089

Donovan, R.N. & Meyerhoff, A.A. 1982. Comment on: Paleomagnetic evidence for a large (~2000 km) sinistral offset along the Great Glen fault during Carboniferous time, *Geology*, **10**, 604-605, https://doi.org/10.1130/0091-7613(1982)10<487b:CAROPE>2.0.CO;2

Faleiros, F.M., Moraes, R., Pavan, M.; Campanha, C. 2016. A new empirical calibration of the quartz c-axis opening-angle deformation thermometer. *Tectonophysic*s, **671**, 173-182. https://doi.org/10.1016/j.tecto.2016.01.014

Fazio, E., Fiannacca, P., Russo, D. & Cirrincione, R. 2020. Submagmatic to solid-state deformation microstructures recorded in cooling granitoids during exhumation of Late-Variscan crust in North-East Sicily. *Geosciences*, **10**, https://doi.org/10.3390/geosciences10080311

Fettes, D. and Macdonald, R. 1978. Glen Gary vein complex. *Scottish Journal of Geology*, **4**, 335-358, https://doi.org/10.1144/sjg14040335

Fletcher, T.P., Auton, C.A., Highton, A.J., Merritt, J.W., Robertson, S. & Rollin, K.E. 1996. *Geology of the Fortrose and Eastern Inverness District.* Memoir of the British Geological Survey Sheet 84W (Scotland). HMSO for the British Geological Survey, London, 137 pp.

Flinn, D. 1961. Continuation of the Great Glen Fault beyond the Moray Firth. *Nature*, **191**, 589–591, https://doi.org/10.1038/1911190a0

Flinn, D. 1992. The history of the Walls Boundary fault, Shetland: the northward continuation of the Great Glen fault from Scotland. *Journal of the Geological Society, London*, **149**, 721–726, https://doi.org/10.1144/gsjgs.149.5.0721.

Flinn, D.; Stone, P. & Stephenson, D. 2013. The Dalradian rocks of the Shetland Islands, Scotland, *Proceedings of the Geologists' Association*, **124,** *393-409, https://doi.org/10.1016/j.pgeola.2012.07.007*

Garson, M.S., Coats. J.S., Rock, N.M.S. & Dean T. 1984. Fennites, breccia dykes, albitites, and carbonatitic veins near the Great Glen Fault, Inverness, Scotland. *Journal of the Geological Society, London*, **141**, 711-732, https://doi.org/10.1144/gsjgs.141.4.0711

Glover, B.W. 1993. The sedimentology of the Neoproterozoic Grampian Group and the significance of the Fort William Slide between Spean Bridge and Rubha Cuil-cheanna, Inverness-shire. *Scottish Journal of Geology*, **29**, 29-43, https://doi.org/10.1016/j.jsg.2014.07.015

Grotenhuis, S.M. ten, Trow, R.A.J. and Passchier, C.W. 2003. Evolution of mica fish in mylonitic rocks. *Tectonophysics*, **372**, 1-21, https://doi.org/10.1016/S0040-1951(03)00231-2

Harris, A.L. 1995. The nature and timing of orogenesis in the Scottish Highlands and the role of the Great Glen Fault. *In:* Hibbard, J., Van Staal, C.R. & Cawood, P.A. (eds) *Current Perspectives in the Appalachian-Caledonian Orogen.* Geological Association of Canada, Special Paper, **41**, 65-79.

Hall, J., Brewer, J.A., Matthews, D.H. & Warner, M. 1984. Crustal structure across the Caledonides from the WINCH seismic reflection profile: influences on the evolution of the Midland Valley of Scotland. *Transactions of the Royal Society of Edinburgh: Earth Sciences*, **75**, 97–109, https://doi.org/10.1017/S0263593300013766

Heilbronner, R. and Tullis, J., 2002. The effect of static annealing on microstructures and crystallographic orientations of quartzites experimentally deformed in axial compression and shear. In: De Meer, S., Drury, M.R., De Bresser, J.H.P., Pennock, G.M. (Eds.), Deformation Mechanisms, Rheology and Tectonics: Current Status

and Future Perspectives, *Geological Society of London, Special Publications*, **200**, 111-208, https://doi.org/10.1144/GSL.SP.2001.200.01.12

Heilbronner, R. and Tullis J., 2006. Evolution of c-axis pole figures and grain size during dynamic recrystallization: results from experimentally sheared quartzite. *Journal of Geophysical Research*, **111**, B10202, http://dx.doi.org/10.1029/2005JB004194

Hentschel, F., Trepmann, C.A. & Janots, E. 2019. Deformation of feldspar at greenschist facies conditions – the record of mylonitic pegmatites from the Pfunder Mountains, Eastern Alps. *Solid Earth*, **10**, 95-116, https://doi.org/10.5194/se-10-95-2019

Highton, A.J. 2009. Cromarty and Rosemarkie Inliers. *In*: Mendum, J.R., Barber, A.J., Butler, R.W.H., Flinn, D., Goodenough, K.M., Krabbendam, M., Park, R.G. & Stewart, A.D. (eds) 2009. *Lewisian, Torridonian and Moine rocks of Scotland*. Geological Conservation Review Series, Joint Nature Conservation Committee, Peterborough, 458-464.

Hirth, G. & Tullis, J. 1992. Dislocation creep regimes in quartz. *Journal of Structural Geology*, **14**, 145-159, https://doi.org/10.1016/0191-8141(92)90053-Y

Holdsworth, R.E., Stewart, M., Imber, J. & Strachan, R.A. 2001. The structure and rheological evolution of reactivated continental fault zones: a review and case study. *In:* Miller, J.A., Holdsworth, R.E., Buck, I.S. & Hand, M. (eds) *Continental Reactivation and Reworking. Geological Society, London*, Special Publications, **184**, 115–137, https://doi.org/10.1144/GSL.SP.2001.184.01.07

Holgate, N. 1969. Palaeozoic and Tertiary transcurrent movements on the Great Glen Fault. *Scottish Journal of Geology*, **5**, 97–139, https://doi.org/10.1144/sjg05020097

Horne, J. 1923. *The Geology of the Lower Findhorn and Lower Strath Nairn, Including Part of the Black Isle Near Fortrose) with contributions by B.N. Peach, L.W. Hinxman, R.G. Carruthers and E.M. Anderson and a Petographical Chapter by J.S. Flett).* Memoir of the Geological Survey of Great Britain, Sheet 84 and part of Sheet 94 (Scotland. HMSO, Edinburgh, 128 pp.

Hutton, D.H.W. 1988. Igneous emplacement in a shear zone termination: The biotite granite at Strontian, Scotland. *Geological Society of America Bulletin*, **100**, 1392–1399, https://doi.org/10.1130/0016-7606(1988)100<1392:IEIASZ>2.3.CO;2

Hutton, D.H.W. & McErlean, M. 1991. Silurian and Early Devonian sinistral deformation of the Ratagain granite, Scotland: constraints on the age of Caledonian movements on the Great Glen fault system. *Journal of the Geological Society, London,* **148**, 1–4, https://doi.org/10.1144/gsjgs.148.1.0001

Hutton, D.H.W., Stephens, W.E., Yardley, B. McErlean, M. & Halliday, A.N. 1993. Ratagain Pluton Complex. *In:* May, F., Peacock, J.D., Smith, D.I. & Barber, A.J. (eds), Geology of the Kintail District. Memoir of the British Geological Survey, Sheet 72W and part of 71E (Scotland), pp. 52-56. HMSO, London.

Kemp, S.J., Gillespie, M.R., Leslie, G.A., Zwingmann, H. & Campbell, S.D.G. 2019. Clay mineral dating of displacement on the Sronlairig Fault: implications for Mesozoic and Cenozoic tectonic evolution in northern Scotland. Clay Minerals, 54, 181-196, https://doi.org/10.1180/clm.2019.25

Kennedy, W.Q. 1946. The Great Glen Fault, *Quarterly Journal of the Geological Society of London*, **102**, 41–76, https://doi.org/10.1144/GSL.JGS.1946.102.01-04.04

Krabbendam, M., Ramsay, J.G., Leslie, A.G., Tanner, P.W.G., Dietrich, D. & Goodenough, K. 2017. Caledonian and Knoydartian overprinting of a Grenvillian

inlier and the enclosing Morar Group rocks: structural evolution of the Precambrian Proto-Moine Nappe, Glenelg, NW Scotland. *Scottish Journal of Geology, **54**, 13–35, https://doi.org/10.1144/sjg2017-006*

Krabbendam, M., Strachan, R. & Prave, T. 2021. Stratigraphic framework for early Neoproterozoic successions of Scotland. *Journal of the Geological Society, London,* **179,** https://doi.org/10.1144/jgs2021-054

Law, R. 2014. Deformation thermometry based on quartz c-axis fabrics and recrystallization microstructures: A review. *Journal of Structural Geology*, **66**, 129-161, https://doi.org/10.1016/j.jsg.2014.05.023

Law, R.D., Thigpen, J.R., Mazza, S.E., Mako, C., Ashley, K.T., Krabbendam, M., Strachan, R.A. & Davis, E. 2021. Tectonic transport directions, shear senses and deformation temperatures indicated by quartz c-axis fabrics and microstructures in a NW-SE transect across the Moine and Sgurr Beag thrust sheets, Caledonian Orogen of northern Scotland. *Geosciences*, **11**(10), 441. https://doi.org/10.3390/geosciences11100411

Law, R.D., Strachan, R.A., Thirlwall, M.F. & Thigpen, J.R. in review. Chapter 8: The Caledonian orogeny: Late Ordovician to Early Devonian tectonic and magmatic events associated with closure of the Iapetus Ocean. In: Smith, M. & Strachan, R.A. (editors) *Geology of Scotland* (5th edition). Geological Society of London.

Lawrence, A., Maffione, M. & Stevenson, C. T. E. 2022. Mush ado about the Ratagain Complex, NW Scotland: insights into Caledonian granitic magmatism and emplacement from magnetic fabric analyses, *Scottish Journal of Geology*, **58**, 1-25, https://doi.org/10.1144/sjg2021-018?ref=pdf&rel=cite-as&jav=VoR.

Le Breton, E., Cobbold, P.R. & Zanella, A. 2013. Cenozoic reactivation of the Great Glen fault, Scotland: additional evidence and possible causes. *Journal of the Geological Society, London*, **170**, 403-415, https://doi.org/10.1144/jgs2012-067

Lister, G.S. 1977. Discussion: Crossed-girdle c-axis fabrics in quartzites plastically deformed by plane strain and progressive simple shear. *Tectonophysics*, **39**, 51-54, https://doi.org/10.1016/0040-1951(77)90087-7

Lister, G.S. and Snoke, A.W. 1984. S-C mylonites. *Journal of Structural Geology,* **6**, 617-638, https://doi.org/10.1016/0191-8141(84)90001-4

Lister, G.S. and Williams, P.F. 1979. Fabric development in shear zones: theoretical controls and observed phenomena. *Journal of Structural Geology,* **1**, 283-298. https://doi.org/10.1016/0191-8141(79)90003-8

Lister, G.S. and Hobbs, B.E. 1980. The simulation of fabric development during plastic deformation of quartzite and its application to quartzite: the effect of deformation history. *Journal of Structural Geology,* **2**, 355-370. https://doi.org/10.1016/0191-8141(80)90023-1

Marshall, J.A.E., Astin, T.R., Brown, J.F., Mark-Kurik, E. & Lazauskiene, J. 2007. Recognizing the Kačák Event in the Devonian terrestrial environment and its implications for understanding land-sea interactions. *In*: Becker, R.T. & Kirchgasser, W.T. (eds) *Devonian Events and Correlations*. Geological Society, London, Special Publications, **278**, 133-155, https://doi.org/10.1144/SP278.6

Marston, R.J. 1971. The Foyers granitic complex, Inverness-shire. *Quarterly Journal of the Geological Society, London,* **126**, 331–338, https://doi.org/10.1144/gsjgs.126.1.0331

May, F., Peacock, J.D., Smith, D.I. & Barber, A.J. 1993. Geology of the Kintail District. Memoir of the British Geological Survey, Sheet 72W and part of 71E (Scotland). HMSO, London. ISBN 0 11 884484 9

May, F., Highton, A.J., Clark, G.C. & Chacksfield, B.C. 1997. *Geology of the Invermoriston District: Memoir for 1:50000 Geological Sheet 73W (Scotland).* Memoir of the British Geological Survey. HMSO.

McBride, J.H. 1994. Investigating the crustal structure of a strike-slip 'step-over' zone along the Great Glen. *Tectonics*, **13**, 1550-1160, https://doi.org/10.1029/94TC00539

McErlean, M.A. 1993. Granitoid emplacement and deformation: A case study of the Thorr Pluton, Ireland, with contrasting examples from Scotland., Unpublished PhD thesis, Durham University, UK.

McGeary, S. 1989. Reflection seismic evidence for a Moho offset beneath the Walls Boundary strike slip fault. *Journal of the Geological Society, London*, **146**, 261–269, https://doi.org/10.1144/gsjgs.146.2.0261.

McLaren, A. & Pryer, L. L. 2001. Microstructural investigation of the interaction and interdependence of cataclastic and plastic mechanisms in feldspar crystals deformed in the semi-brittle field. *Tectonophysics*, **335**, 1–15, https://doi.org/10.1016/S0040-1951(01)00042-7

Means, W.D. 1981. The concept of steady-state foliation. *Tectonophysics*, **78**, 179-199, https://doi.org/10.1016/0040-1951(81)90013-5

Mendum, J.R. 2009. Moine (South) – Introduction. *In*: Mendum, J.R., Barber, A.J., Butler, R.W.H., Flinn, D., Goodenough, K.M., Krabbendam, M., Park, R.G. & Stewart, A.D. (eds) 2009. *Lewisian, Torridonian and Moine rocks of Scotland*. Geological Conservation Review Series, Joint Nature Conservation Committee, Peterborough, 547-569.

Mendum, J.R. & Noble, S.R. 2010. Mid-Devonian sinistral transcurrent movements on the Great Glen Fault: the rise of the Rosemarkie Inlier and the Acadian Event in Scotland. *In:* Law, R.D., Butler, R.W.H., Holdsworth, R.E., Krabbendam, M. & Strachan, R.A. (eds) *Continental Tectonics and Mountain Building – The Legacy of Peach and Horne.* Geological Society, London, Special Publications, **335**, 161–187, https://doi.org/10.1144/SP335.8

Milne, E.J.M., Neill, I., Bird, A.C., Millar, I.L., McDonald, I., Dempsey, E.D., Olive, V., Odling, N. & Waters, E.C. 2023. Caledonian hot zone magmatism in the 'Newer Granites': insight from the Cluanie and Clunes plutons, Northern Scottish Highlands. *Journal of the Geological Society, London*, **180**, https://doi.org/10.1144/jgs2022-076

Munro, M. 1973. Structures in the south-eastern part of the Strontian Granite Complex, Argyllshire. *Scottish Journal of Geology*, **9**, 99-108, https://doi.org/10.1144/sjg09020099

Murphy, J. B. & Keppie, J. D. 2005. The Acadian Orogeny in the Northern Appalachians. *International Geology Review*, **47**, 663-687, https://doi.org/10.2747/0020-6814.47.7.663

Mykura, W. 1982. The Old Red Sandstone east of Loch Ness, Inverness-shire. *Institute of Geological Sciences, Report*, **82-13**, Edinburgh.

Mykura, W. 1991. Old Red Sandstone. *In:* Craig, G.Y. (ed) *Geology of Scotland* (3rd edition) Geological Society, London, 297-346.
Mykura, W. & Owens, B. 1983. The Old Red Sandstone of the Mealfuorvonie outlier, west of Loch Ness, Inverness-shire. *Institute of Geological Sciences, Report*, 83/7.
Nicholls, G. D. 1951. The Glenelg-Ratagain igneous complex. *Quarterly Journal Geological Society of London,* **106**, 302–321, https://doi.org/10.1144/GSL.JGS.1950.106.01-04.17
Oliver, G. J. H. 2001. Reconstruction of the Grampian episode in Scotland: its place in the Caledonian Orogeny. *Tectonophysics*, **332**, 23-49, https://doi.org/10.1016/S0040-1951(00)00248-1
Oliver, G.J.H., Wilde, S.A. & Wan, Y. 2008. Geochronology and geodynamics of Scottish granitoids from the late Neoproterozoic break-up of Rodinia to Palaeozoic collision. *Journal of the Geological Society, London,* **165**, 661–674, https://doi.org/10.1144/0016-76492007-105
Pankhurst, R.J. 1979. Isotope and trace element evidence for the origin and evolution of Caledonian granites in the Scottish Highlands. *In:* Atherton, M.P. & Tarney, J (eds) *Origin of Granitic Batholiths*, Orpington, 18-33.
Parnell, J. T. 1982. Comment on: Paleomagnetic evidence for a large (~2000 km) sinistral offset along the Great Glen fault during Carboniferous time. *Geology*, **10**, 605, https://doi.org/10.1130/0091-7613(1982)10<605:CAROPE>2.0.CO;2
Passchier, C.W. & Trouw, R.A.J. 2005. *Microtectonics, 2nd Edition*. Springer, New York.
Paterson, S.R., Vernon, R.H., & Tobisch, O.T. 1989. A review of criteria for the identification of magmatic and tectonic foliations in granitoids. *Journal of Structural Geology*, **11**, 349-363, https://doi.org/10.1016/0191-8141(89)90074-6
Paterson, B.A., Rogers, G., Stephens, W.E. & Hinton, R.W. 1993. The longevity of acid-basic magmatism associated with a major transcurrent fault. *Geological Society of America, Abstracts with Programs*, **25**, no. 6, A42.
Peach, B.N., Horne, J.,Woodward, H.B., Clough, C.T., Harker, A. & Wedd, C.B. 1910. *The Geology of Glenelg, Lochalsh and South-East Part of Skye (Explanation of one-inch map 71).* Memoirs of the Geological Survey, Edinburgh, Scotland.
Piasecki, M.A.J., van Breemen, O., & Wright, A.E. 1981. Late Precambrian geology of Scotland, England and Wales. *In:* Kerr, J.W. & Fergusson, A.J. (eds) *Geology of the North Atlantic Borderlands*. Memoir of the Canadian Society of Petroleum Geologists, **7**, 57-94, https://archives.datapages.com/data/cspg_sp/data/007/007001/57_cspgsp00700057.htm
Pidgeon, R.T. & Aftalion, M. 1978. Cogenetic and inherited zircon U-Pb systems in granites: Palaeozoic granites of Scotland and England. *In:* Bowes, D.R. & Leake, B.E. (eds) *Crustal evolution in northwestern Britain and adjacent regions.* Geological Journal Special Issue pp. 183-220.
Pitcher, W.S., Elwell, R.W.D., Tozer, C.F. & Cambray, F.W. 1964. The Leannan Fault. *Quarterly Journal of the Geological Society, London,* **120**, 241–273, https://doi.org/10.1144/gsjgs.120.1.0241
Ramsay, J.G. 1955. A camptonitic dyke suite at Monar, Ross-shire and Inverness-shire. *Geological Magazine,* **92**, 297–308, https://doi.org/10.1017/S0016756800064347

Rathbone, P.A. & Harris, A.L. 1980. Moine and Lewisian near the Great Glen Fault in Easter Ross. *Scottish Journal of Geology*, **16**, 51-64, https://doi.org/10.1144/sjg16010051

Rogers, G. & Dunning, G.R. 1991. Geochronology of appinitic and related granitic magmatism in the W Highlands of Scotland: constraints on the timing of transcurrent fault movement. *Journal of the Geological Society, London* 148, 17–27 https://doi.org/10.1144/gsjgs.148.1.0017

Rogers, D.A., Marshall, J.E.A. & Austin, T.R. 1989. Devonian and later movements on the Great Glen fault system, Scotland. *Journal of the Geological Society, London,* **146**, 369–372, https://doi.org/10.1144/gsjgs.146.3.0369

Schmid, S.M., Casey, M. 1986. Complete fabric analysis of some commonly observed quartz c-axis patterns. American Geophysical Union, Geophysical Monograph **36**, 263-286. https://agupubs.onlinelibrary.wiley.com/doi/10.1029/GM036p0263

Searle, M. P. 2021. Tectonic evolution of the Caledonian orogeny in Scotland: a review based on the timing of magmatism, metamorphism and deformation. *Geological Magazine*, **159**, 124-152, https://doi.org/10.1017/S0016756821000947

Searle, M.P. 2022. Reply to Dewey and Ryan Comment on Searle, MP (2021) 'Tectonic evolution of the Caledonian orogeny in Scotland: a review based on the timing of magmatism, metamorphism and deformation'. *Geological Magazine*, **158**, 1837-1845, https://doi.org/10.1017/S0016756822000838

Séranne M. 1992. Devonian extensional tectonics versus Carboniferous inversion in the northern Orcadian basin. *Journal of the Geological Society, London,* **149**, 27–37, https://doi.org/10.1144/gsjgs.149.1.0027

Singleton, J.S., Rahl, J.M**.** & Befus, K.S. 2020. Rheology of a coaxial shear zone in the Virginia Blue Ridge: Wet quartzite dislocation creep at ~250-280°C. *Journal of Structural Geology*, **140**, 104-109, https://doi.org/10.1016/j.jsg.2020.104109

Smith, D.I. & Watson, J. 1983. Scale and timing of movements on the Great Glen fault, Scotland. *Geology*, **11**, 523-526, https://doi.org/10.1130/0091-7613(1983)11<523:SATOMO>2.0.CO;2

Soper, N.J., Strachan, R.A., Holdsworth, R.E., Gayer, R.A. & Greiling, R.O. 1992. Sinistral transpression and the Silurian closure of Iapetus. *Journal of the Geological Society, London,* **149**, 871–880, https://doi.org/10.1144/gsjgs.149.6.0871

Speight, J.M. & Mitchell, J.G. 1979. The Permo-Carboniferous dyke-swarm of northern Argyll and its bearing on dextral displacement on the Great Glen Fault. *Journal of the Geological Society, London*, **139**, 3–11, https://doi.org/10.1144/gsjgs.136.1.0003

Stephens, W.E. 1999. Glen More. In: Stephenson, D. et al. (eds.) Caledonian Igneous Rocks of Great Britain. Geological Conservation Review Series, Joint Nature Conservation Committee, Peterborough, 409-412.

Stephenson, D., Mendum, J.R., Fettes, D.J & Leslie, A.G. 2013. The Dalradian rocks of Scotland: an introduction. *Proceedings of the Geologists' Association*, **124**, 3-82.

Stewart, M. 1997. *Kinematic evolution of the Great Glen Fault Zone, Scotland*. PhD Thesis, Oxford Brookes University.

Stewart, M. 2010. Excursion 14 - Great Glen. *In:* Strachan, R.A., Alsop, I., Friend, C.R.L. & Miller, S. (eds) *An Excursion Guide to the Moine Geology of the Northern*

Highlands of Scotland. Edinburgh Geological Society & Geological Society of Glasgow, Edinburgh, Scotland, 266-281.

Stewart, M., Strachan, R. A. & Holdsworth, R. E. 1997. Direct field evidence for sinistral displacements along the Great Glen Fault Zone: late Caledonian reactivation of a regional basement structure? *Journal of the Geological Society, London*, **154**, 135-139, https://doi.org/10.1144/gsjgs.154.1.0135

Stewart, M., Strachan, R.A. & Holdsworth, R.E. 1999. Structure and early kinematic history of the Great Glen Fault Zone, Scotland. *Tectonics*, **18**, 326–342, https://doi.org/10.1029/1998TC900033

Stewart, M., Holdsworth, R.E. & Strachan, R.A. 2000. Fault-rock evolution during early movements along the Great Glen Fault Zone, Scotland: An insight into deformation processes in the frictional- to viscous-creep transition zone. *Journal of Structural Geology*, **22**, 543–560, https://doi.org/10.1016/S0191-8141(99)00164-9

Stewart, M., Strachan, R. A., Martin, M. W. & Holdsworth, R. E. 2001. Constraints on early sinistral displacements along the Great Glen Fault Zone, Scotland: structural setting, U–Pb geochronology, and emplacement of the syn-tectonic Clunes tonalite. *Journal of the Geological Society, London*, **158**, 821-830, https://doi.org/10.1144/jgs.158.5.821

Stipp, M., Heilbronner, R., Stunitz, H. & Schmid, S. M. 2002a. Dynamic recrystallization of quartz: correlation between natural and experimental conditions. *In*: De Meer, S., Drury, M.R., De Bresser, J.H.P. & Pennock, G.M. (eds) *Deformation Mechanisms, Rheology and Tectonics: Current Status and Future Perspectives. Geological Society of London Special Publications*, **200**, 171-190, https://doi.org/10.1144/GSL.SP.2001.200.01.11

Stipp, M., Stünitz, H., Heilbronner, R. & Schmid, S. M. 2002b. The eastern Tonale fault zone: A 'natural laboratory' for crystal plastic deformation of quartz over a temperature range from 250 to 700 °C. *Journal of Structural Geology*, **24**, 1861–1884, https://doi.org/ 10.1016/S0191-8141(02)00035-4

Stocker, M.S. 1982. Old Red Sandstone sedimentation and deformation in the Great Glen fault Zone, NW of Loch Linnhe. *Scottish Journal of Geology*, **18**, 147-156, https://doi.org/10.1144/sjg18020147

Strachan, R. A. 1985. The stratigraphy and structure of the Moine rocks of the Loch Eil area, West Inverness-shire, *Scottish Journal of Geology*, **21**, 9-22, https://doi.org/10.1144/sjg21010009

Strachan, R.A., Harris, A.L., Fettes, D.J. & Smith, M. 2002. The Highland and Grampian terranes. *In:* Trewin, N.H. (ed) *The Geology of Scotland*, 4th edition. The Geological Society, London, 81-148. ISBN: 1862391262 9781862391260.

Strachan, R.A., Holdsworth, R.E., Krabbendam, M. & Alsop, G.I. 2010. The Moine Supergroup of NW Scotland: insights into the analysis of polyorogenic supracrustal sequences. In: Law, R.D., Butler, R.W.H., Holdsworth, R., Krabbendam, M. & Strachan, R.A. (eds) *Continental Tectonics and Mountain Building - The Legacy of Peach and Horne.* Geological Society, London, Special Publication, 335, 233-254. doi.org/10.1144/SP335.11

Stünitz, H., FitzGerald, J., & Tullis, J. 2003. Dislocation generation, slip systems, and dynamic recrystallization in experimentally deformed plagioclase single crystals, *Tectonophysics*, **372**, 215 – 233, https://doi.org/10.1016/S0040-1951(03)00241-5

Thomson, K. & Underhill, J.R. 1993. Controls on the development and evolution of structural styles in the Inner Moray Firth Basin. *In:* Parker, J.R. (ed) *Petroleum Geology of Northwest Europe: Proceedings of the 4th Conference*. Geological Society, London, 1167–1178, http://dx.doi.org/10.1144/0041167

Tribe, I.R. & D'Lemos, R.S. 1996. Significance of hiatus in decreasing temperature fabric development within syn-tectonic quartz diorite complexes, Channel Islands, U.K. *Journal of the Geological Society, London*, **153**, 127–138, https://doi.org/10.1144/gsjgs.153.1.0127

Tullis, J. 1977. Preferred orientation of quartz produced by slip during plane strain. *Tectonophysics*, **39**, 87-102. https://doi.org/10.1016/0040-1951(77)90090-7

Tullis, J. 2002. Deformation of granitic rocks: Experimental studies and natural examples. *Reviews in Mineralogy and Geochemistry*, 51, 51–95, https://doi.org/10.2138/gsrmg.51.1.51

Tullis, J. & Yund, R. A. 1987. The brittle-ductile transition in feldspar aggregates: An experimental study. *International Geophysics*, **51**, 89–117, https://doi.org/10.1016/S0074-6142(08)62816-8

Underhill, J.R. 1991. Implications of Mesozoic- Recent basin development in the Western Inner Moray Firth. *Journal of Marine and Petroleum Geology*, **8**, 359-369, https://doi.org/10.1016/0264-8172(91)90089-J

Underhill, J.R. & Brodie, J.A. 1993. Geology of Easter Ross, Scotland: implications for movement on the Great Glen fault zone. *Journal of the Geological Society, London,* **150**, 515–527, https://doi.org/10.1144/gsjgs.150.3.0515

Urai, J.L., Means,W.D. and Lister, G.S. 1986. Dynamic recrystallization of minerals. *American Geophysical Union, Geophysical Monograph Series*, **36**, 161–199.

Vernon, R.H. 2004. A Practical Guide to Rock Microstructure. Cambridge University Press., Cambridge, UK.

Watson, J.V. 1984. The ending of the Caledonian orogeny in Scotland. *Journal of the Geological Society, London,* **141**, 193–214, https://doi.org/10.1144/gsjgs.141.2.0193

Watts, L.M., Holdsworth, R.E., Sleight, J.A., Strachan, R.A. & Smith, S.A.F. 2007. The movement history and fault rock evolution of a reactivated crustal-scale strike-slip fault: the Walls Boundary Fault Zone, Shetland. *Journal of the Geological Society, London*, **164**, 1037–1058, https://doi.org/10.1144/0016-76492006-156

Wilson, J.T. 1962. Cabot Fault, an Appalachian equivalent of the San Andreas and Great Glen Faults and some implications for continental displacement. *Nature,* **195**, 135-138, https://doi.org/10.1038/195135A0

Winchester, J.A. 1973. Pattern of regional metamorphism suggests a sinistral displacement of 160 km along the Great Glen Fault. *Nature,* **246**, 81-84, https://doi.org/10.1038/physci246081a0